Fall 2020

The Role of HIV-1 Tat-Mediated Inhibition of the Dopamine and Norepinephrine Transporters in the Neuropathology of HIV-1 Associated Neurocognitive Disorders

Matthew Strauss

The Role of HIV-1 Tat-mediated Inhibition of the Dopamine and Norepinephrine Transporters in the Neuropathology of HIV-1 Associated Neurocognitive Disorders

by

Matthew Strauss

Doctor of Pharmacy
University of South Carolina, 2015

Submitted in Partial Fulfillment of the Requirements

For the Degree of Doctor of Philosophy in

Pharmaceutical Sciences

College of Pharmacy

University of South Carolina

2020

Approved by:

Jun Zhu, Major Professor

Michael Wyatt, Committee Member

Doug Pittman, Committee Member

Kim Creek, Committee Member

David Mott, Committee Member

Cheryl L. Addy, Vice Provost and Dean of the Graduate School

DEDICATION

To my wife Caroline, without her encouragement, love, sacrifices, support, and inspiration this work would not have been possible…

ACKNOWLEDGEMENTS

First of all, I would like to express my utmost gratitude to my mentor, Dr. Jun Zhu, whose mentorship has instilled in me an immeasurable respect for science. In Dr. Zhu I have also found a great friend with whom I have shared many laughs and had a multitude of great discussions about all aspects of life.

I am very grateful to all past and present members of the Zhu lab who have become friends and colleagues, particularly Dr. Pam Quizon for being a great friend and with whom I shared many memorable moments through the years, I could not have succeeded without her mentorship and guidance. I would also like to thank Dr. Wei-Lun Sun for his guidance and advice, as well as Sarah Davis for taking the torch to lead the next group of young scientists in the Zhu lab, I wish you the best of luck.

I also extend my gratitude to the members of my dissertation committee: Drs. Kim Creek, Doug Pittman, Michael Wyatt, and David Mott for their invaluable guidance and critiques. I would also like to thank Dr. Jay Mclaughlin for his advice and friendship through both scientific and personal adventures.

Finally, I want to thank my family for their continued and unwavering support throughout my academic career. To my parents, I only hope to be as supportive to my growing family as you have been to me my entire life. To my wife, Caroline, none of this would have been possible without you, and your constant love and support means more than you could ever know.

ABSTRACT

Despite the success of combinatorial antiretroviral therapy (cART) in controlling peripheral HIV infection and improving the lives of HIV-1 patients, roughly 50% of this population continues to develop a group of neurological complications including cognitive dysfunction, motor deficits, and dementia collectively referred to as HIV-associated neurocognitive disorders (HAND). The continuing presence of the transactivator of transcription (Tat) protein in cART-treated HIV-1 patients has been suggested to play a crucial role in the neurotoxicity and cognitive impairment evident in HAND. HIV-1 Tat protein has been detected in dopamine (DA) -rich brain areas, and long-term viral protein exposure has been found to accelerate damage to the mesocorticolimbic DA system. Previous reports from our laboratory indicate that HIV-1 Tat-mediated damage to the dopaminergic system involves a direct allosteric interaction between HIV-1 Tat and the DA transporter (DAT). Importantly, in the central nervous system, in addition to the DAT, the norepinephrine (NE) transporter (NET) is also responsible for maintaining DA homeostasis. Due to its high level of homology with the DAT it is possible that HIV-1 Tat may induce DA dysregulation through interactions with this transporter as well. Based on these findings, this research project investigated the hypothesis that *via direct inhibitory allosteric interactions with the dopamine and norepinephrine transporters, the HIV-1 Tat*

protein dysregulates dopamine homeostasis, resulting in the neuropsychiatric dysfunction prominently featured in HAND.

First, the possibility that HIV-1 Tat inhibition of DA uptake involves both DAT and NET was investigated. Via site-directed mutagenesis of the Tyrosine467 (Y467) residue of the NET to a phenylalanine (Y467F) or a histidine (Y467H), which correlates with Tyrosine470 on the DAT, it was determined that not only is HIV-1 Tat capable of inhibiting DA uptake through NET, but that this interaction involved similar residues as the HIV-1 Tat/DAT interaction. Building on this finding, the next step was to establish if HIV-1 Tat-mediated inhibition of the DA and NE transporters could be replicated in an animal model of HAND. Utilizing an inducible HIV-1 Tat transgenic mouse model (iTat-tg), it was determined that HIV-1 Tat inhibited both the DA and NE transporters to a similar extent in the prefrontal cortex (PFC) of the iTat-tg mice.

The critical question following these findings was if HIV-1 Tat-mediated dysregulation of the dopaminergic system could be prevented, what effect would this have on the development of cognitive deficits observed in HAND? This possibility was investigated via generation of a mutant Tyrosine88 to phenylalanine (Y88F) DAT mouse model, which was crossed with the iTat-tg mouse. The Y88F DAT mutation proved capable of both preventing HIV-1 Tat-mediated inhibition of the DAT in the PFC, as well as learning and memory deficits which had been previously reported in the iTat-tg mice. These results demonstrate that prevention of the HIV-1 Tat/DAT interaction is sufficient to prevent DA dysregulation and associated neurocognitive deficits in HAND.

Furthermore, this interaction is highlighted as a potential target for the development of novel therapies which may serve as adjunct therapy to improve the lives of HIV-1 infected patients.

TABLE OF CONTENTS

LIST OF TABLES

LIST OF FIGURES

LIST OF ABBREVIATIONS

aCSF …… Artificial cerebrospinal fluid

AIDS …….. Acquired immunodeficiency virus

ANI …….. Asymptomatic neurocognitive impairment

ANOVA …… Analysis of variance

BBB ……Blood-brain barrier

B_{max} ……..… Maximal binding

cART ……..……Combinatorial antiretroviral therapy

CNS …….. Central nervous system

CSF ……Cerebrospinal fluid

DA ……..…. Dopamine

DAT ……Dopamine transporter

DMI …… Desipramine

DOPAC ……Dihydroxyphenylacetic acid

Dox ……..Doxycycline

GFAP ……Glial fibrillary acidic protein

G-tg …… iTat-tg mice lacking HIV-1 Tat expression

HAD ……..HIV-1 associated dementia

HAND ……...HIV-associated neurocognitive disorders

hDAT …….. ……Human dopamine transporter

HIV …… Human immunodeficiency virus

hNET ……...Human norepinephrine transporter

HIP ……...Hippocampus

HPLC ……...High-performance liquid chromatography

IC50 …… Half maximal inhibitory concentration

iTat-tg ……Inducible HIV-1 Tat transgenic

K_d …… Dissociation constant

K_m ……Michaelis-Menton constant

KRH ……Krebs-Ringer-HEPES

MND ……...Mild neurocognitive disorder

NE …… Norepinephrine

NET …….. Norepinephrine transporter

NIH …… National Institute of Health

PFC …… Prefrontal Cortex

S1 ……Primary substrate binding site

S2 ……... Secondary substrate binding site

SDS ……Sodium dodecyl sulfate

SEM …… Standard error of the mean

SERT ……..Serotonin transporter

Tat …….. Trans-activator of transcription

TETON …… Tetracycline-on

TM10 ……Transmembrane helix 10

V_{max} …… Maximal velocity

WT ……Wild type

CHAPTER 1

INTRODUCTION

1.1 HIV-ASSOCIATED NEUROCOGNITIVE DISORDERS

Untreated human immunodeficiency virus type 1 infection (HIV-1) continually weakens the immune system of infected patients, ultimately manifesting in the development of acquired immunodeficiency syndrome (AIDS) (Vahlne 2009). Opportunistic infections, which are a direct consequence of the development of AIDS, have decreased following the advent of combinatorial antiretroviral therapy (cART) in the late 1990's (Carpenter et al., 1996; Deeks et al., 2013), transitioning HIV-1 infection from a terminal to a chronic diagnosis. Due to the subsequent dramatic reduction in mortality, improvement in life expectancy, and increased access to cART, the number of people living with HIV-1 worldwide has steadily risen throughout the decades (Simioni et al., 2010; Bonnet et al., 2013). Currently there are over 37 million people infected with HIV-1 and nearly another 2 million are becoming infected each year (Figure 1.1). These conditions have resulted in dramatically altered patient demographics, as individuals over 50 years old now make up the largest percentage of the HIV-1 infected population (Centers for Disease Control and Prevention 2017). This shift in patient demographics correlated with increased observation of a range of neurological symptoms including cognitive dysfunction, behavioral changes,

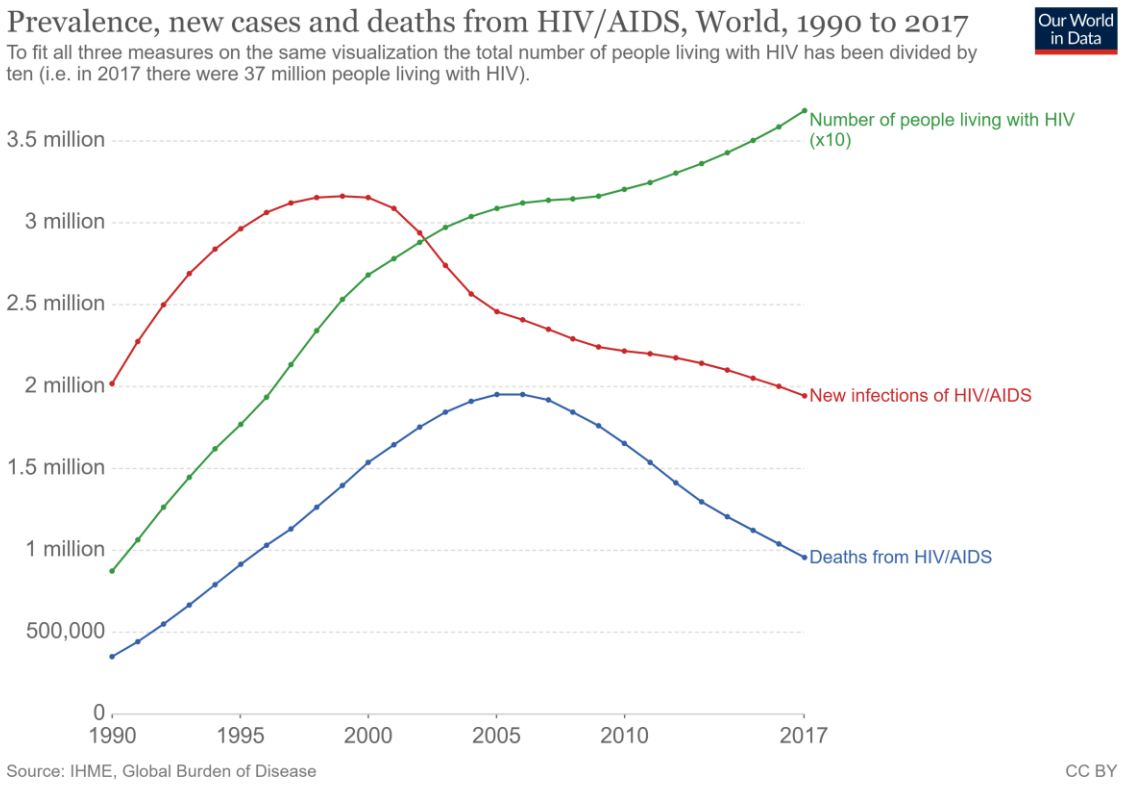

Figure 1.1 Current state of the HIV-1 pandemic. Each point represents data from a single year from the Institute for Health Metrics and Evaluation (IHME). The green line represents the number of people currently infected with HIV-1 worldwide (x10), the red line represents new infections in that year, and the blue line represents the number of deaths caused by HIV-1 infection in that year.

motor deficits, and dementia which are collectively referred to as HIV-associated neurocognitive disorders (HAND).

The first reports of HAND were described as early as the 1980's, with the only well-defined neurological complication of HIV-1 being HIV-associated dementia (HAD) (Sanmarti et al., 2014). Since this time, evidence indicates a shifting pattern of the neurocognitive impairment observed in HIV-1 patients, from deficits in motor ability, the speed of information processing, and verbal speed in the pre-cART era to deficits in memory and executive function in the post-cART era (Heaton et al., 2011). In 2007, the Frascati Criteria was introduced, which revised the HAND classification system into a spectrum of neurocognitive disorders ranging from the very mild to the most severe (Figure 1.2) (Antinori et al., 2007; Mind Exchange Working Group et al., 2013). The mildest stage of HAND, Asymptomatic Neurocognitive Impairment (ANI), affects about 33% of HIV-1 infected patients and is characterized by neuropsychological impairment in at least two cognitive domains without affecting daily living. The next level, Mild Neurocognitive Disorder (MND), affects 20-30% of HIV-1 infected patients and is defined as mild to moderate impairment in at least two cognitive domains with a disruption in activities of daily living. The most severe form, HAD, affects between 2-8% of HIV-1 infected patients and is classified by cognitive impairment in at least two cognitive domains and accompanied by significant impairment of daily living. The diagnosis of HAND emphasizes that there must be no evidence of cognitive impairment that does not have HIV-1 as the underlying cause (Mind Exchange Working Group et al., 2013).

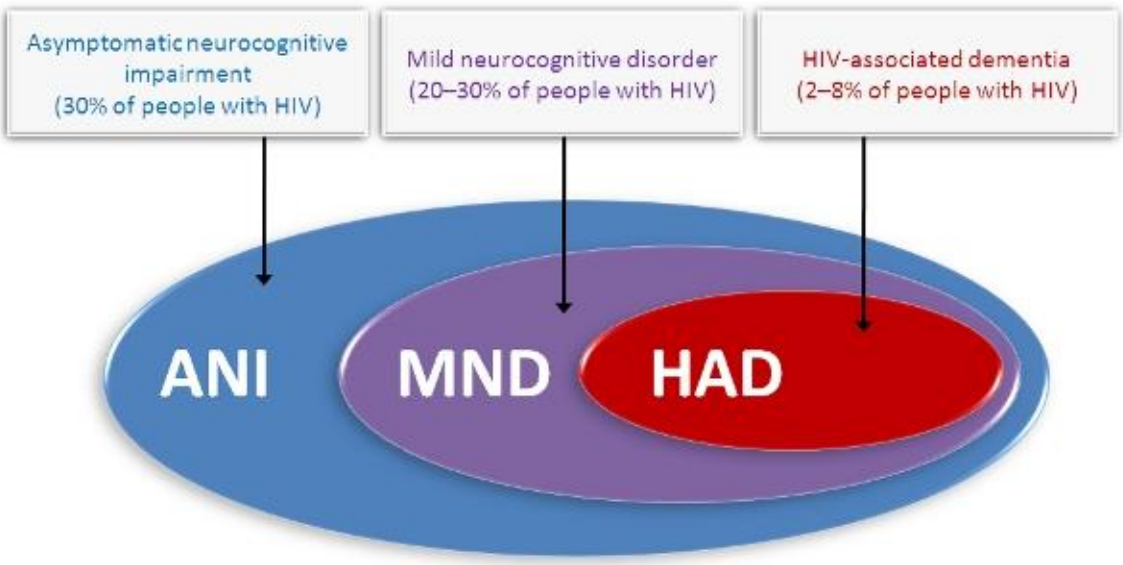

Figure 1.2 Classification of HIV-1 associated neurocognitive impairments. Asymptomatic neurocognitive impairment (ANI) and is characterized by neuropsychological impairment in at least two cognitive domains without affecting daily living. The next level, Mild Neurocognitive Disorder (MND), affects 20-30% of HIV1- infected patients and is defined as mild to moderate impairment in at least two cognitive domains with a disruption in activities of daily living. The most severe form, HAD, affects between 2-8% of HIV-1 infected patients and is classified by cognitive impairment in at least two cognitive domains and accompanied by significant impairment of daily living. Adapted from

The development of HAND results, in part, because most cART medications cannot cross the blood-brain barrier (BBB). In contrast, the HIV-1 virus is capable of bypassing the BBB by piggybacking on infected monocytes and lymphocytes that migrate into the CNS (Clements et al., 2002; Orandle et al., 2002; Williams et al., 2014), leaving it as a reservoir for HIV-1 viral replication (Gray et al., 2014). Once in the CNS, infected monocytes mature into HIV-1 infected perivascular macrophages that produce virions and facilitate the spread of the virus through production of neurotoxic viral particles, proteins, and cytokines (Albright et al., 2003; Brown et al., 2006). This production facilitates continued infection, neurotoxicity, and subsequent neuronal injury which are central to the development of HAND (Thompson et al., 2011; Desplats et al., 2013).

Because there is currently no treatment for HAND, the patient and healthcare burden of these disorders will continue to rise, as estimates have suggested that the number of HIV-1 patients with HAND will increase from 5- to 10-fold by the year 2030 (Cysique et al., 2011). Thus, novel therapeutics, which are capable of preventing HAND in the early stages of HIV-1 infection, will greatly enhance HIV-1 infected patients' quality of life as well as the economic burden on the healthcare system.

1.2.1 HIV-1 VIRAL PROTEINS

The HIV-1 virus is composed of at least nine genes which are flanked by a long terminal repeats (LTRs). These genes code for specific proteins which can be classified into three distinct categories: (1) the major structural proteins – Gag,

Pol, and Env; (2) regulatory proteins – Tat and Rev; and (3) accessory proteins – Vpu, Vpr, Vif, and Nef (Gallo et al., 1988). Each of these proteins has distinct functions which are required at various stages of the virus' life cycle.

Structural proteins

The gag gene gives rise to the 55-kilodalton Gag precursor protein (p55), which is expressed from the unspliced viral mRNA. Following post-translational modifications, the membrane-associated Gag polyprotein triggers the budding of the viral particle from the surface of an infected cell. After budding, p55 is cleaved by the virally encoded protease (a product of the pol gene) into four smaller proteins: matrix (p17) – facilitates nuclear transport of the viral genome; capsid (p24) – forms the conical core of the viral particle; nucleocapsid (p9) – recognizes packaging signals and helps in reverse transcription; and p6 – which aids in the interaction of p55 and vpr, as well as the release of viral particles from infected cells (Göttlinger et al., 1989; King, 1994; Lee et al., 2012). The Gag and Pol genes are initially expressed as a single precursor protein (p160). p160 is generated by a ribosomal frame shifting event, which is triggered by a specific cis-acting RNA motif (Parkin et al., 1992). During viral maturation, the virally encoded protease cleaves the Pol polypeptide away from Gag and further digests it into four separate enzymes: reverse transcriptase – transcribes DNA from the RNA template; RNase H – facilitates complementary DNA strand synthesis by cleaving the original RNA template; integrase – required for integration of proviral DNA into the host genome; and protease – involved with cleaving of the p55 protein (Lee et al., 2012). Env (envelope) migrates through

the Golgi complex where it undergoes glycosylation, which is required for infectivity (Capon et al., 1991). A cellular protease cleaves Env (gp160) to generate gp41 and gp120. gp41 contains the transmembrane domain of Env, and serves as an anchor for the viral envelope, while gp120 mediates HIV-1 infection through interactions with the CD4 receptor that is present on lymphocytes (King, 1994; merk and Subramaniam, 2013).

Regulatory proteins

Tat (trans-activator of transcription) is essential for HIV-1 viral replication Ruben et al., 1989) and acts as an RNA binding protein, binding to a short-stem loop structure, known as the transactivation response element (TAR), that is located at the 5' terminus of HIV RNAs (Ruben et al., 1989; Feinberg et al., 1991). The Tat protein is discussed in further detail below. Rev (regulator of expression of virion proteins) in another RNA-binding protein. Rev binds to the Rev response element (RRE) within the second intron of the HIV-1 genome and is essential to activate late genes and for the synthesis of viral proteins to produce virions (Zapp and Green, 1989; Vercruysse and Daelemans, 2014).

Accessory proteins

The accessory proteins are not absolutely required for viral replication in all *in vitro* systems but represent critical virulence factors *in vivo*. Nef, Vif, Vpr, and Vpu have multifaceted activities that are mostly involved in the evasion of innate and adaptive immune systems. Specifically, Nef and Vpu are capable of manipulating the localization and functional aspects of host cell membrane proteins, facilitating viral entry (Miller et al., 1994). Vif and Vpr protect the virus by

inhibition of cytoplasmic host defense molecules and by modifying the host cell intracellular environment. The effects of the accessory proteins greatly influence viral replication and aid the virus in escaping the host immune system.

1.2.2 HIV-1 TAT PROTEIN

Of the aforementioned HIV-1 viral proteins, the HIV-1 Tat protein has been one of the most well studied in the context of HAND pathology (Gaskill et al., 2017; Zhu et al., 2018), and the reasons for our specific focus on this viral protein are twofold. The first is that HIV-1 Tat protein has been detected in the plasma, serum, and cerebrospinal fluid (CSF) of HIV-1 infected patients (Westendorp et al., 1995; Xiao et al., 2000). The levels of HIV-1 Tat in the plasma and CSF have been reported to be in the low nanomolar range, however, the authors (Westendorp et al., 1995; Xiao et al., 2000) argued that these concentrations may be lower than the actual concentration present in the system due to the close proximity of HIV-1 infected cells in the brain (Hayashi et al., 2006). Regardless of the exact concentration of HIV-1 Tat in the CNS, the second reason for the focus on this viral protein is due to its potent neurotoxicity (Sabatier et al., 1991; King et al., 2006). Specifically, the continued presence of HIV-1 Tat in cART-treated HIV-1 patients (Johnson et al., 2013; Henderson et al., 2019) has been suggested to play a critical role in the cognitive impairment evident in HAND (Rappaport et al., 1999; King et al., 2006).

HIV-1 Tat is a small (86 amino acid) nonstructural polypeptide composed of six protein domains that are encoded by two exons (Figure 1.3). Amino acids 1-72 represent the first five domains and are encoded from the first exon, which

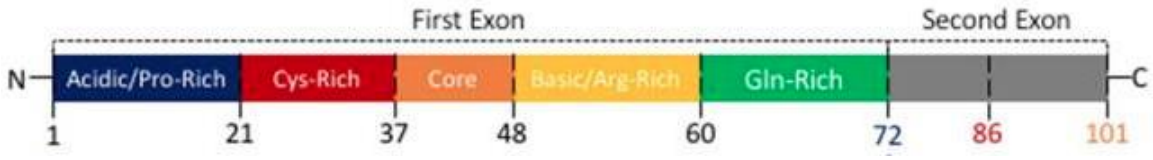

Figure 1.3 HIV-1 trans-activator of transcription protein organization. Amino acids 1-21 (blue) indicate the acidic/proline-rich domain, 22-37 (red) the cysteine-rich domain, 38-48 (orange) the hydrophobic core domain, 48-57 (yellow) the basic/arginine-rich domain, and 58-72 (green) the glutamine-rich domain. The second axon (carboxyl terminus) varies in length and can be found in both 73-86 (Tat_{1-86}) or 73-101 (Tat_{1-101}) variants. Adapted from Gaskill et al., 2017.

is critical to the transcriptional activity of HIV-1 Tat. These domains consist of an acidic domain (residues 1-21), a cysteine-rich domain (residues 22-37), the hydrophobic core domain (residues 38-48), a basic domain (residues 48-57), and a glutamine-rich domain (residues 58-72). The sixth domain is a C-terminus domain which varies in length (Bertrand et al., 2013), resulting in two HIV-1 Tat variants: the 101 amino acid variant (Tat_{1-101}), which represents the major variant isolated from HIV-1 clinical samples, and the 86 amino acid variant (Tat_{1-86}), which is primarily utilized for research purposes (Gaskill et al., 2017). Importantly, studies comparing the two variants have shown no marked differences between these types (Ma and Nath 1997; Bertrand et al., 2013; Midde et al., 2013). The studies reported in this dissertation utilized the Tat_{1-86} variant.

In the CNS HIV-1 Tat is secreted by HIV-1 infected macrophages and microglia and is subsequently absorbed into uninfected cells (Frankel and Pabo 1988; Vivès et al., 1997; Frankel and Young 1998). HIV-1 Tat has been found to have various neurotoxic effects, including but not limited to activation of dormant T-lymphocytes (Ott, 1997), induction of cellular apoptosis (Li et al., 1995; Westendorp et al., 1995), modulation of gene expression via disruption of intracellular signaling cascades (Westendorp et al., 1995; Nath and Geiger 1998; Jeang et al,. 1999), and increasing BBB permeability (Toborek et al., 2005). Furthermore, HIV-1 Tat has been detected in dopamine (DA) rich brain areas (Del Valle et al., 2000; Hudson et al., 2000; Lamers et al., 2010) and where it perturbs the dopaminergic system, which has been implicated in the neuropathology of HAND (Purohit et al., 2011; Wang et al., 2004; Gaskill et al.,

2017; Zhu et al., 2018). The effects of HIV-1 Tat on the dopaminergic system in the context of HAND is discussed in detail in the following section.

1.3 HIV-1 TAT AND THE DOPAMINERGIC SYSTEM

1.3.1 Role of dopamine in the central nervous system

Dopamine (DA) plays a crucial role in multiple CNS functions, including but not limited to motor control, reward, cognition, executive function, and maternal behavior (Beaulieu and Gainetdinov, 2011; Klanker et al., 2013; Nieoullon, 2002; Nutt et al., 2015). The majority of DA neurotransmission occurs within four known pathways: the nigrostriatal pathway, the tuberoinfundinbular pathway, and the mesolimbic and mesocortical pathways. This dissertation focuses primarily on brain regions which are involved in the mesolimbic and mesocortical pathways (the prefrontal cortex (PFC) and striatum), as these pathways are frequently associated with reward-related cognition and executive functions (Ikemoto, 2010), which are often affected in HAND. In the CNS, DA is synthesized in dopaminergic and adrenergic neuron terminals, where the conversion of L-tyrosine to L-DOPA, the precursor of DA, by tyrosine hydroxylase is the rate-limiting step (Flatmark, 2000; Hornykiewicz, 2002). Once synthesized, DA can be released via two distinct mechanisms, classical vesicular release and DA transporter (DAT)- mediated efflux (Goodwin et al., 2009; Wall et al., 1995). Following release, DA may either bind to post-synaptic receptors, be metabolized, or, most frequently, be transported back into the pre-synaptic terminal via DAT-mediated reuptake (Figure 1.4) (Eisenhofer et al., 2004). Importantly, DA may also be transporter back into the pre-synaptic terminal by

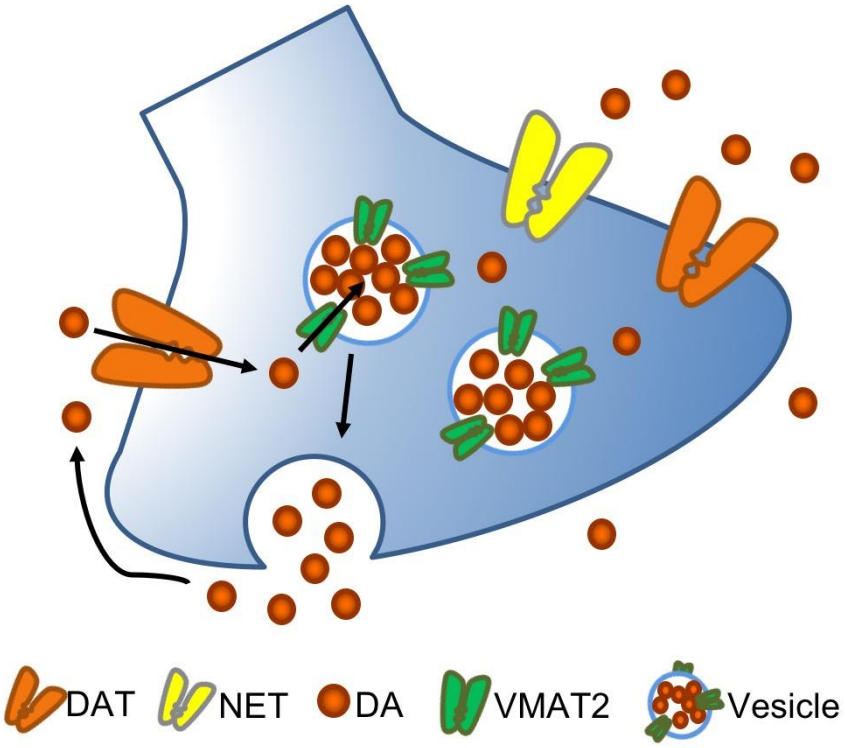

Figure 1.4 Representation of pre-synaptic dopaminergic terminal. In the pre-synaptic terminal dopamine (DA) can is stored in synaptic vesicles which, upon action potential firing, are released into the synaptic cleft. In the synaptic cleft DA can either bind to post-synaptic receptors, be metabolized by enzymes or glia cells, or, most frequently, be transported back into the pre-synaptic cytosol by the dopamine (DAT) or norepinephrine (NET) transporters. Once in the pre-synaptic cytosol, DA is repackaged into synaptic vesicles via the vesicular monoamine transporter (VMAT-2).

the norepinephrine (NE) transporter (NET), in brain areas with low levels of DAT expression, particularly the PFC (Morón et al., 2002). The specific effects of HIV-1 on transporter function are discussed in detail in section 1.5 of this dissertation.

1.3.2 HIV-1 Tat and dopaminergic neurotransmission

HIV-1 Tat has been shown to be neurotoxic to a wide variety of components of the CNS, each of which may play a role in the development of HAND symptoms. However, due the strong evidence linking HIV-1 to dysregulation of the dopaminergic system, and the evident impact of this dysregulation in the development of HAND, this dissertation focuses solely on the effects of HIV-1 on the dopaminergic system, although future studies investigation the effects of HIV-1 Tat on other CNS systems will be beneficial to uncover alternate potential mechanisms of this viral protein in the pathology of HAND.

Studies utilizing both human subjects and animal models have demonstrated that HIV-1-mediated damage to the dopaminergic system occurs early in HIV-1 infection, often while patients are still asymptomatic (Lopez et al., 1999; Koutsilieri et al, 2002b; Scheller et al., 2005). This damage has been identified in both cART naïve (Kieburtz et al., 1991; Berger et al., 1994; Sardar et al., 1996) and cART treated patients (Kumar et al., 2009, 2011; Scheller et al., 2010; Horn et al., 2013), highlighting the pressing need to address these pathologic observations. *In vitro* studies have found that increased levels of DA may enhance viral replication in infected lymphocytes and macrophages (Scheller et al., 2000; Koutsilieri et al., 2002), promoting oxidative stress which

subsequently causes neuronal death. This effect creates a vicious cycle by which dopaminergic dysfunction spurs greater infection, thereby enhancing dopaminergic damage (Gaskill et al., 2017). As noted in the previous section, there are multiple connections of dopaminergic neurons in throughout the brain, with the striatum, ventral tegmental area (VTA), and PFC representing the most clinically relevant regions. Interestingly, despite resembling each other in many respects, dopaminergic neurons in these regions mediate distinct functions and exhibit dissimilar responses to toxins and addictive agents (Choi et al., 2015; Teo et al., 2004). It is currently unclear whether HIV-1 Tat protein differentially affects these distinct regions, and this topic has been of particular interest in the context of HIV-1 infection. For example, a recent study found that HIV-1 Tat expression in a mouse model produced excitatory effects in medial prefrontal cortical pyramidal neurons but was inhibitory in hippocampal pyramidal neurons (Cirino et al., 2020). This selective vulnerability has also been found in the dopaminergic system, where HIV-1 Tat exposure selectively decreased tyrosine hydroxylase immunoreactivity in the substantia nigra but not in the VTA (Miller et al., 2018). Studies such as this highlight the need for region-specific investigations into the effects of HIV-1 Tat on the CNS, which may aid in identifying the underlying molecular mechanisms of disease-related pathology.

The neurotoxic effects of HIV-1 Tat were first described using neuroblastoma cells (Sabatier et al., 1991), which, although these cells are not dopaminergic, provided an initial picture of the interaction between HIV-1 Tat and neurons. Specifically, studies utilizing HIV-1 Tat exposed cultured human fetal

neurons and microinjection of HIV-1 Tat into striatal neurons demonstrated that HIV-1 Tat promotes neurotoxicity by triggering inflammatory cascades that eventually induce neuronal death by apoptosis (New et al., 1997; Jones et al., 1998; Zauli et al., 2000; Aksenov et al., 2001). Moreover, direct application of HIV-1 Tat on dopaminergic neurons increases intracellular calcium levels, thereby activating caspases and the subsequent generation of reactive oxygen species (Kruman et al., 1998; Bonavia et al., 2001; Haughey and Mattson, 2002; Mattson et al., 2005). Furthermore, an *in vivo* microdialysis study found compromised DA levels in the striatum of HIV-1 Tat treated animals (Ferris et al., 2009b) and HIV-1 Tat protein contributes to alterations in expression levels of dopaminergic markers including tyrosine hydroxylase and dopamine receptor-1 (Zauli et al., 2000; Silvers et al., 2006; Silvers et al., 2007). As HIV-1 Tat has been detected in DA-rich brain areas (Del Valle et al., 2000; Hudson et al., 2000; Lamers et al., 2010), and antibodies against HIV-1 Tat have been found to inversely correlate with HAND progression (Bachani et al., 2013), continued investigation into the precise molecular mechanisms resulting in the aforementioned neurotoxic effects of HIV-1 Tat on the dopaminergic system are critical to the development of novel therapeutics which may prevent or delay HAND progression.

1.3.3 Animal models of HAND

To understand the onset of disease related neuropathology and progression, as well as to develop and test adjunctive therapies along with antiretroviral drugs, animal models for HAND have proven extremely useful.

Ideally, non-human primates such as chimpanzees would be utilized to mimic HIV-1 infection and disease given their genetic similarity to humans (Van Maanen and Sutton, 2003). However, due to financial considerations, maintenance, difficulty in obtaining sufficient numbers to achieve statistically significant outcomes and public apprehensions, their use has been limited in HAND research. In contrast, rodent models have been extensively utilized to study HIV-1 and associated neurologic dysfunction in spite of the challenges to model disease associated with the species-specific nature of HIV-1 infection. These models offer several advantages such as low cost, easy maintenance, and a well characterized genome that can be exploited to alter a particular cell or region of interest (Gorantla et al., 2012). These models have been created by employing several approaches including stereotaxic injection of viral proteins directly into the brain, expressing viral transgenes in animals, and transplantation of infected human cells into immunodeficient rodents (Van Duyne et al., 2009; Barreto et al., 2014).

One specific rodent model which has been utilized is the HIV-1 transgenic (HIV-1 Tg) rat, which was developed by Reid et al., (2001). This model is derived from the Fisher344/ BHsd rat strain and carry proviral DNA that is devoid of Gag and Pol genes, making this model noninfectious. These mice display immune, motor, and behavioral abnormalities similar to HAND patients (Reid et al., 2001). Deficits in learning and cognition associated with asymptomatic HIV-1 infection have been reported in these animals (Vigorito et al., 2007; Lashomb et al., 2009). Furthermore, these animals demonstrate alterations in dopaminergic function,

neuroinflammation, as well as deficits in several synaptic proteins (Persidsky and Fox, 2007; Webb et al., 2010; Rao et al., 2011; Zhu et al., 2016). Despite the utility of this model in the study of HAND neuropathology, it does have several drawbacks. First, because this model expresses seven HIV-1 viral proteins, it is impossible to determine the specific mechanisms of a single viral protein, and second, because the viral proteins are expressed from birth it does not allow for the determination of dose- and duration-dependent effects of these viral proteins. Thus, while the HIV-1 Tg rat model allows for investigation of the overarching neuropathological alterations observed in HAND, models which allow for precise and controlled expression of single viral proteins may prove more useful in discovering the precise mechanisms underlying HAND neuropathology.

One such model is the inducible HIV-1 Tat transgenic mouse model (iTat-tg) which was first described by Kim et al., (2003), and is utilized in chapters 3 and 4 of this dissertation. This model possesses a “tetracycline-on (TETON)” promoter that becomes transcriptionally active when a tetracycline (in this case doxycycline, Dox) is present. In these mice the TETON promoter is coupled to an HIV-1 Tat protein coding gene, and thus HIV-1 Tat expression may be induced by the administration of Dox. This TETON/HIV-1 Tat system is integrated into the regulator for the astrocyte-specific glial fibrillary acidic protein (GFAP) promoter, which confers brain specific expression of HIV-1 Tat protein. Importantly, although inducible expression of HIV-1 Tat in this model is not equivalent to human HIV-1 infection and does not induce the same host response, this model recapitulates many aspects of the neuropathologies and neurocognitive

impairments observed in HIV-1 infected individuals (Kim et al., 2003). Specifically, these mice demonstrate learning and memory impairments (Carey et al., 2012), increased anxiety-like behavior (Paris et al., 2013), gray matter density reductions (Carey et al., 2013), and altered cocaine-mediated psychostimulation (Paris et al., 2014). Due to the potential for precise and controlled expression of HIV-1 Tat protein in this model (Carey et al., 2012) it offers specific advantages to investigate the precise molecular mechanisms underlying HIV-1 Tat-mediated dysregulation of the dopaminergic system.

1.4 THE DOPAMINE AND NOREPINEPHRINE TRANSPORTERS

1.4.1 The neurotransmitter: sodium symporter family

Neurotransmitter: sodium symporters (NSSs) play an essential role in the nervous system by terminating synaptic transmission and recycling neurotransmitters for reuse (Rudnick, 2002). NSSs are members of the solute carrier 6 (SLC6) family of transporters including the DA, NE, serotonin, and GABA transporters and are comprised of around 600-800 amino acids in their primary sequence. These transporters possess 12 transmembrane (TM) helices which display significant sequence identities (~50-70%) even amongst NSSs that transport diverse substrates (Kristensen et al., 2011). Intracellular amino and carboxyl termini help to control uptake and substrate recognition via multiple putative post-translational modification sites (Foster et al., 2002; Fog et al., 2006; Wu et al., 2015), although the variations in amino acid sequence between transporters does result in distinct properties (Wang et al., 2015). NSSs are secondary active transporters that utilize the Na^+ gradient across the plasma

membrane to catalyze the uptake of a variety of neurotransmitters from the extracellular milieu against their concentration gradient in a cotransport mechanism (Torres et al., 2003). Active substrate translocation follows an alternating access model (Jardetzky, 1966; Yamashita et al., 2005). This model suggests that substrate translocation is a dynamic process which requires conformational transition between an outward, occluded, and inward facing states.

Both the DA and NE transporters are capable of translocating DA in distinct brain regions, and therefore spatial and temporal modulation of DA signaling in the brain is dependent upon regulation of both of these transporters. DAT- and NET-mediated behavioral and physiological function are dynamically controlled by a variety of signaling cascades, macromolecules, and exogenous factors (Joseph et al., 2019). Despite the lack of a complete understanding of DAT and NET regulation in the CNS, a multitude of research suggests that affecting molecules achieve their function through ligand-transporter interactions, trafficking, post-translational modifications, and protein-protein interactions (Navratna et al., 2018). For example, several studies have implied that synthetic compounds like N-(3,3-diphenylpropyl)-2-phenyl-4-quinazolinamine (SoRI-20041) as well as point mutations at specific residues on the DAT cause subtle alterations in transporter conformation which in turn have differential effects on inward transport and efflux properties (Guptaroy et al., 2009; Rothman et al., 2009). For the purposes of this dissertation, I will focus specifically on the

allosteric regulatory mechanism which is relevant to the interaction between HIV-1 Tat protein and the DA and NE transporters.

1.4.2 Allosteric dependent regulation

Molecular dynamics and simulation studies provided initial evidence for the existence of an allosteric binding site for DA, a modulatory binding site on the transporter that is topographically distinct from the primary binding site (Shi et al., 2008; Shan et al., 2011). These studies suggest that direct interaction of ligands and ions at allosteric binding sites may elicit progressive rearrangements in transporter structure, shifting the conformational state in order to transport substrate DA. Although the discovery of biological ligands which interact with this allosteric site remain elusive, DAT/NET ligands including tricyclic antidepressants and selective reuptake inhibitors have been shown to interact with this allosteric binding site (Zhou et al., 2007; Zhou et al., 2009; Cheng and Bahar, 2019). Synthetic compounds which interact with allosteric binding sites have also been developed (Pariser et al., 2008). The synthetic compounds utilized in this study (including SoRI-20041) inhibit the binding of [^{125}I]3beta-(4'-iodophenyl) tropan-2beta-carboxylic acid methyl ester ([^{125}I]RTI-55) to the substrate binding site by following allosteric inhibitory patterns. This was indicated by the finding that these synthetic compounds do not follow the classical dose-dependent competitive inhibition paradigm irrespective of the concentration of [^{125}I]RTI-55. These modulators also slowed the dissociation rate of pre-bound [^{125}I]RTI-55 and presented a decrease in B_{max} and an increase in K_d values for [^{125}I]RTI-55 binding, verifying the allosteric binding of these 4-quinazolinamine derivatives.

Taken together, these findings demonstrate that various ligands may allosterically modulate local rearrangements in the structural elements of NSS transporters, which ultimately contribute to a functionally unique conformation of the transporter.

1.5 HIV-1 TAT AND DOPAMINE TRANSPORTER FUNCTION

Within the last decade there has been significant interest in describing the effects of HIV-1 Tat on DAT activity (Midde et al., 2013, 2015; Zhu et al., 2016; Yuan et al., 2015a, 2016; Bucci, 2015). While these and other recent studies suggest HIV-1 Tat may modulate DAT function, technical limitations such as the lack of available HIV-1 Tat specific antibodies and the large amount of HIV-1 Tat used in the studies limits interpretation (Gaskill et al., 2017). Despite these limitations, these studies suggest the effects of HIV-1 infection on the dopaminergic system may, at least in part, be mediated by HIV-1 Tat specific effects on DAT function (Figure 1.5) (Chang et al., 2008; Maragos et al., 2003; Perry et al., 2010; Wang et al., 2004). HIV-1 infected patients with dementia have decreased DAT levels compared to both healthy controls as well as those with HIV who do not have dementia (Wang et al., 2004). Specifically, the loss of DAT molecules is most apparent in the caudate and putamen, similar to Parkinson's disease and other frontal-striatal pathologies (Itoh et al., 2000). Several studies have reported that HIV-1 Tat, in the absence of viral replication, may negatively affect dopamine transmission by targeting DAT activity, without affecting total DAT levels in striatal homogenates (Aksenova et al., 2006; Wallace et al., 2006; Zhu et al., 2009), although changes in cellular distribution of DAT were not

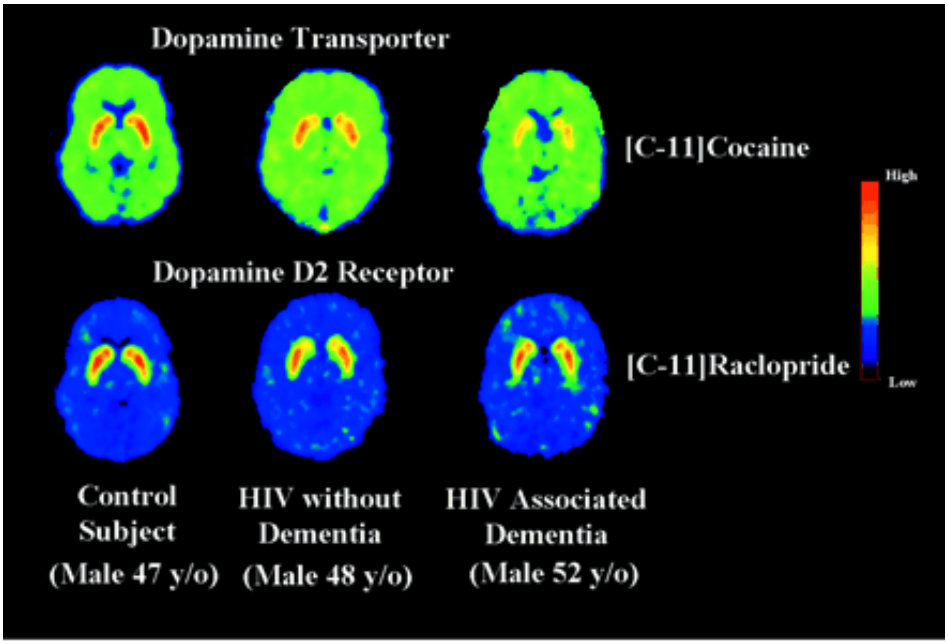

Figure 1.5 Dopamine transporter and receptor expression in the context of HIV-1 associated dementia. Distribution volume ratio images of PET with [C^{11}]cocaine (dopamine transporter, top row) and [C^{11}]raclopride (dopamine receptor, bottom row) in a 47-year-old control subject (left), a 48-year-old no dementia subject (middle), and a 52-year-old HAD subject (middle), at the level of the basal ganglia. The images are scaled with respect to the maximum value obtained in the control subject and presented using the rainbow scale (red color = high value, violet = low value). Adapted from Wang et al., 2004.

examined in these studies. A study by Midde et al., (2012) examined this phenomenon and suggested that HIV-1 Tat may induce DAT internalization via a protein kinase C (PKC) dependent mechanism. Furthermore, given the relatively high percentage of HIV-1 infected patients who abuse psychostimulants (Beyrer et al., 2010; Mathers et al., 2008), and that these psychostimulants may impact DAT trafficking (Holton et al., 2005; Hong and Amara, 2013; Mortenson et al., 2008), a careful critical mechanistic information on how HIV-1 Tat regulates dopamine neurotransmission.

Surface plasmon resonance analysis performed in rat striatal synaptosomes suggests that HIV-1 Tat directly interacts with DAT in a concentration-dependent manner (Zhu et al., 2009). Further investigation into this interaction using a computational modeling and experimental validation approach has aided in characterization of the direct allosteric interaction between HIV-1 Tat and DAT (Midde et al., 2013; 2015a; Yuan et al., 2015; Yuan et al., 2016; Quizon et al., 2016; Sun et al., 2019). These studies suggest HIV-1 Tat may stabilize the inward facing conformation of DAT, limiting the availability of extracellular DA binding sites on the transporter, thereby attenuating DA uptake.

1.6 RESEARCH OBJECTIVES

The overarching hypothesis of this dissertation was that *via direct inhibitory allosteric interactions with the dopamine and norepinephrine transporters, the HIV-1 Tat protein dysregulates dopamine homeostasis, resulting in the neuropsychiatric dysfunction prominently featured in HAND.*

Chapter 2 builds upon previous work demonstrating that HIV-1 Tat inhibits DAT-mediated DA uptake via a direct allosteric interaction with specific residues on the DAT. Due to the high level of homology between the DA and NE transporters, including that several of the residues determined to be involved in the HIV-1 Tat/DAT interaction are identical between DAT and NET, I hypothesized that the inhibitory interaction between HIV-1 Tat and DAT extends to the NET. I investigated this hypothesis by performing a single point mutation at Tyrosine467 (Y467) on the NET to a phenylalanine (Y467F) or a histidine (Y467H). These mutants were evaluated to determine their effects on the functional and kinetic properties of the NET as well as for their potential role in the HIV-1 Tat/NET interaction.

Chapter 3 utilized the inducible HIV-1 Tat transgenic mouse model (iTat-tg) which was described earlier in this chapter. The primary objective of the research outlined in chapter 3 was to determine if the inhibitory effects of HIV-1 Tat on DAT and NET function could be replicated in an *in vivo* model of HAND. Furthermore, we sought to determine if this inhibition would result in global aberrations in the dopaminergic system, or if the effects of HIV-1 Tat on the dopamine system would be observed in a region-specific manner.

Chapter 4 utilized an approach that combined previous *in vitro* findings as well as those identified in Chapter 3 to determine what affect attenuation of HIV-1 Tat mediated inhibition of DAT function would have on behavioral outcomes associated with HAND. To this end, a mutant DAT mouse model was generated which possesses a Tyrosine88 to phenylalanine mutation (Y88F). This mutation

was previously shown to attenuate the inhibitory effects of HIV-1 Tat on DAT *in vitro*. These mice were evaluated to determine if this mutation had any effects on basal transporter function or behavior. Finally, the Y88F DAT mutant mice were crossed with the iTat-tg mice, allowing the Y88F DAT mutant mice to biologically express HIV-1 Tat. We investigated the effects of the Y88F DAT mutation on the findings reported in Chapter 3, as well as on previously reported cognitive deficits observed in the iTat-tg mice.

Overall, the research outlined in this dissertation aims to clarify the mechanism and role of HIV-1 Tat-mediated dysregulation of the dopaminergic system in the context of HIV-1 associated neurocognitive disorders, with the ultimate goal of providing novel therapeutic targets for the treatment of this condition.

CHAPTER 2

HIV-1 TAT-INDUCED INHIBITION OF DOPAMINE TRANSPORT BY THE HUMAN NOREPINEPHRINE TRANSPORTER IS ATTENUATED BY TYROSINE-467 MUTATIONS[1]

[1] Strauss, M., Quizon, P.M., Davis S.E., Yuan, Y., Martinez-Muniz, G., Porter, K.D., Zhan, C., & Zhu, J (2020). HIV-1 Tat-induced inhibition of dopamine transport by the human norepinephrine transporter is attenuated by tyrosine-467 mutations. *In preparation for submission to The Journal of NeuroImmune Pharmacology.*

ABSTRACT: The HIV-1 Tat protein is capable of disrupting normal dopaminergic transmission, which has been implicated as a central factor in the development of HIV-1 associated neurocognitive disorders. We have previously demonstrated that HIV-1 Tat inhibits dopamine (DA) re-uptake through the human DA transporter (hDAT) by interacting with specific residues on hDAT, including tyrosine470. Based on computational modeling and simulations, we predicted that HIV-1 Tat may also inhibit the human norepinephrine (NE) transporter (hNET) by interacting with a similar residue on hNET, tyrosine467. Thus, the current study sought to examine the effects of mutating NET tyrosine467 to a histidine (Y467H) or a phenylalanine (Y467F). Compared to wild type hNET (WT hNET), Y467F displayed an 85% increase in the K_m of [^{3}H]NE uptake, while no other changes were observed in the V_{max} or K_m of [^{3}H]DA or [^{3}H]NE uptake, or surface expression of hNET. The B_{max} or K_d of [^{3}H]WIN 35,428 binding was not altered in either mutant, although the B_{max} of [^{3}H]Nisoxetine binding for Y467H was decreased by 30% compared to WT hNET, with no observed differences in K_d. Additionally, the affinity of nisoxetine to inhibit [3H]DA uptake was increased by 40% in Y467H compared to WT hNET, with no other alterations in inhibitory activity for DA, nisoxetine, or cocaine observed for [^{3}H]DA or [^{3}H]NE uptake. Both Y467H and Y467F were able to attenuate the Tat-induced inhibition in [^{3}H]DA uptake, providing mechanistic insight for the development of novel small molecules which may attenuate the Tat/DAT and Tat/NET interaction.

GRAPHICAL ABSTRACT

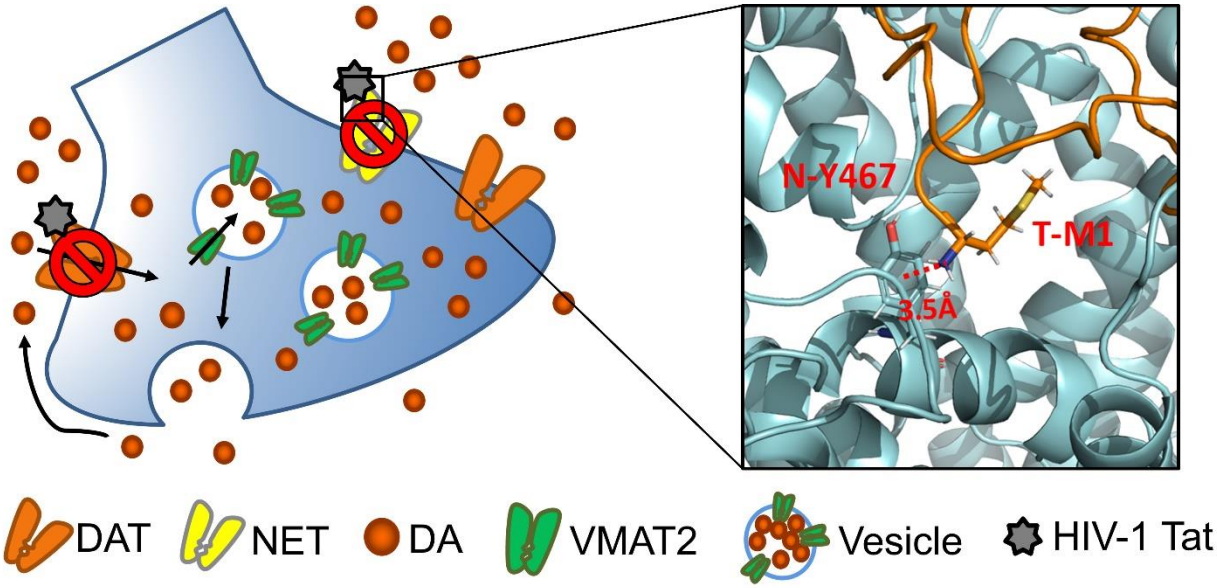

HIV-1 Tat inhibits dopamine uptake through human norepinephrine (hNET) transporter on the presynaptic terminal via a direct allosteric interaction. hNET Tyrosine 467 is predicted to have a cation-π interaction with HIV-1 Tat Methionine 1. Mutating Tyrosine 467 to Histidine or Phenylalanine attenuates this inhibitory effect by disrupting the Tat-hNET interaction.

2.1 INTRODUCTION

Despite the success of combinatorial antiretroviral therapy (cART) in controlling peripheral HIV infection and improving the lives of HIV patients, roughly 50% of the 38 million HIV-positive patients (HIV.gov) will develop neurological complications including cognitive dysfunction, motor deficits, and dementia collectively referred to as HIV-associated neurocognitive disorders (HAND; Heaton et al., 2010). Most cART medications cannot cross the blood-brain barrier, while infected macrophages carrying the virus can (Buckner et al., 2006), allowing the CNS to serve as an HIV-viral reservoir (Brack-Werner, 1999; Marban et al., 2016). The replication and expression of viral proteins in the CNS

is associated with the persistence of HIV-related neuropathology and subsequent neurocognitive deficits (Brack-Werner, 1999; Frankel and Young, 1998, Johnston et al., 2001; Power et al., 1998) and is central to the development of HAND (Gaskill et al., 2009). Specifically, the continuing presence of the transactivator of transcription (Tat) protein in cART-treated HIV patients (Johnson et al., 2013) may play a crucial role in the neurotoxicity and cognitive impairment evident in HAND (King et al., 2006; Rappaport et al., 1999). Considering long-term viral protein exposure can accelerate damage to the mesocorticolimbic dopamine (DA) system (Nath et al., 1987; Berger and Arendt, 2000; Koutsilieri et al., 2002), and HIV-1 Tat has been detected in DA-rich brain areas (Del Valle et al., 2000; Hudson et al., 2000; Lamers et al., 2010), defining the molecular mechanism(s) by which HIV-1 Tat impairs the DA system and affects the progression of HAND may provide valuable insight into the development of novel therapies for this population.

Converging lines of clinical observations, supported by imaging (Chang et al., 2008; Wang et al., 2004), neuropsychological performance testing (Kumar et al., 2011; Meade et al., 2011), and postmortem examinations (Gelman et al., 2012), have demonstrated that DA dysregulation is correlated with the abnormal neurocognitive function observed in HAND. Exposure to viral proteins may lead to elevated DA and decreased DA turnover in the early stages of HIV-infection (Scheller et al., 2010), while long-lasting exposure results in a dopamine transporter (DAT) deficit that potentiates HAND severity and accelerates its progress (Purohit et al., 2011; Chang et al., 2008; Wang et al., 2004). DA

transporter (DAT)-mediated DA re-uptake is critical for maintaining normal DA homeostasis, and our previously published work has demonstrated that exogenous application of recombinant HIV-1 Tat_{1-86} protein decreases DAT activity in cells (Midde et al., 2013; Midde et al., 2015; Quizon et al., 2016) and rat brain synaptosomes (Zhu et al., 2009b) via a direct allosteric mechanism (Yuan et al., 2015; Yuan et al., 2016).

In addition to the DAT, the norepinephrine transporter (NET) may also participate in DA re-uptake in brain regions with relatively low levels of DAT expression, particularly the prefrontal cortex (Moron et al., 2002; Masana et al., 2011; Devoto & Flore, 2006), a brain area underlying many of the cognitive capabilities frequently affected in HAND. Our previous work on the DAT has utilized a computational modeling and experimental validation approach to determine the key residues on the DAT which are involved in the Tat/DAT interaction. For example, we determined that a single point mutation of DAT at tyrosine470 (to a histidine, Y470H) alters basal DA uptake but attenuated the inhibitory effects of HIV-1 Tat_{1-86} on DA transport (Midde et al., 2013). Importantly, the NET displays identical residues to those which we have identified as being critical to the Tat/DAT interaction (Yuan et al., 2016), one of which is DAT-Tyr470, which aligns with NET-Tyr467. To the best of our knowledge, the mechanism(s) of Tat interacting with NET has been heretofore unexplored. In the present study, we mutated NET-Tyr467 to either a histidine (Y470H) or a phenylalanine (Y470F) in order to determine the role of this residue in basal DA transport and the Tat/NET interaction. Ultimately, identifying specific

binding sites which are similar between Tat/DAT and Tat/NET and their respective roles in the DA transport process may be beneficial to attenuating the inhibitory effect of Tat on dopaminergic transmission by providing a molecular basis for the development of novel compounds, which may serve as an early intervention strategy in HIV-1 infection.

2.2 MATERIALS AND METHODS

2.2.1 *Predicting the interaction site between hNET and HIV-1 Tat*

The complex structure of hNET binding with HIV-1 Tat was constructed based on our previous reported hDAT/Tat complex structure (Yuan et al., 2015) via homology modelling. Sequence alignment among three major monoamine transporters was performed by using PROMALS3D server (http://prodata.swmed.edu/promals3d/; Pei et al., 2008) on the amino acid sequences of the human norepinephrine transporter (NET, accession number as P23975 in protein sequence database of UniProt (Yuan 2011), the human DAT (hDAT, accession number of Q01959), and the human serotonin transporter (SERT, accession number as P31645). The Modeller module of Discovery Studio 2.5 (Studio, D. 2009) was used to build the structure of hNET/Tat complex with using the structure of hDAT/Tat complex as template. 1ns backbone-restrained MD simulations were performed on the energy-minimized hNET/Tat complex at the physiological environment.

2.2.2 Construction of Plasmids

The Tyr467 mutation was chosen based on predictions of computational modeling and simulations (Figure 2.1) and our previous studies investigating a

homologous residue (Tyr 470) on the dopamine transporter (Midde et al., 2013; Midde et al., 2015; Yuan et al., 2016; Yuan et al., 2015). Mutation of Tyr467 to Histidine (Y467H) or Phenylalanine (Y467F) is expected to abolish a critical hydrogen bond between hNET and HIV-1 Tat. The 467H and 467F mutations were generated based on the wild type hNET (WT hNET) sequence (NCBI, cDNA clone MGC: 190603 IMAGE: 100062757) by site-directed mutagenesis. Synthetic cDNA encoding hNET subcloned into pcDNA3.1+ was used as a template to generate mutants using the QuikChange™ site-directed mutagenesis Kit (Agilent Tech, Santa Clara CA). The sequences of the mutant constructs were confirmed at the University of South Carolina EnGenCore facility. DNA plasmids were propagated and purified using a Qiagen Plasmid Maxi Kit (Valencia, CA).

2.2.3 Cell culture and DNA transfection

Rat pheochromocytoma cells (PC12 cells, CRL-1721, American Type Culture Collection (ATCC), Manassas, VA), which were maintained in Dulbecco's modified eagle medium (DMEM, Life Technologies, Carlsbad, CA) and supplemented with 15% horse serum, 2.5% bovine calf serum, 2 mM glutamine and antibiotics, 100 U/mL penicillin and 100 µg/mL streptomycin. Cells were cultured at 37 °C in a 5% CO_2 incubator. For the intact cell experiments, once cells grew to 100% confluence on 10 cm plates they were seeded at a density of 1×10^5 cells/cm^2 in 24-well plates and transfected with 0.8 µg of WT hNET, Y467H, or Y467F plasmid DNA per well using Lipofectamine 2000 (Life Technologies) 24 hours after seeding. Intact cells seeded in 24-well plates were used for experiments 24 hours following transfection. For cell suspension assays,

100% confluent 10 cm plates were transfected with 24 μg of WT hNET, Y467H, or Y467F plasmid DNA using Lipofectamine 2000 (Life Technologies) and used for experiments 24 hours later.

2.2.4 [^{3}H]Dopamine and [^{3}H]Norepinephrine uptake assays

The maximal velocity (V_{max}) and Michaelis-Menton constant (K_m) of [^{3}H]Dopamine ([^{3}H]DA) or [^{3}H]Norepinephrine ([^{3}H]NE) uptake was evaluated in PC12 cells transfected with WT, Y467H, or Y467F hNET using a procedure modified from our previous reports (Sun et al., 2019; Sun et al., 2017; Midde et al., 2013). 24 hours following transfection, intact cells in 24-well plates were washed twice with Krebs-Ringer-HEPES (KRH) buffer (final concentration in mM: 125 NaCl, 5 KCl, 1.5 $MgSO_4$, 1.25 $CaCl_2$, 1.5 KH_2PO_4, 10 D-glucose, 25 HEPES, 0.1 EDTA, 0.1 pargyline, and 0.1 L-ascorbic acid; pH 7.4). Cells were then preincubated for 10 min at room temperature in 450 μL of KRH buffer with or without 10 μM nomifensine (for [^{3}H]DA uptake) or 10 μM desipramine (for [^{3}H]NE uptake) to determine nonspecific binding. Following the 10 min incubation, cells were incubated for an additional 8 min at room temperature in the presence of one of six concentrations of unlabeled DA or NE (final concentrations 0.03-5 μM) combined with a fixed concentration of [^{3}H]DA (500,000 dpm/well, specific activity 40 Ci/mmol; PerkinElmer Life and Analytical Sciences, Boston MA) or [^{3}H]NE (500,000 dpm/well, specific activity 14.5 Ci/mmol; PerkinElmer Life and Analytical Sciences, Boston MA), respectively. Specific hNET-mediated DA or NE uptake was calculated by subtracting the non-specific uptake (in the presence of nomifensine or desipramine) from the total uptake. The reaction was terminated

by the removal of solution from the wells followed quickly by three washes with ice-cold KRH buffer. Cells were then lysed in 500 µL of 1% SDS for one hour and radioactivity was measured using a liquid scintillation counter (Tri-Carb 2900TR; PerkinElmer Life and Analytical Sciences, Waltham, MA). To determine if the Y467H or Y467F mutations alter the affinity of NET substrates or inhibitors, we performed competitive inhibition of DA or NE uptake in intact PC12 cells transfected as described above. Cells were preincubated with a series of final concentrations of DA (1 nM – 1 mM), nisoxitine (0.1 nM – 100 µM), or cocaine (1 nM – 100 µM) at room temperature for 10 min followed by an additional 8 min incubation with a fixed concentration of [^{3}H]DA (50 nM, final concentration).

To assess whether the Y467H or Y467F mutations could attenuate the inhibitory effects of HIV-1 Tat on hNET, we performed [^{3}H]DA uptake in PC12 cells transfected with WT or mutant hNET in the presence or absence of HIV-1 Tat protein. Cells were dissociated with trypsin/EDTA (0.25%/0.1%, 1 mL for each 10 cm dish), resuspended in culture medium, and incubated at room temperature for 10 min. The dissociated cells were pelleted by centrifugation at 400 × g for 5 min at 4 °C and then washed once with phosphate-buffered saline followed by additional 5 min centrifugation (400 × g, 4 °C). The resulting cell pellets were then resuspended in KRH assay buffer. The cell suspensions from WT, Y467H, or Y467F mutants were then preincubated with or without recombinant $Tat_{1–86}$ ($rTat_{1–86}$, 140 nM, final concentration, ImmunoDx, Woburn MA) at room temperature for 20 min followed by additional 8 min incubation with mixed [^{3}H]DA (50 nM, final concentration). Non-specific [^{3}H]DA uptake was

determined in the presence of 10 µM desipramine. The reaction was terminated by immediate filtration through Whatman GF/B glass filters (presoaked for 2 h with 1 mM pyrocatechol) followed by three washes with ice-cold KRH buffer containing pyrocatechol using a Brandel cell harvester (model M-48; Brandel Inc., Gaithersburg, MD). Radioactivity was determined as described above.

2.2.5 [^{3}H]WIN 35,428 and [^{3}H]Nisoxetine binding assays

Binding assays were used in order to determine the kinetic parameters (B_{max} and K_d) of [^{3}H]WIN 35,428 and [binding in PC12 cells in suspension transfected with WT, Y467H, or Y467F mutants (cell suspension preparation and transfection as described above). Following cell suspension preparation, the cell pellet was resuspended in 1 mL of binding buffer (15 mM Na2HPO4, 30 mM NaH2PO4, 122 mM NaCl, 5 mM KCl, 1 mM MgSO4, 10 mM glucose, 1 mM CaCl, and 10 nM EDTA; adapted from Zhen et al., 2012). 25 µL of cell suspension was added to tubes containing 200 µL of assay buffer with or without 10 µM desipramine (for nonspecific binding) and preincubated for 5 min at 25 °C. Following preincubation, 25 µL of one of six concentrations of unlabeled β-CFT (final concentrations 1-30 nM) combined with a fixed concentration of [^{3}H]WIN 35,428 (250,000 dpm/well, specific activity 82.9 Ci/mmol; PerkinElmer Life and Analytical Sciences, Boston MA) was added to each tube (final volume 250 µL) and incubated for an additional 15 min at 25 °C. The reaction was terminated by immediate filtration through Whatman GF/B glass filters (presoaked for 2 h with 1 mM pyrocatechol) followed by three washes with ice-cold assay buffer using a

Brandel cell harvester (model M-48; Brandel Inc., Gaithersburg, MD) and radioactivity was determined as described above.

The [^{3}H]Nisoxetine binding assays were performed identically to the [^{3}H]WIN 35,428 binding assays with the following modifications: (1) The same concentrations of unlabeled and [^{3}H]Nisoxetine (250,000 dpm/well, specific activity 82.0 Ci/mmol) were used instead of [3H]WIN 35,428, and (2) instead of being resuspended in 1 mL assay buffer, for the [3H]Nisoxetine binding assays the cells were counted after being suspended in 1 mL assay buffer, and then diluted to a concentration of 100,000 cells/ 25 µL.

2.2.6 Cell Surface Biotinylation

To determine if the hNET mutations alter NET surface expression, biotinylation assays were performed as described previously (Quizon et al., 2016). PC12 cells were cultured on 6-well plates at a density of 10^5 cells/well. 24 hours after seeding in the 6-well plates, PC12 cells were transfected with WT, Y467H, or Y467F hNET as described. Cells were incubated with 1 mL of 1.5 mg/mL of sulfo-NHS-SS biotin (Pierce, Rockford, IL) in PBS/Ca/Mg buffer (138 mM NaCl, 2.7 mM KCl, 1.5 mM KH_2PO_4, 9.6 mM Na_2HPO_4, 1 mM $MgCl_2$, and 100 nM $CaCl_2$, pH 7.3). After incubation, cells were washed 3 times with 1 mL of ice-cold PBS/Ca/Mg buffer containing 100 mM glycine and incubated for 30 min at 4 °C in the same buffer. Cells were then washed 3 times with 1 mL of ice-cold PBS/Ca/Mg buffer and then lysed by addition of 500 ml of Lysis buffer (1% Triton X-100, 10 mM Tris HCl, 150 mM NaCl, 1 mM EDTA, and 250 µM phenylmethylsulfonyl fluoride), followed by incubation and continuous shaking for

20 min at 4 °C. Cells were transferred to 1.5 mL tubes and centrifuged at 20,000 × g for 20 min. The resulting pellets were discarded, and 100 µL of the supernatants were stored at −20 °C for determination of total NET. Remaining supernatants were incubated with continuous shaking in the presence of monomeric avidin beads in Triton X-100 buffer (100 µL/tube) for 1 h at room temperature. Samples were centrifuged subsequently at 17,000 × g for 4 min at 4 °C, and supernatants (containing the non-biotinylated, intracellular protein fraction) were stored at −20 °C. Resulting pellets containing the avidin-absorbed biotinylated proteins (cell-surface fraction) were resuspended in 1 mL of 1.0% Triton X-100 buffer and centrifuged at 17,000 × g for 4 min at 4 °C, and pellets were resuspended and centrifuged twice. Final pellets consisted of the biotinylated proteins adsorbed to monomeric avidin beads. Biotinylated proteins were eluted by incubating with 50 µl of Laemmli buffer for 20 min at room temperature and stored at −20 °C for western blotting.

To obtain immunoreactive NET protein in total synaptosomal, intracellular, and cell surface fractions, samples were thawed and subjected to gel electrophoresis and western blotting. Samples were separated by 10% SDS-polyacrylamide gel electrophoresis for ~90 min at 125V. Samples were then transferred to Immobilon-P transfer membranes (0.45 µm pore size; Millipore Co., Bedford MA, USA) in transfer buffer (50 mM Tris, 250 mM glycine, 3.5 mM SDS) using a Mini Trans-Blot Electrophoretic Transfer Cell (Bio-Rad; Hercules, CA) for 90 min at 75 V. The membranes were then incubated with blocking buffer (5% milk powder in PBS containing 0.5% Tween-20) for 1 h at room temperature,

followed by incubation with mouse anti-NET (MAb tech, 17-1 monoclonal antibody, diluted 1:1,000 in blocking buffer) overnight at 4 °C. Transfer membranes were then washed three times with blocking buffer at room temperature followed by incubation with anti-mouse-HRP (Cell Signaling, catalog number 7076S diluted 1:5,000 in blocking buffer) for 1 h at room temperature. Membranes were then washed an additional three times in PBS containing 0.5% Tween-20 (Sigma-Aldrich; St. Louis, MO). Immunoreactive proteins on the transfer membranes were detected using Amersham ECL prime western blotting detection reagent (GE life sciences; Chicago, IL) and developed on Hyperfilm (GE life sciences; Chicago, IL). After detection and quantification of NET each blot was washed and re-probed with rabbit anti-Calnexin (Santa Cruz, Biotechnology, catalog number SC-11397 polyclonal antibody, diluted 1:10,000 in blocking buffer), an endoplasmic reticular protein, to monitor protein loading between all groups. Multiple autoradiographs were obtained using different exposure times, and immunoreactive bands within the linear range of detection were quantified by densitometric scanning using Scion image software. Band density measurements, expressed as relative optical density, were used to determine levels of NET in the total synaptosomal fraction, the intracellular fraction (non-biotinylated), and the cell surface fraction (biotinylated).

2.2.7 Statistical Analysis

Results are presented as mean ± SEM, and *n* represents the number of independent experiments for each experiment group. Kinetic parameters ($V_{max,}$ K_m, B_{max}, and K_d) were determined from saturation curves by nonlinear

regression analysis using a one-site model with variable slope. IC_{50} values for substrate and inhibitors for [^{3}H]DA or [^{3}H]NE uptake were determined from inhibition curves by nonlinear regression analysis using a one-site model with variable slope. For experiments involving comparisons between unpaired samples, unpaired Student's *t* test was used to assess any difference in the kinetic parameters (V_{max}, K_m, B_{max}, K_d or IC_{50}) between WT and hNET mutants; log-transformed values of IC_{50}, K_m or K_d were used for the statistical comparisons. Significant differences between samples were analyzed with separate ANOVAs followed by post-hoc tests, as indicated in the results Section of each experiment. All statistical analyses were performed using IBM SPSS Statistics version 26, and differences were considered significant at $p < 0.05$.

2.3 RESULTS

2.3.1 Computational modeling: Tyr467 and functional relevant residues of human NET

The computationally modeled NET-Tat binding mode is depicted in Figure 2.1. According to the modeled binding structure, the aromatic side chain of Y467 residue of NET has a favorable cation-π interaction with the positively charged amine group of M1 residue of Tat. Based on this computational insight, mutation of Y467 to another residue with a non-aromatic side chain should considerably weaken the favorable NET-Tat binding.

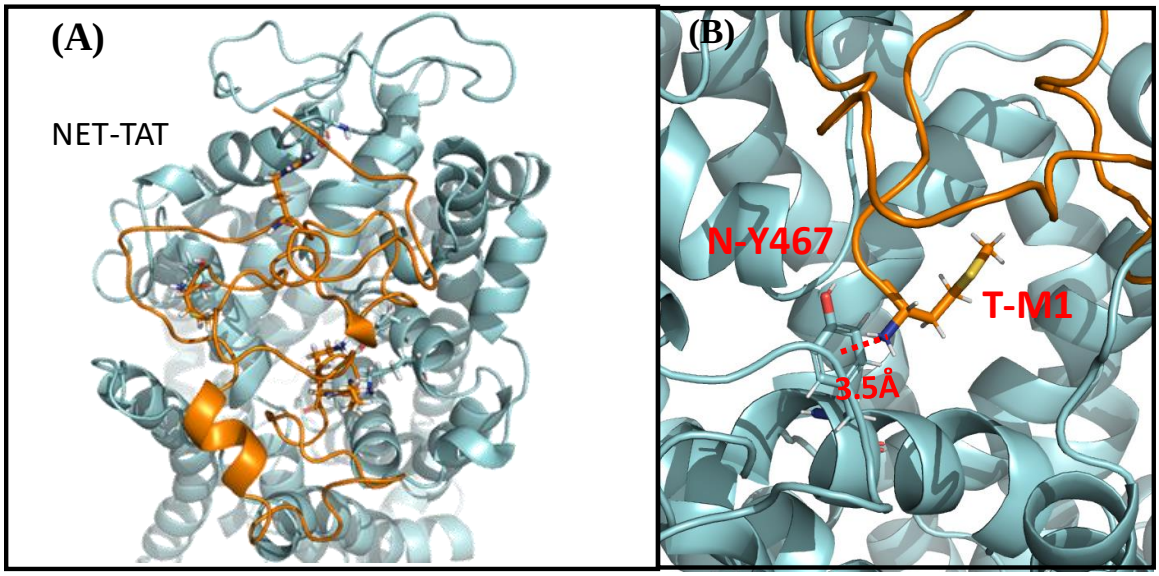

Figure 2.1 Overview of hNET/TAT complex. (A) hNET and Tat are shown in cyan and gold surface style, respectively. (B) Local view of cation- π interaction between hNET-Y467 and TAT-M1 with labeled distance.

2.3.2 Mutational effects of Tyr467 on hNET differentially influence DA or NE uptake kinetics

To determine the functional influence of Tyr467 mutations on hNET function, kinetic analysis of [^{3}H]Dopamine ([^{3}H]DA) or [^{3}H]Norepinephrine ([^{3}H]NE) uptake was performed in PC12 cells transfected with WT-, Y467A-, or Y467F-hNET. As shown in Table 2.1, compared to WT hNET (V_{max}: 57.0 ± 6.3 fmol/min/10^6 cells, K_m: 0.219 ± 0.063 μM), neither V_{max} or K_m of [^{3}H]DA uptake was altered in Y467H (V_{max}: 54.3 ± 6.7 fmol/min/10^6 cells, K_m: 0.225 ± 0.049 μM) and Y467F (V_{max}: 59.3 ± 5.2 fmol/min/10^6 cells, K_m: 0.129 ± 0.017 μM). For [^{3}H]NE uptake, no difference in V_{max} was observed among WT hNET (52.6 ± 15 fmol/min/10^6), Y467H (74.4 ± 16 fmol/min/10^6), and Y467F (86.2 ± 30 fmol/min/10^6). Compared to WT hNET (0.179 ± 0.018 μM), Km was not significantly altered in Y467H (0.596 ± 0.23 μM), but was increased in Y467F (0.332 ± 0.026 μM, [$t_{(6)} = 4.7$; $p < 0.01$, unpaired Student's *t* test]).

To determine whether mutations of Tyr467 alter subcellular distribution of NET, surface biotinylation followed by Western blot was performed. Three subcellular fractions were prepared from PC12 cells transfected with WT, Y467H, and Y467F hNET. NET immunoreactivity in both total, intracellular (non-biotinylated), and the cell surface fraction (biotinylated) were examined (Figure 2.2). No differences between WT-, Y467H- or Y467F-hNET were found in the ratio of total, nonbiotinylated or biotinylated NET to calnexin immunoreactivity, indicating that mutations of Tyr467 do not alter NET surface expression.

Table 2.1 Kinetic properties of the reuptake of [^{3}H]DA and [^{3}H]NE in PC12 cells expressing WT hNET and its mutants

	WT hNET	Y467H	Y467F
	[^{3}H]DA uptake		
V_{max} (fmol/min/10^6)	57.0 ± 6.3	54.3 ± 6.7	59.3 ± 5.2
K_m (μM)	0.219 ± 0.063	0.225 ± 0.049	0.129 ± 0.017
	[^{3}H]NE uptake		
V_{max} (fmol/min/10^6)	52.6 ± 15	74.4 ± 156	86.2 ± 30
K_m (μM)	0.179 ± 0.018	0.597 ± 0.23	0.332 ± 0.026*

*T=4.7, df = 6 p =0.0034

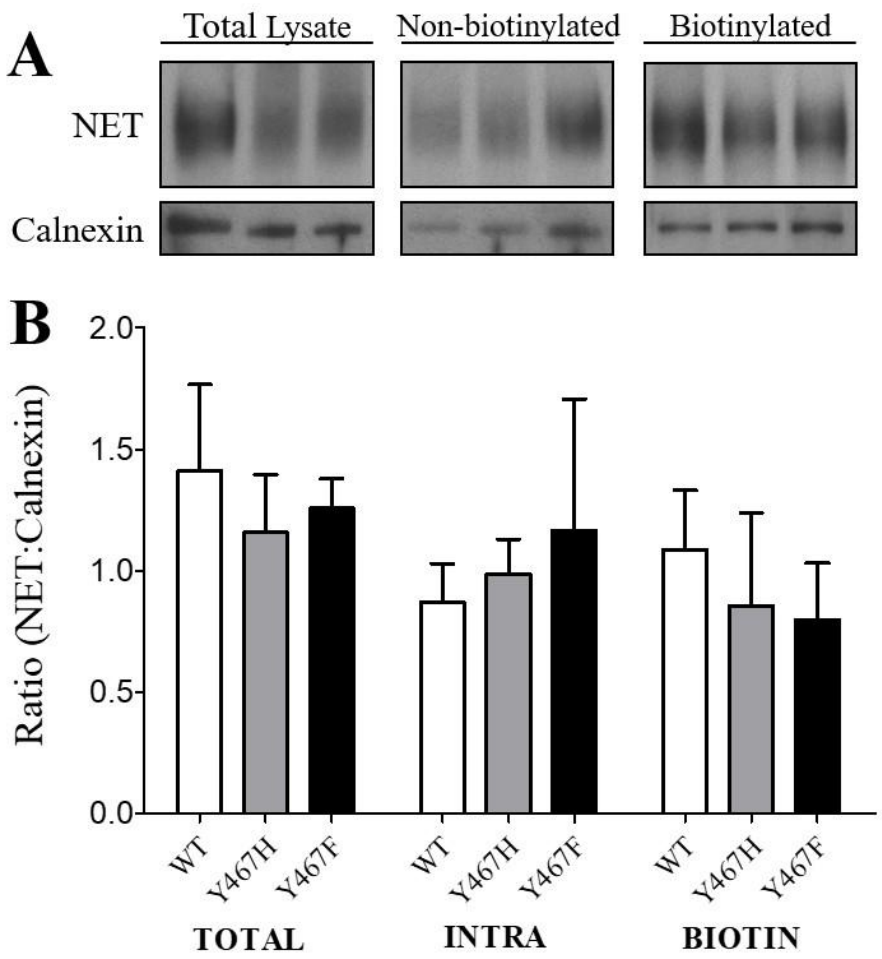

Figure 2.2 Biotinylation and Western blotting to determine cell surface expression of WT-, Y467F-, and Y467H-hNET. (A) Representative immunoreactive blots for NET and calnexin (as control protein) in total, non-biotinylated (intracellular) and biotinylated (surface expression) fractions. (B) NET immunoreactivity for total, non-biotinylated and biotinylated expression is expressed as mean ± S.E.M. densitometry units from 5 independent experiments.

2.3.3 Mutations of Tyr467 did not alter [^{3}H]WIN 35,428 or [^{3}H]Nisoxetine binding to NET

Since both WIN35,428 and Nisoxetine label different locations on hNET (Zhen et al., 2012), we examined the B_{max} and K_d values of [^{3}H]WIN 35,428 or [^{3}H]Nisoxetine to WT-, Y467H-, and Y467F-hNET. As shown in Table 2.2, compared to WT hNET (B_{max}: 0.267 ± 0.063 pmol/10^6 cells, Kd: 24.7 ± 3.1 nM), the B_{max} of [^{3}H]WIN35,428 binding was not altered in Y467H (B_{max}: 0.209 ± 0.034 pmol/10^6 cells) or Y467F (B_{max}: 0.322 ± 0.078 pmol/10^6 cells). The K_d value was not altered in Y467H (31.0 ± 3.1 nM), however it was increased in Y467F (34.2 ± 1.9 nM,[$t_{(6)}$ = 2.5; p < 0.05, unpaired Student's t test]).For [^{3}H]Nisoxetine binding (Table 2.2), compared to WT hNET (0.261 ± 0.023 pmol/10^6 cells), the B_{max} value was decreased in Y467H (0.183 ± 0.019 pmol/10^6 cells, [$t_{(9)}$ = 2.5; p < 0.05, unpaired Student's t test]) but not altered in Y467F (0.273 ± 0.031 pmol/10^6 cells). Additionally, no changes to the K_d value of [^{3}H]Nisoxetine binding were found between WT hNET (8.86 ± 1.0 nM) and Y467H (9.43 ± 1.3 nM) or Y467F (9.62 ± 1.2 nM).

2.3.4 Mutational effects of Tyr467 on uptake inhibition potency of substrate and inhibitors

We determined the ability of substrate (DA or NE) and NET inhibitors (nisoxetine and cocaine) to inhibit [^{3}H]DA or [^{3}H]NE uptake in WT-, Y467H-, and Y467F hNET to investigate whether Tyr467 mutations influence selective binding sites on hNET (Table 2.3). For [^{3}H]DA uptake, compared to WT hNET, the apparent affinity (IC_{50}) values for DA (1734 ± 20 nM) and cocaine (4377 ± 904

Table 2.2 Kinetic properties of [^{3}H] WIN35,428 and [^{3}H] Nisoxetine binding in PC12 cells expressing WT hNET and its mutants

	WT hNET	Y467H	Y467F
[^{3}H]WIN 35,428			
B_{max} (pmol/10^6)	0.267 ± 0.063	0.209 ± 0.034	0.322 ± 0.078
K_d (nM)	24.7 ± 3.1	31.0 ± 3.1	34.2 ± 1.8
[^{3}H]Nisoxetine			
B_{max} (pmol/10^6)	0.261 ± 0.023	0.183 ± 0.019*	0.27 ± 0.03
K_d (nM)	8.86 ± 1.0	9.44 ± 1.3	9.61 ± 1.2

*T=2.5, df = 9 p =0.0331

Table 2.3 Inhibitory affinity of substrates and inhibitors for [^{3}H]DA and [^{3}H]NE uptake in WT hNET and its mutants

	WT hNET	Y467H	Y467F
	IC_{50} for [^{3}H]DA uptake (nM)		
DA	174 ± 20	236 ± 21	125 ± 12
Nisoxetine	26.7 ± 4.0	15.9 ± 5.0*	21.1 ± 5.1
Cocaine	4377 ± 904	3920 ± 1010	4814 ± 964
	IC_{50} for [^{3}H]NE uptake (nM)		
NE	775.6 ± 218	894.4 ± 258	802.4 ± 106
Nisoxetine	10.1 ± 2.3	9.69 ± 4.7	8.00 ± 3.4
Cocaine	6959 ± 2130	2258 ± 899	2888 ± 1320

*T=3.0, df = 4 p =0.0381

nM) were not altered in Y467H (DA: 236 ± 21 nM, Cocaine: 3920 ± 1010 nM), or Y467F (DA: 125 ± 12 nM, Cocaine: 4814 ± 964 nM). Compared to WT hNET (26.7 ± 4.0 nM), the IC_{50} for nisoxetine inhibiting [^{3}H]DA uptake was significantly reduced in Y467H (15.9 ± 5.0 nM, [$t_{(4)}$ = 3.0; $p < 0.05$, unpaired Student's *t* test]) but not altered in Y467F (21.1 ± 5.1 nM). For [^{3}H]NE uptake, compared to WT hNET, the IC_{50} values for NE (775 ± 218), nisoxetine (10.1 ± 2.3 nM), and cocaine (6959 ± 2130 nM) were not altered in Y467H (NE: 894 ± 258 Nisoxetine: 9.69 ± 4.7 nM, Cocaine: 2258 ± 899 nM) or Y467F (NE: 802 ± 106, Nisoxetine: 8.00 ± 3.4 nM, Cocaine: 2888 ± 1320 nM).

2.3.5 Mutations of Tyr467 on hNET attenuate Tat-induced inhibition of DA transport

We examined specific [^{3}H]DA uptake in WT hNET and the Tyr467 mutants in the presence or absence of 140 nM recombinant Tat_{1-86}. The inhibitory effects of Tat_{1-86} on DA uptake via WT-, Y467H-, and Y467F-hNET are presented as the ratio of [^{3}H]DA uptake in the presence of Tat_{1-86} compared to [^{3}H]DA uptake in the absence of Tat for each respective mutant (Figure 2.3). One-way ANOVA revealed a significant main effect of genotype. Post hoc analysis revealed 140 nM Tat_{1-86} produced a 35% decrease in the specific [^{3}H]DA uptake in WT hNET relative to its control [in DPM: Tat (2367 ± 426) vs control (3439 ± 443),[$t(16)$ = 2.5; $p < 0.05$, unpaired Student's *t* test]; however, no effect of Tat on DA uptake was observed in Y467H [in DPM: Tat (2291 ± 568) vs control (2321 ± 569)] or Y467F [in DPM: Tat (2881 ± 145) vs control (3227 ± 458)], suggesting that

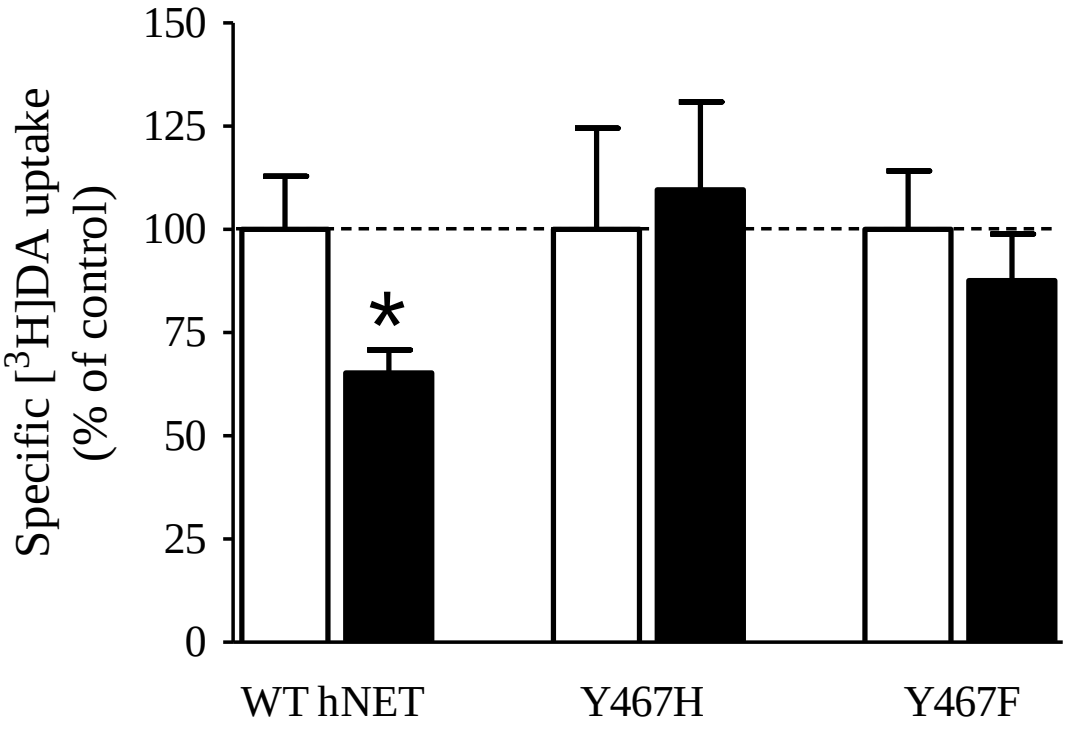

Figure 2.3 Effects of Tat_{1-86} on the specific [^{3}H]DA uptake in WT-, Y467H-, and Y467F-hNET. PC12 cells transfected with the WT hNET or mutants were preincubated with (white bars) or without (black bars) recombinant Tat_{1-86} ($rTat_{1-86}$, 140 nM, final concentration) at room temperature for 20 min followed by the addition of [^{3}H]DA (50 nM, final concentration) for an additional 8 min at room temperature. In parallel, nonspecific uptake was determined in the presence of 10 μM desipramine. Data are expressed as means ± S.E.M. from 4-9 independent experiments. * $p < 0.05$ compared to control value (in the absence of Tat, unpaired Student's *t* test).

mutations of tyrosine 467 on hNET to a histidine or phenylalanine attenuate Tat-induced inhibition of DA uptake.

2.4 DISCUSSION

Our previous studies have demonstrated that DA uptake through the DAT is inhibited by HIV-1 Tat through an allosteric interaction with specific residues on the DAT. In addition to the DAT, the NET is also responsible for DA uptake in the PFC, a critical brain region underlying cognitive capabilities frequently diminished in HAND. For this reason, and because the NET displays identical residues to the DAT at locations which we have demonstrated to be crucial for the Tat/DAT interaction, the present study sought to determine if HIV-1 Tat interacts with a similar group of residues on the NET. Computational modeling and simulations predicted that the Tyr467 residue of the NET, which mimics Tyr470 on the DAT, is crucial for HIV-1 Tat induced inhibition of DA transport. Consistent with this prediction, our findings indicate that mutation of Tyr467 can attenuate the HIV-1 Tat induced inhibition of DA uptake observed in WT hNET. Our pharmacological function assays suggest that mutation of Tyr467 may alter the affinity of both substrates and inhibitors, as evidenced by changes in the Michaelis constant (K_m) of [^{3}H]NE uptake and the maximal binding and inhibitory potency of nisoxetine. Transmembrane 10 (TM10) of the NET, where Tyr467 is located, makes up part of the secondary substrate binding site (S2), thus it is feasible that the observed changes in affinity are due to conformational disruptions in this pocket. Taken together, our results provide novel molecular insight into the HIV-1

Tat/NET interaction and highlight the role of this residue in the substrate transport process.

The long-range electrostatic attraction between the positively charged HIV-1 Tat molecule and the negatively charged extracellular surface of NET (Ravna et al., 2009) likely represents the driving force for the association of these proteins. Our computational prediction of the binding mode is based on a series of computational modeling studies including homology modeling, Brownian (Gabdoulline and Wade, 1998) and molecular dynamics simulations. Considering the fundamental question of how HIV-1 Tat interacts with the NET through specific recognition binding sites to interrupt NET-mediated DA transmission, our computational model predicted Tyr467 to have a favorable cation-π interaction with HIV-1 Tat Met1. In support of the proposed model, our results demonstrate that mutating Tyr467 alters the conformational state of the S2 binding site on NET and, importantly, attenuates HIV-1 Tat induced inhibition of DA transport. Additionally, these results provide evidence that our computationally simulated model of the HIV-1 Tat/NET complex is a reliable method to predict the intermolecular interactions between HIV-1 Tat and the NET, and support the idea that the HIV-1 Tat/NET interaction involves similar residues as we previously reported between HIV-1 Tat and the DAT (Midde et al., 2013; Midde et al., 2015). Although mutation of Tyr467 was able to attenuate HIV-1 Tat-induced inhibition of NET-mediated DA transport, our computational modeling and previous work with the DAT suggest that multiple residues are likely involved in the HIV-1 Tat/NET interaction. With this in mind, determining the influence of additional

single and multiple mutations to predicted recognition residues on the NET will be an essential task for our future studies.

Tyr467 is located within a hydrophobic pocket of transmembrane helix 10 (TM10) of the NET where it makes up a portion of the S2 binding pocket (Wang et al., 2012). The S2 binding pocket is functionally responsible for allosterically triggering conformational changes from the occluded state to the inward-facing state, facilitating the release of ions and substrate, and the residues located in this pocket may take part in binding molecules before they reach the primary substrate binding site (S1; Góral et al., 2020; Anderson et al., 2015). Because of the critical role of both of these binding pockets in the uptake process they represent common targets of NET inhibitors. Nisoxetine, a potent and selective NET inhibitor, has been shown to induce inhibition through its interaction with the S2 binding site (Manepalli et al., 2012; Anderson et al., 2015), whereas WIN 35,428, a cocaine analog, induces inhibition via interactions with the S1 binding site (Manepalli et al., 2012; Ravna et al., 2006). Although these binding pockets are located in close proximity, the binding of these two molecules to the NET has been demonstrated to be mutually exclusive (Zhen et al., 2012). Our study determined that mutation of Tyr467 to His (Y467H) or Phe (Y467F) did not have a significant effect on the affinity of [^{3}H]Nisoxetine or [^{3}H]WIN 35,428 binding to the transporter, although we did observe a decrease in the maximal binding (B_{max}) of [^{3}H]Nisoxetine to the Y467H mutant. A previous report (Wang et al., 2012) also found that mutation of Tyr467 reduced the B_{max} of [^{3}H]Nisoxetine and suggested that it was due to a decrease in transporter expression. Regarding this

possibility, we performed cell surface biotinylation for WT NET and the Tyr467 mutants to assess total and surface NET expression. Our results did not find any significant difference in total or plasma membrane expression of the NET in either mutant, suggesting that this decrease in binding was not due to a decreased number of binding sites, although it is possible that this assays lacks the necessary sensitivity to identify the relatively small decrease in B_{max} (~30%).

Although [^{3}H]nisoxetine and [^{3}H]WIN 35,428 binding were unchanged in the mutants, we did identify alterations in uptake kinetics and inhibitor activity. We observed an ~85% increase in the K_m of NE uptake in Y467F compared to WT NET, indicating this mutant has a lower affinity for NE. This effect may be due to the aforementioned role of TM10 in allosterically mediating conformational transitions of the NET, as well as effects on the Y545-Y467-Y548 motif, which may be involved in conformational conversions required for the transport of NE, similar to the DA transport process of DAT (Yuan et al., 2016; Sun et al., 2019). Despite the alterations in NE affinity, we did not identify any alterations in DA uptake kinetics in these mutants, which may be due to the role of the S2 binding pocket in controlling the entry pathway of substrates into S1 in the NET, where mutations may differentially affect DA or NE interactions (Anderson et al., 2015). We also found that the inhibition potency for nisoxetine to prevent [^{3}H]DA uptake was increased in Y467H, whereas the inhibition potencies of cocaine and DA were unchanged. This is likely due to an altered conformation of the S2 binding pocket (the target of nisoxetine), where Tyr467 is located, with the S1 binding pocket (the target of cocaine and DA) being left intact. Collectively, the effects of

the Tyr467 mutants on basal uptake kinetics and NET conformational integrity are in agreeance with previous work and computational predictions suggesting a role of this residue in the S2 binding pocket and nisoxetine binding.

Consistent with our computational modeling prediction, a vital finding in the present study is that mutation of NET Tyr467 attenuates HIV-1 Tat induced inhibition of NET reuptake functionality. Our modeling suggests that the Met1 residue of HIV-1 Tat forms a cation-π interaction with NET Tyr467. This prediction is supported by our results demonstrating that mutation of Tyr467 to a non-aromatic amino acid (His) attenuates this interaction. Interestingly, mutation of Tyr 467 to an alternative aromatic amino acid (Phe) still produces attenuation of the inhibitory effects of HIV-1 Tat. This result has several possible explanations. One possibility is that, as noted above, mutation of Tyr467 may induce conformational changes in the NET. These conformational changes may alter the allosteric binding pocket on NET with which HIV-1 Tat interacts, thereby attenuating its ability to inhibit reuptake. Additionally, as the driving force between the Met-aromatic interaction is likely a combination of van der Waals, electrostatic, and hydrophobic forces (Tatko & Waters, 2004; Rotello 1998), the precise differences between the Met-Tyr and Met-Phe interactions will likely require future investigation.

In conclusion, we provide novel evidence that inhibition of DA uptake by HIV-1 Tat extends beyond the DAT and affects DA uptake via the NET as well. Attenuation of HIV-1 Tat induced inhibition of NET reuptake via mutation of NET Tyr467 supports our computational modeling prediction of the HIV-1 Tat/NET

interaction and suggests that this interaction may be similar to our previously reported HIV-1 Tat/DAT interaction. Future studies will aim to investigate the contribution of multiple residues on NET which have been predicted to be involved in the HIV-1 Tat/NET interaction, which may provide molecular insight into the development of novel allosteric DAT/NET modulators that are capable of attenuating the inhibitory effects of HIV-1 Tat on DA reuptake.

CHAPTER 3

[^{3}H]DOPAMINE UPTAKE THROUGH THE DOPAMINE AND NOREPINEPHRINE TRANSPORTERS IS DECREASED IN THE PREFRONTRAL CORTEX OF TRANSGENIC MICE EXPRESSING HIV-1 TAT PROTEIN[2]

[2] Strauss, Matthew, et al. "[3H] Dopamine Uptake through the Dopamine and Norepinephrine Transporters is Decreased in the Prefrontal Cortex of Transgenic Mice Expressing HIV-1 Transactivator of Transcription Protein." *Journal of Pharmacology and Experimental Therapeutics* 374.2 (2020): 241-251.

ABSTRACT: Dysregulation of dopamine neurotransmission has been linked to the development of HIV-1 associated neurocognitive disorders (HAND). To investigate the mechanisms underlying this phenomenon, this study utilized an inducible HIV-1 transactivator of transcription (Tat) transgenic (iTat-tg) mouse model, which demonstrates brain-specific Tat expression induced by administration of doxycycline. We found that induction of Tat expression in the iTat-tg mice for either 7 or 14 days resulted in a decrease (~30%) in the V_{max} of [^{3}H]DA uptake via both the dopamine transporter (DAT) and norepinephrine transporter (NET) in the prefrontal cortex (PFC), which was comparable to the magnitude (~35%) of the decrease in B_{max} for [^{3}H]WIN 35,428 and [^{3}H]Nisoxetine binding to DAT and NET, respectively. The decreased V_{max} was not accompanied by a reduction of total or plasma membrane expression of DAT and NET. Consistent with the decreased V_{max} for DAT and NET in the PFC, the current study also found an increase in the tissue content of DA and dihydroxyphenylacetic acid (DOPAC) in the PFC of iTat-tg mice following 7-day administration of doxycycline. Electrophysiological recordings in layer V pyramidal neurons of the prelimbic cortex from iTat-tg mice found a significant reduction in action potential firing, which was not sensitive to selective inhibitors for DAT and NET, respectively. These findings provide a molecular basis for using the iTat-tg mouse model in the studies of NeuroHIV. Determining the mechanistic basis underlying the interaction between Tat and DAT/NET may reveal novel therapeutic possibilities for preventing the increase in comorbid conditions as well as HAND.

3.1 INTRODUCTION

Acquisition of the Human Immunodeficiency Virus (HIV) leads to the development of acquired immunodeficiency syndrome (AIDS) and continues to be a global public health problem, with an estimated 37 million HIV-1 positive individuals worldwide. Despite the success of combinatorial antiretroviral therapy (cART) in controlling peripheral HIV infection and improving the life of HIV patients, roughly 50% of HIV-1 patients develop a group of neurological complications including cognitive dysfunction, motor deficits, and dementia collectively referred to as HIV-associated neurocognitive disorders (HAND) (Heaton et al., 2010). Persistent viral replication and expression of HIV-1 viral proteins within the CNS are central to the development of HAND (Gaskill et al., 2009), particularly since most cART medications cannot cross the blood-brain barrier, while infected macrophages carrying the virus can (Buckner et al., 2006). Considering long-term viral protein exposure can accelerate damage to the mesocorticolimbic dopamine (DA) system (Nath et al., 1987; Berger and Arendt, 2000; Koutsilieri et al., 2002), there is a pressing need to define the molecular mechanism(s) by which HIV-1 infection impairs the DA system and affects the progression of HAND. HIV-1 viral proteins are associated with the persistence of HIV-related neuropathology and subsequent neurocognitive deficits (Frankel and Young, 1998; Power et al., 1998; Brack-Werner, 1999; Johnston et al., 2001). Specifically, the continuing presence of the transactivator of transcription (Tat) protein in CART-treated HIV patients (Johnson et al., 2013; Henderson et al., 2019), may play a crucial role in the neurotoxicity and cognitive impairment

evident in neuroAIDS (Rappaport et al., 1999; King et al., 2006), as the HIV-1 Tat protein has been detected in DA-rich brain areas (Del Valle et al., 2000; Hudson et al., 2000; Lamers et al., 2010) and in the sera (Westendorp et al., 1995; Xiao et al., 2000) of HIV-1 infected patients (Johnson et al., 2013).

Maintaining a normal physiological DA system is essential for a variety of brain activities involved in attention, learning, memory (Nieoullon, 2002; Cools, 2006), and motivation (Lammel et al., 2012; Tye et al., 2013). Converging lines of clinical observations, supported by imaging (Wang et al., 2004; Chang et al., 2008), neuropsychological performance testing (Kumar et al., 2011; Meade et al., 2011), and postmortem examinations (Gelman et al., 2012), have demonstrated that DA dysregulation is correlated with the abnormal neurocognitive function observed in HAND (Berger and Arendt, 2000; Purohit et al., 2011). Therapy-naïve HIV patients demonstrate increased levels of DA and decreased DA turnover in the early stages of HIV infection (Scheller et al., 2010), which may initiate compensatory mechanisms eventually resulting in decreased DA levels (Sardar et al., 1996; Kumar et al., 2009; Kumar et al., 2011) and dopaminergic neuron damage (Wang et al., 2004; Chang et al., 2008) in the advanced stages of HIV infection.

DA transporter (DAT)-mediated DA reuptake is critical for maintaining normal DA homeostasis. Human DAT (hDAT) activity is strikingly reduced in HIV-1-infected patients, particularly those with a history of cocaine abuse, correlating with the severity of HIV-1 associated cognitive deficits (Wang et al., 2004; Chang et al., 2008). Our published *in vitro* work has demonstrated that exogenous

application of recombinant Tat_{1-86} protein decreases DAT activity in cells (Midde et al., 2013; Midde et al., 2015; Quizon et al., 2016) and rat brain synaptosomes (Zhu et al., 2009b). This research raises a critical question of whether the *in vitro* Tat-dysregulated DAT function can be replicated with *in vivo* biological expression of Tat protein in an animal model, which may contribute to the neurocognitive deficits observed in both these animals and HIV infected individuals. Moreover, the prefrontal cortex is an important brain region for higher cognitive function, where not only the DAT but also the norepinephrine (NE) transporter (NET) is capable of DA reuptake (Moron et al., 2002). For this reason, it is possible that Tat-induced dysfunction of DA system could be mediated by inhibition of both DAT and NET. The inducible Tat transgenic (iTat-tg) mouse model recapitulates many aspects of the neuropathologies and neurocognitive impairments observed in HAND (Kim et al., 2003) and represents clinically relevant model of symptomatic NeuroHIV. Thus, investigating the neuropathogenic role of DAT/NET-mediated dopaminergic transmission in the brain of iTat-tg mice may provide mechanistic insight into the development of cognitive deficits in HIV-1 infected population. This iTat-tg mouse model allows for determination of how *in vivo* Tat protein expression influences dopaminergic neurotransmission by inhibiting DAT and NET, which may contribute to the development of HAND.

3.2 MATERIALS AND METHODS

3.2.1 Animals

Male iTat-tg and G-tg mice breeding stock were provided by Dr. Jay P. McLaughlin at the University of Florida College of Pharmacy (Gainesville, FL). Mice in this colony were established from progenitors originally derived by Dr. Johnny J. He (Kim et al., 2003), at the Rosalind Franklin University of Medicine and Science (Chicago, IL). The iTat-tg mouse line genetically expresses a "tetracycline-on (TETON)" system, which is integrated into the regulator for the astrocyte-specific glial fibrillary acidic protein (GFAP) promoter and coupled to the Tat_{1-86} coding gene, allowing astrocyte (brain)-specific Tat_{1-86} expression induced by doxycycline (Dox) administration (Kim et al., 2003). The iTat-tg mouse model facilitates the needed focus on Tat protein, allowing us to study Tat-mediated dysregulation of DAT and NET. In contrast, the G-tg mice possess the TETON system integrated into GFAP but lack the Tat_{1-86} coding gene, rendering them incapable of Tat expression, but highly suitable as control subjects. Since the iTat-tg and G-tg mice are developed from C57BL/6J mouse strain, C57BL/6J mice (obtained from the Jackson Laboratory, Bar Harbor, ME) were used as another control mouse line. Mice used for all experiments were between the age of 9-14 weeks (see Table A.4). This age range was chosen based on the previous reports which found both physiological (Carey et al., 2013; Cirino et al., 2020) and behavioral deficits (Carey et al., 2012; Paris et al., 2014; Paris et al., 2015) in the iTat-tg mice using an identical age range. At the completion of all experiments, we conducted the correlation analysis on the age

with the respective experimental data values from individual animals following 7- or 14-day administration of Dox, which revealed no correlation between age and the respective experimental data values. Mice were housed (4-5 mice/cage) in a temperature (21 ± 2 °C)- and humidity (50 ± 10%)-controlled vivarium, which were maintained on a 12:12 h light/dark cycle (lights on at 07:00 h) with ad libitum access to food and water. Animals were maintained in accordance with the Guide for the Care and Use of Laboratory Animals under the National Institute of Health (NIH) guidelines in the Assessment and Accreditation of Laboratory Animal Care accredited facilities. The experimental protocol was approved by the Institutional Animal Care and Use Committee (IACUC) at the University of South Carolina, Columbia.

3.2.2 Drug administration and Synaptosomal preparation

Male iTat-tg, G-tg, and C57BL/6J mice were administered either Dox (100 mg/kg/day, Sigma-Aldrich; St. Louis, MO) or saline (10 µl/gram body weight) via intraperitoneal injection for 7 or 14 consecutive days. The optimized dose of Dox was chosen because it has been previously proven efficacious for induction of Tat (Zou et al., 2007; Carey et al., 2012; Paris et al., 2014b) and findings showing that iTat so induced is biologically active during the period of behavioral testing (Zou et al., 2007). The 7- or 14-Dox or saline treatment paradigm was chosen for the kinetic analysis of DA uptake based on the previous behavior studies (Carey et al., 2012; Carey et al., 2013; Paris et al., 2014a). In addition, based on the previous report showing no significant difference in Tat immunoreactivity in whole brain of iTat-tg mice following 7- or 14-day

administration of Dox (Paris et al., 2014b), and because no difference in the inhibitory effects of Tat on DA uptake were observed between these time points, only 7-day administration paradigm was used in the subsequent studies. Selection of animals for saline or Dox treatment was made randomly among littermates.

All mice were rapidly decapitated 24 h after last saline or Dox injection. Brain tissue dissected from prefrontal cortex (PFC, prelimbic and infralimbic cortices combined), striatum, and hippocampus was pooled from a group of three mice (constituting a single sample for each region), which was used as a single replicate (*n*) for conducting independent experiments. Thus, "*n*" refers the number of independent experiments conducted, rather than the number of mice used. Synaptosomes were prepared using our published method (Zhu et al., 2004). The PFC region was a focus of the current study because it is a critical brain region for higher cognitive function (Miller and Cohen, 2001; Dalley et al., 2004; Ridderinkhof et al., 2004), where the NET also plays a role in DA uptake (Horn, 1973a; Raiteri et al., 1977). Given that DA uptake through DAT or NET is not identical throughout various brain regions, the DA uptake through DAT in striatum and NET in hippocampus were examined in addition to the PFC. The striatum and hippocampus were also selected due to their central role in DA neurotransmission (Horn, 1973b; Raiteri et al., 1977; Borgkvist et al., 2012). The tissue was homogenized immediately in 20 mL of ice-cold 0.32 M sucrose buffer containing 2.1 mM of NaH_2PO_4 and 7.3 mM of Na_2HPO_4, pH 7.4; with 16 up-and-down strokes using a Teflon pestle homogenizer (clearance approximately 0.003

in.). Homogenates were centrifuged at 1,000g for 10 min at 4°C and the resulting supernatants were then centrifuged at 12,000g for 20 min at 4°C. The resulting pellets were resuspended in the respective buffer for each individual assay as noted below.

3.2.3 Kinetic analysis of synaptosomal [^{3}H]DA uptake assay

To determine whether Dox-induced biological Tat expression alters DA uptake via DAT or NET, the maximal velocity (V_{max}) and Michaelis-Menten constant (K_m) of synaptosomal [^{3}H]DA uptake were examined using a previously described method (Zhu et al., 2016). In a pilot study, we measured the synaptosomal [^{3}H]DA uptake via DAT, NET, or the serotonin transporter (SERT) in whole C57BL/6J mouse brain with the utilization of selective inhibitors for the individual transporters and found that the portion of DA uptake via DAT, NET or SERT is 80%, 17%, and 3%, respectively (data not shown). Due to the minimal level of DA uptake via SERT, this transporter was not examined in the current study. Importantly, although NET density is overall lower in the whole mouse brain, in the PFC the NET is more concentrated than the DAT and plays a primary role in reuptake of DA (Moll et al., 2000; Moron et al., 2002), and thus warranted the present investigation. Because DA is transported by DAT, NET, and SERT in the PFC (Moron et al., 2002; Williams and Steketee, 2004), kinetic analysis of [^{3}H]DA uptake via DAT in the PFC was assessed in the presence of desipramine (1 uM) and paroxetine (5 nM) to prevent DA uptake into norepinephrine- and serotonin-containing nerve terminals, respectively, whereas [^{3}H]DA uptake via NET in the PFC was assessed in the presence of GBR12909

(100 nM) and fluoxetine (100 nM) to prevent DA uptake into dopaminergic- and serotonin-containing nerve terminals, respectively. In brief, the resulting pellets described above were resuspended in Krebs-Ringer-HPES assay buffer (125 mm NaCl, 5 mm KCl, 1.5 mm $MgSO_4$, 1.25 mm $CaCl_2$, 1.5 mm KH_2PO_4, 10 mm glucose, 25 mm HEPES, 0.1 mm EDTA, 0.1 mm pargyline and 0.1 mm L-ascorbic acid, saturated with 95% O_2 / 5% CO_2, pH 7.4). Aliquots of synaptosomal tissue (50 µg/25 µL) were incubated with one of 6 mixed [^{3}H]DA concentrations containing a range of DA (Sigma-Aldrich; St. Louis, MO) concentrations (1 nM - 5 µM) and fixed [^{3}H]DA (12 nM, Perkin Elmer; Waltham, MA) for 8 minutes at 37 °C. Incubation was terminated by the addition of 3 mL of ice-cold assay buffer, followed by immediate filtration through Whatman GF/B glass fiber filters (presoaked with 1 mM pyrocatechol for 3 h). Filters were washed three times with 3 mL of ice-cold assay buffer using a Brandel cell harvester (Model MP-43RS; Biochemical Research and Development Laboratories Inc., Gaithersburg, MD). Radioactivity was determined by liquid scintillation spectrometry (Model B1600TR, Packard Corporation Inc., Meriden, CT). Bovine serum albumin (Sigma-Aldrich; St. Louis, MO) was used as a standard (Bradford, 1976) to measure protein concentration for all samples. Nonspecific uptake of [^{3}H]DA into DAT or NET was determined in the presence of 10 µM nomifensine (Sigma-Aldrich; St. Louis, MO) or 10 µM desipramine, respectively.

3.2.4 [^{3}H]WIN 35,428 and [^{3}H]Nisoxetine binding assays

[^{3}H]WIN 35,428 and [^{3}H]Nisoxetine (both purchased from Perkin Elmer; Waltham, MA) represent substrate binding sites on the DAT and the NET, respectively. To determine whether biological HIV-1 Tat expression alters these substrate binding sites, we performed the saturation binding of [^{3}H]WIN 35,428 and [^{3}H]Nisoxetine for DAT and NET, respectively, using a previously described method (Reith et al., 2005; Zhu et al., 2009a). Saturation binding assays were conducted in duplicate in a final volume of 250 µL for PFC, striatum, and hippocampus. For [^{3}H]WIN 35,428 binding, 50 µL aliquots (50 µg protein) of synaptosomes were incubated in 0.32M sucrose buffer (pH: 7.4) containing 2.1 mM NaH_2PO_4 and 7.3 mM Na_2HPO_4 (chemicals purchased from Sigma-Aldrich; St. Louis, MO) with six concentrations of [^{3}H]WIN 35,428 (1, 5, 10, 15, 25, 30 nM) on ice for 2 h. Desipramine (1 µM) was included to inhibit [^{3}H]WIN 35,428 binding to the NET in the PFC. Nonspecific binding was determined in the presence of 10 µM cocaine in the striatum and 10 µM nomifensine in the PFC. For [^{3}H]Nisoxetine binding, 50 µL aliquots (50 µg protein) of synaptosomes were incubated in assay buffer (150 mM Na_2HPO_4, 300 mM NaH_2PO_4, 1.22 M NaCl, 50 mM KCl, 12 mM $MgSO_4$, 100 mM glucose, 10 mM CaCl, and 1 µM EDTA; pH: 7.4) with one of six Nisoxetine concentrations (0.5-30 nM) that was mixed with a fixed concentration of [^{3}H]Nisoxetine (3 nM) on ice for 2 h. 0.1 µM GBR 12909 was included to inhibit [^{3}H]Nisoxetine binding to the DAT. Non-specific binding was determined in the presence of 10 µM desipramine. The reaction was terminated by rapid filtration onto Whatman GF/B glass filter filters, presoaked for

2 h with assay buffer containing 10% polyethylenimine, through a Brandel cell harvester (Model MP-43RS; Biochemical Research and Development Laboratories Inc., Gaithersburg, MD). Filters were washed three times with 3 mL of ice-cold assay buffer. Radioactivity was determined by liquid scintillation spectrometry (Model B1600TR, Packard Corporation Inc., Meriden, CT), and bovine serum albumin (Sigma-Aldrich; St. Louis, MO) was used as a standard (Bradford, 1976) to measure protein concentration for all samples.

3.2.5 Biotinylation and Western Blot Assay.

Biotinylation was performed to determine alterations in plasmalemmal surface expression of DAT in the PFC and striatum and NET in the PFC and hippocampus following Dox-induced Tat expression. Following 7-day administration of Dox or saline, synaptosomes were prepared as described above. The biotinylation assay was performed as described previously (Zhu et al., 2009a). Synaptosomes (800 µg/sample) prepared freshly were incubated in 500 µL of PBS Ca/Mg buffer (138 mM NaCl, 2.7 mM KCl, 1.5 mM KH_2PO_4, and 9.6 mM Na_2HPO_4; with 1 mM $MgCl_2$ and 0.1 mM $CaCl_2$; Sigma-Aldrich; St. Louis, MO) containing 1.5 mg/mL EZ-link sulfo-NHS-biotin at 4 °C for 1 h. After incubation, samples were centrifuged at 8000g for 4 min at 4 °C. To remove the free sulfo-NHS-biotin, the resulting pellets were resuspended and centrifugated three times with 1 mL of ice-cold 100 mM glycine in PBS/Ca/Mg buffer and centrifugated at 8000g for 4 min at 4 °C. Final resulting pellets were resuspended in 1 mL of ice-cold 100 mM glycine in PBS/Ca/Mg buffer and incubated with continual shaking for 30 min at 4 °C. Samples were centrifuged

subsequently at 8000g for 4 min at 4°C, the resulting pellets were resuspended in 1 ml of ice-cold PBS/ Ca/Mg buffer, and the resuspension and centrifugation step were repeated twice. Final pellets were lysed by sonication for 2 to 4 seconds in 500 µL of Triton X-100 buffer (10 mM Tris, 150 mM NaCl, 1 mM EDTA, 1.0% Triton X-100, 1 µg/ml aprotinin, 1 µg/ml leupeptin, 1 µM pepstatin, 250 µM phenylmethysulfonyl fluoride, pH 7.4), followed by incubation and continual shaking for 20 min at 4°C. Lysates were centrifuged at 21,000g for 20 min at 4°C. Pellets were discarded, and 100 µL of supernatant was saved for assessing total DAT or NET expression. Monomeric avidin beads (100 µL, Thermo Scientific; Waltham, MA) were added to the remaining supernatant and incubated for one hour at room temperature. The samples were then centrifuged at 17,000g for 4 min, and 100 µL of the resulting supernatant was saved for the intracellular (non-biotinylated) fraction. Resulting pellets containing the avidin-absorbed biotinylation proteins (cell surface fraction) were resuspended in 1mL of 1.0% Triton X-100 buffer and centrifuged at 17,000g for 4 min at 4°C, which was repeated twice. Final pellets containing the biotinylated DAT and NET absorbed to monomeric avidin beads were eluted by addition of 50 µL of laemmeli buffer (Sigma-Aldrich; St. Louis, MO) and incubated for 20 min at room temperature. The total, intracellular and surface fractions were stored at -20 °C until Western blot assay.

To obtain immunoreactive DAT and NET protein in total synaptosomal, intracellular, and cell surface fractions, samples were thawed and subjected to gel electrophoresis and western blotting. Samples were separated by 10% SDS-

polyacrylamide gel electrophoresis for ~90 min at 125V. Samples were then transferred to Immobilon-P transfer membranes (0.45 µm pore size; Millipore Co., Bedford MA, USA) in transfer buffer (50 mM Tris, 250 mM glycine, 3.5 mM SDS) using a Mini Trans-Blot Electrophoretic Transfer Cell (Bio-Rad; Hercules, CA) for 90 min at 75 V. The membranes were then incubated with blocking buffer (5% milk powder in PBS containing 0.5% Tween-20) for 1 h at room temperature, followed by incubation with either goat anti-DAT (Santa Cruz, C-20 polyclonal antibody, diluted 1:500 in blocking buffer) or mouse anti-NET (MAb tech, 05-1 monoclonal antibody, diluted 1:5,000 in blocking buffer) overnight at 4 °C. Transfer membranes were then washed three times with blocking buffer at room temperature followed by incubation with either anti-goat-HRP (Jackson Laboratory, catalog number 305-035-045 diluted 1:10,000 in blocking buffer) or anti-mouse-HRP (Cell Signaling, catalog number 7076S diluted 1:15,000 in blocking buffer) for 1 h at room temperature. Membranes were then washed an additional three times in PBS containing 0.5% Tween-20 (Sigma-Aldrich; St. Louis, MO). Immunoreactive proteins on the transfer membranes were detected using Amersham ECL prime western blotting detection reagent (GE life sciences; Chicago, IL) and developed on Hyperfilm (GE life sciences; Chicago, IL). After detection and quantification of DAT or NET each blot was washed and re-probed with rabbit anti-Calnexin (Santa Cruz, Biotechnology, catalog number SC-11397 polyclonal antibody, diluted 1:10,000 in blocking buffer), an endoplasmic reticular protein, to monitor protein loading between all groups. Multiple autoradiographs were obtained using different exposure times, and immunoreactive bands within

the linear range of detection were quantified by densitometric scanning using Scion image software. Band density measurements, expressed as relative optical density, were used to determine levels of DAT and NET in the total synaptosomal fraction, the intracellular fraction (non-biotinylated), and the cell surface fraction (biotinylated).

3.2.6 HPLC analysis of DA and dihydroxyphenylacetic acid (DOPAC) tissue contents in brain regions

Concentrations of DA and DOPAC in PFC, nucleus accumbens, and striatum in iTat-tg and G-mice following 7-day administration of saline or Dox were determined using a high performance liquid chromatography (HPLC) system coupled with electrochemical detection (HPLC–EC) as described previously (Zhu et al., 2004). Twenty-four hours after the last injection of saline or Dox, whole brains from individual mice were removed and immediately stored in liquid nitrogen, and then stored at −80° C. To prepare samples for HPLC assay, whole brains were sliced on top of an ice-cold plate and brain regions were dissected by biopsy punches with a plunger system (Miltex). Brain tissues were individually stored in 10 volume/tissue weight of 0.1 N perchloric acid at −80° C until assay. Upon assay, samples were thawed on ice, sonicated and centrifuged at 30,000 × g for 15 min at 4° C. For each sample, 20 µl of the resulting supernatant was injected onto the HPLC system. Chromatograms were recorded using EZ Chrom Elite software (Agilent, Santa Clara, CA). Retention times of DA and DOPAC standards were used to identify respective peaks. Peak heights were used to calculate the detected amounts of DA and DOPAC based on a

standard curve generated from external standards. The HPLC–EC system (Coulochem III, ThermoFisher Scientific, Columbia MD) consisted of a 582 solvent delivery system, an autosampler (Model 542), a reverse phase HPLC column (MD-150, 3.2 x 150 mm, 3µm, product no 70-0636) and electrochemical detector (cell 5014B). The mobile phase contained 124 mM citric acid monohydrate, 50 mM Na_2HPO_4, 10 mM NaCl, 0.1 mM EDTA, 0.2% octylsulfonic acid–sodium salt and 5% methanol (pH 3.0), using a flow rate of 0.5 ml/min. Samples were kept at 4^o C in a cooling tray in the autosampler.

3.2.7 Patch-clamp Electrophysiology

iTat and C57 mice were decapitated following isoflurane anesthesia 24 h after the last Dox or saline injection. Brains were rapidly removed and coronal slices (300 µm) containing the PFC were cut using a Vibratome (VT1000S; Leica Microsystems) in an ice-cold artificial cerebrospinal fluid (aCSF, in mM: 130 NaCl, 3 KCl, 1.25 NaH_2PO_4, 26 $NaHCO_3$, 10 glucose, 1 $MgCl_2$, and 2 $CaCl_2$, pH 7.2–7.4, saturated with 95% O_2 and 5% CO_2) solution in which NaCl was replaced with an equiosmolar concentration of sucrose. Slices were incubated in aCSF at 32–34°C for 45 min and kept at 22–25°C thereafter, until transfer to the recording chamber. All solutions had osmolarity between 305 and 315 mOsm. Slices were viewed under an upright microscope (Eclipse FN1; Nikon Instruments) with infrared differential interference contrast optics and a 40 × water-immersion objective. For recordings, the chamber was continuously perfused at a rate of 1–2 mL/min with oxygenated aCSF heated to 32 ± 1°C using an automated temperature controller (Warner Instruments). Recording

pipettes were pulled from borosilicate glass capillaries (World Precision Instruments) to a resistance of 4–7 MΩ when filled with the intracellular solution. The intracellular solution contained the following (in mM): 145 potassium gluconate, 2 $MgCl_2$, 2.5 KCl, 2.5 NaCl, 0.1 BAPTA, 10 HEPES, 2 Mg-ATP, and 0.5 GTP-Tris, pH 7.2–7.3, with KOH, osmolarity 280–290 mOsm. Layer V pyramidal neurons of the prelimbic cortex were identified by their morphology. The layer V pyramidal neurons of the medial prefrontal cortex were selected for two reasons: first, dopamine (D1) receptor expression is enriched in deeper layers of the prefrontal cortex (Santana and Artigas, 2017), which are primarily affected by HIV-1 Tat protein (Brailoiu et al., 2017; Kesby et al., 2017), second, the neurons projects to subcortical nuclei have been suggested to play a critical role in cognitive functioning (Douglas and Martin, 2004; Riga et al., 2014). Current step protocols (from -500 to +500 pA; 20 pA increments; 500 ms step duration) were run to determine action potential frequency versus current (*f-I*) relationship. Drugs were applied via the Y-tube perfusion system modified for optimal solution exchange in brain slices (Hevers and Luddens, 2002). Dopamine (10 nM, final concentration) was initially applied alone, followed by the combined application of dopamine (10 nM) and GBR-12909 (100 nM), followed by the combined application of dopamine (10 nM), GBR-12909 (100 nM) and desipramine (1 µM). All data were collected after a minimum of 2 min of drug exposure. Currents were low-pass filtered at 2 kHz and digitized at 20 kHz using a Digidata 1440A acquisition board (Molecular Devices) and pClamp10 software (Molecular Devices). Access resistance (10–30 MΩ) was monitored during

recordings by injection of 10 mV hyperpolarizing pulses. All analyses were completed using Clampfit 10 (Molecular Devices).

3.2.8 Data analysis

Data are expressed as mean ± S.E.M., and *n* refers to the number of individual experiments for each group. To analyze the kinetic parameters (V_{max}/K_m and B_{max}/K_d) of [^{3}H]DA uptake or [^{3}H]WIN 35,428 and [^{3}H]Nisoxetine binding, best fit non-linear regression analysis using a single site model was conducted for each individual experiment using GraphPad Prism 8 software. To determine whether a relationship existed between individual mouse age and the respective experimental data, separate Pearson correlation analysis was conducted. The kinetic parameters were then compared between the saline and Dox treated groups for C57BL/6J or G-tg mice (to rule out any non-specific effects of Dox administration) and subsequently for the iTat-tg mice using unpaired Student's *t* tests, which were conducted using IBM SPSS statistics version 25. Analyses resulting in $p < 0.05$ were considered significant.

3.3 RESULTS

3.3.1 Expression of HIV-1 Tat produces a decrease in synaptosomal [^{3}H]DA uptake through both DAT and NET in the PFC.

To determine the effects of Dox-induced Tat expression on DA uptake via DAT or NET, kinetic analyses of synaptosomal [^{3}H]DA uptake were performed in iTat-tg mice following 7- or 14-days of Dox administration. After 7-day administration of Dox or saline (Figure 3.1A and B), the V_{max} of [^{3}H]DA uptake via DAT and NET in the PFC was significantly reduced by 27 ± 4.8% [$t_{(7.953)} = 3.981$,

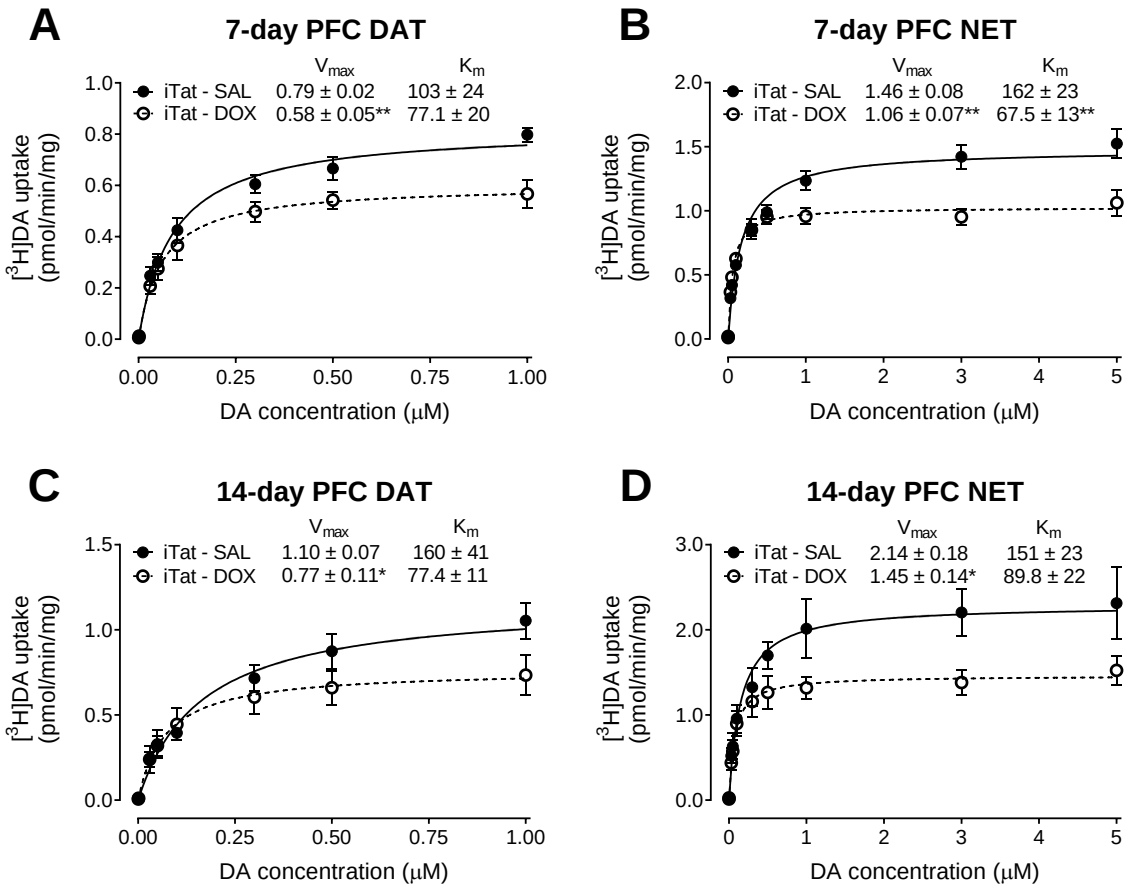

Figure 3.1 Kinetic analysis of synaptosomal [^{3}H]DA uptake was determined in the PFC of iTat-tg mice following 7- or 14-day administration of saline or Dox. Synaptosomes were incubated with a range of mixed DA concentrations (0.1 – 5 μM, final concentration) containing a fixed concentration (12 nM) of [^{3}H]DA. The V_{max} and K_m values for [^{3}H]DA uptake via DAT (A and C) or NET (B and D) in the PFC of iTat-tg (iTat) mice following 7- (A and B) or 14- (C and D) day administration of saline or Dox were calculated using non-linear regression analysis with a one-site binding parameter and represent the means from five to seven independent experiments ± S.E.M. * $p < 0.05$, ** $p < 0.01$ compared to saline control group.

$p < 0.01$] and 27 ± 6.8% [$t_{(11)} = 3.752$, $p < 0.01$], respectively, compared to the respective saline controls (Figure 3.1A and B). No changes in the K_m values of [^{3}H]DA uptake via DAT were observed (Figure 3.1A), however the K_m values of [^{3}H]DA uptake via NET of iTat Dox-treated mice were significantly reduced by 58 ± 6.6% compared to saline-treated controls [$t_{(11)} = 3.708$, $p < 0.01$] (Figure 3.1B). After 14-day administration of Dox or saline, the V_{max} values of [^{3}H]DA uptake via DAT (Figure 3.1C) and NET (Figure 3.1D) in the PFC were significantly decreased by 30 ± 5.9% [$t_{(9)} = 2.356$, $p < 0.05$] and 32 ± 3.1% [$t_{(8)} = 2.952$, $p < 0.05$], respectively compared to saline-treated controls. No significant differences in the K_m of [^{3}H]DA uptake via either DAT or NET were found (Figures 3.1C and D). We also determined the V_{max} and K_m values of [^{3}H]DA uptake in the striatum and hippocampus where DAT and NET are dominantly expressed. Results showed no observable difference in the V_{max} and K_m values of [^{3}H]DA uptake via DAT in the striatum and NET in hippocampus between saline- and Dox-treated iTat-tg mice following either 7- or 14-day administration of Dox (Table 3.1). In the current study, in addition to iTat-tg mice treated with saline as a control for Dox treatment, C57BL/6J and G-tg mice were used as negative controls. No differences in the V_{max} and K_m values of [^{3}H]DA uptake via DAT and NET in those brain regions were observed between saline- or Dox-treated mice (Tables A.1-3).

3.3.2 Expression of HIV-1 Tat does not alter plasmalemmal membrane expression of DAT or NET in the PFC.

To determine whether the Tat expression-induced decrease in the V_{max} of [^{3}H]DA uptake via DAT or NET in PFC was associated with an alteration of the

Table 3.1 Kinetic properties of [^{3}H]DA uptake and [^{3}H]WIN 35,428 binding or [^{3}H]Nisoxetine binding in iTat-tg mice

			Striatum (DAT)		Hippocampus (NET)	
			V_{max} (pmol/min/mg)	K_m (nM)	V_{max} (pmol/min/mg)	K_m (nM)
Treatment duration	7d	iTat-tg Saline	15.6 ± 1.4	97.3 ± 6.6	0.898 ± 0.12	102 ± 23
		iTat-tg Dox	15.6 ± 1.6	91.1 ± 3.4	0.926 ± 0.077	75.4 ± 14
	14d	iTat-tg Saline	67.6 ± 8.5	140 ± 11	1.96 ± 0.19	122 ± 18
		iTat-tg Dox	68.4 ± 8.9	141 ± 10	1.86 ± 0.26	115 ± 24
			B_{max} pmol/mg	K_d (nM)	B_{max} pmol/mg	K_d (nM)
	7d	iTat-tg Saline	22.9 ± 3.7	20.3 ± 5.3	0.611 ± 0.10	13.4 ± 3.3
		iTat-tg Dox	25.4 ± 5.4	18.3 ± 1.8	0.552 ± 0.096	15.4 ± 2.0

Data are expressed as mean ± S.E.M. values from five to seven independent experiments performed in duplicate. 7d indicates 7-days of treatment and 14d indicates 14-days.

subcellular distribution of the transporters, biotinylation and immunoblot assays were performed to assess cell surface and intracellular transporter localization. Three subcellular fractions were prepared from the PFC, striatum, and hippocampus of iTat-tg mice following 7-day Dox or saline administration and DAT or NET immunoreactivity in both total fraction and cell surface fraction (biotinylated) were examined. No differences in DAT or NET immunoreactivity in PFC between saline- and Dox-treated iTat-tg mice were found in the ratio of total or surface transporters to calnexin (Figure 3.2), indicating that the observed decrease in the V_{max} for DAT or NET is not due to alteration of the available transporters on the cell surface. Moreover, no differences in the respective immunoreactivity of DAT in striatum or NET in hippocampus between saline- and Dox-treated iTat-tg mice were found in the ratio of total or surface transporters to calnexin (Figure A.1). Additionally, no differences were observed in DAT or NET immunoreactivity in the PFC, striatum, or hippocampus between saline- and Dox-treated control mice in the ratio of total or surface transporters to calnexin (Figure A.2).

3.3.3 Expression of HIV-1 Tat produces a decrease in [^{3}H]WIN 35,428 and [^{3}H]Nisoxetine binding in the PFC

[^{3}H]WIN 35,428 and [^{3}H]Nisoxetine are highly selective and potent reuptake inhibitors with high affinity for the DAT and NET, respectively (Tejani-Butt, 1992; Pristupa et al., 1994). To determine whether Tat-induced decreases in the V_{max} of [^{3}H]DA uptake via DAT or NET alter the respective substrate binding sites, kinetic analyses of [^{3}H]WIN 35,428 and [^{3}H]Nisoxetine binding were

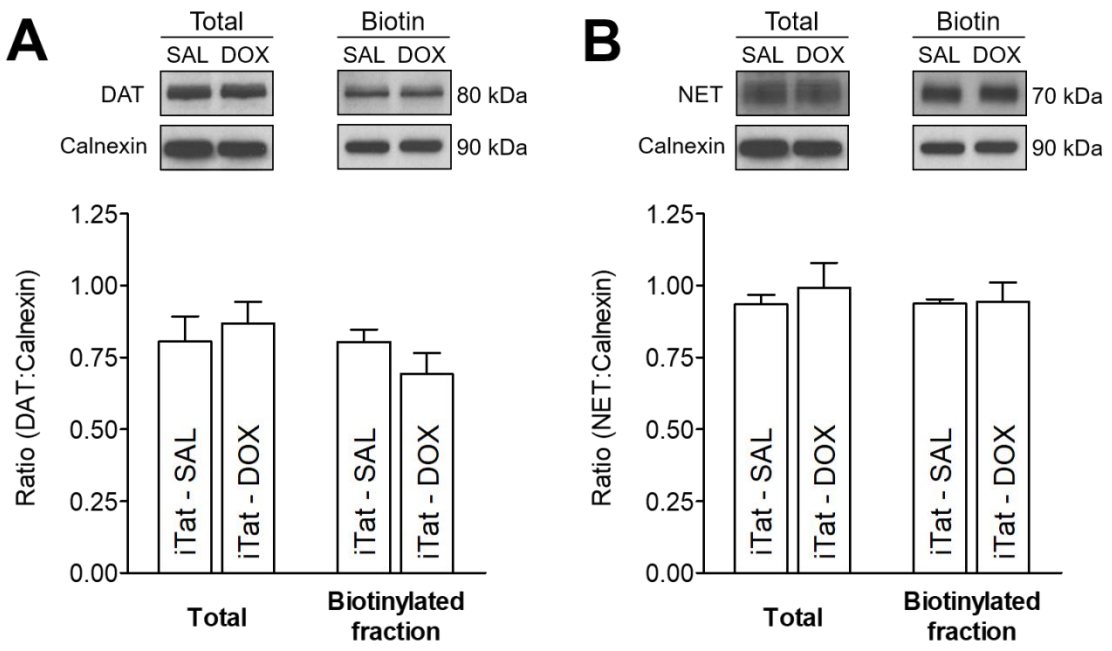

Figure 3.2 Analysis of plasmalemmal surface expression of DAT and NET was determined in the PFC of iTat-tg mice following 7-day administration of saline or Dox. Synaptosomes were incubated with sulfo-NHS-biotin and Pierce monomeric avidin beads and washed multiple times to isolate the DAT or NET, which was present on the plasmalemmal membrane. Top panels: representative immunoblots of total and biotinylated (Biotin) fraction of DAT (A) or NET (B) from the PFC of iTat-tg (iTat) mice from Dox-treated and saline (SAL) control groups. Calnexin was used as control protein. Bottom panels: the ratio of total or biotinylated DAT (A) or NET (B) immunoreactivity to calnexin immunoreactivity expressed as mean ± S.E.M. from five independent experiments.

performed in the brain regions of iTat-tg mice following 7-day Dox or saline administration. For [^{3}H]WIN 35,428 binding sites, in comparison to saline controls, the B_{max} values in PFC of Dox-treated iTat-tg mice were decreased by 28 ± 2.7% [$t_{(7)}$ = 4.396, p < 0.01] (Figure 3.3A), with no change in K_d values. However, no difference was observed in the B_{max} values in striatum between saline-and Dox-treated iTat-tg mice (Table 3.1). For [^{3}H]Nisoxetine binding sites, the B_{max} values in the PFC of Dox-treated iTat-tg mice was reduced by 36 ± 7.7% compared to saline-treated controls [$t_{(7)}$ = 2.479, p < 0.05] (Figure 3.3B). The K_d value was reduced by 40 ± 10% compared to saline-treated controls [$t_{(8)}$ = 2.670, p < 0.05] (Figure 3.3B). No difference in the B_{max} values in hippocampus were found between saline-and Dox-treated iTat-tg mice (Table 3.1). Moreover, no differences were observed between saline- or Dox-treated control mice (Tables A.1 and A.2).

Due to the comparable decreases observed in the V_{max} of [^{3}H]DA uptake and the B_{max} of [^{3}H]WIN 35,428 binding for the DAT in the PFC of Dox-treated iTat mice, comparison of the turnover rate (V_{max}/B_{max}) revealed no significant differences between saline (2.43 ± 0.14) and Dox (2.16 ± 0.29) treated groups (Figure 3.3C). Analysis of the ratio of K_m and K_d for V_{max} of [^{3}H]DA uptake and the B_{max} of [^{3}H]WIN 35,428 binding for the DAT in the PFC also revealed no significant differences between saline (0.014 ± 0.005) and Dox (0.009 ± 0.001) treated mice (Figure 3.3D). No significant differences were found in turnover rate for [^{3}H]DA uptake and [^{3}H]Nisoxetine binding for the NET in the PFC between saline (3.40 ± 0.38) and Dox (3.66 ± 0.19) treated mice (Figure 3.3E), or for the

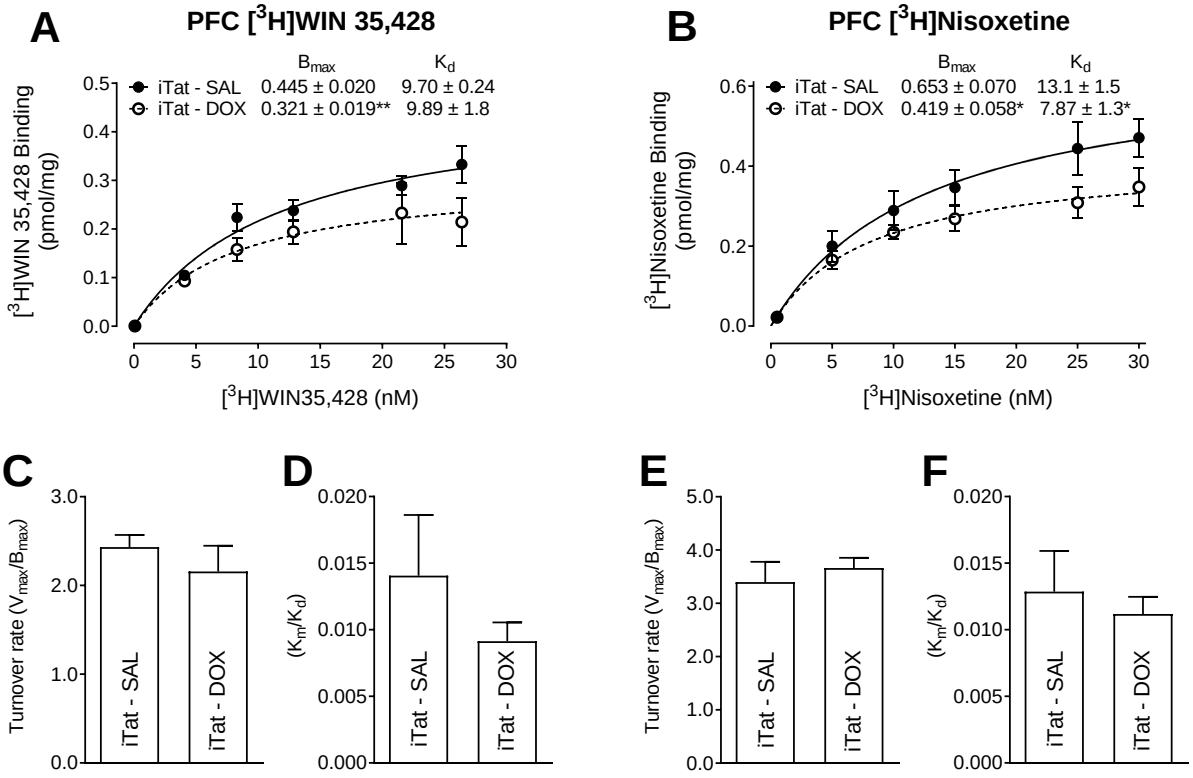

Figure 3.3 Saturation binding of [^{3}H]WIN 35,428 or [^{3}H]Nisoxetine in the PFC of iTat-tg mice following 7- day administration of saline or Dox. For [^{3}H]WIN 35,428 binding to DAT, synaptosomes were incubated in assay buffer with one of six concentrations of [^{3}H]WIN 35,428 (1-30 nM, final concentration) and 1 µM desipramine on ice for 2 h. Nonspecific binding was determined in the presence of 10 µM cocaine. For [^{3}H]Nisoxetine binding to NET, synaptosomes were incubated in assay buffer with one of six concentrations of nisoxetine (0.5-30 nM, final concentration) along with a fixed concentration of [^{3}H]Nisoxetine (3 nM) and 0.1 µM GBR12909 on ice for 2 h. Nonspecific binding was determined in the presence of 10 µM desipramine. The B_{max} and K_d values for [^{3}H]WIN 35,428 (A) or [^{3}H]Nisoxetine (B) binding to DAT or NET in the PFC of iTat-tg (iTat) mice following 7- day administration of saline or Dox were calculated using non-linear regression analysis with a one-site binding parameter and represent the means ± S.E.M. from five independent experiments. * $p < 0.05$, ** $p < 0.01$ compared to saline control group. DA turnover rate values were determined for DAT from (C) the V_{max} of [^{3}H]DA uptake (Figure 3.1A)/B_{max} of [^{3}H]WIN 35,428 binding and (D) the K_m/K_d of [^{3}H]DA uptake (Figure 3.1A)/B_{max} of [^{3}H]WIN 35,428 binding and for NET from (E) the V_{max} of [^{3}H]DA uptake (Figure 3.1B)/B_{max} of [^{3}H]Nisoxetine binding and (F) the K_m/K_d of [^{3}H]DA uptake (Figure 3.1B)/B_{max} of [^{3}H]Nisoxetine binding.

ratio K_m and K_d in the saline (0.013 ± 0.003) and Dox (0.011 ± 0.001) treated groups (Figure 3.3F).

3.3.4 The decreased DAT and NET function in the PFC is consistent with alterations in DA and DOPAC tissue content

Given the critical role of the DAT and the NET in controlling DA homeostasis, a Tat-induced decrease in DA reuptake via DAT or NET in the PFC could result in alterations in the levels of DA and its primary metabolite DOPAC in the respective brain regions. DA and DOPAC content were determined in PFC and striatum from iTat-tg and G-tg mice following 7-day administration of saline or Dox. As shown in Figure 3.4, DA tissue content in PFC from Dox-treated iTat-tg mice was increased by 268% (0.078 ± 0.021 ng/mg tissue) compared to saline (0.021 ± 0.011 ng/mg tissue) treated controls [$t_{(8)} = 2.39$, $p < 0.05$] (Figure 3.4A). Similarly, DOPAC tissue content in the PFC of Dox-treated iTat-tg mice was increased by 144% (0.036 ± 0.006 ng/mg tissue) compared to saline (0.015 ± 0.003 ng/mg tissue) treated controls [$t_{(7)} = 3.344$, $p < 0.05$] (Figure 3.4B). However, neither DA or DOPAC content in striatum of iTat-tg mice differed significantly between saline- and Dox-treated groups (Figure 3.4C and D). We also examined the tissue levels of DA and DOPAC content in the PFC and striatum of G-tg mice, which showed no significant differences between saline- and Dox-treated groups (Figure A.3).

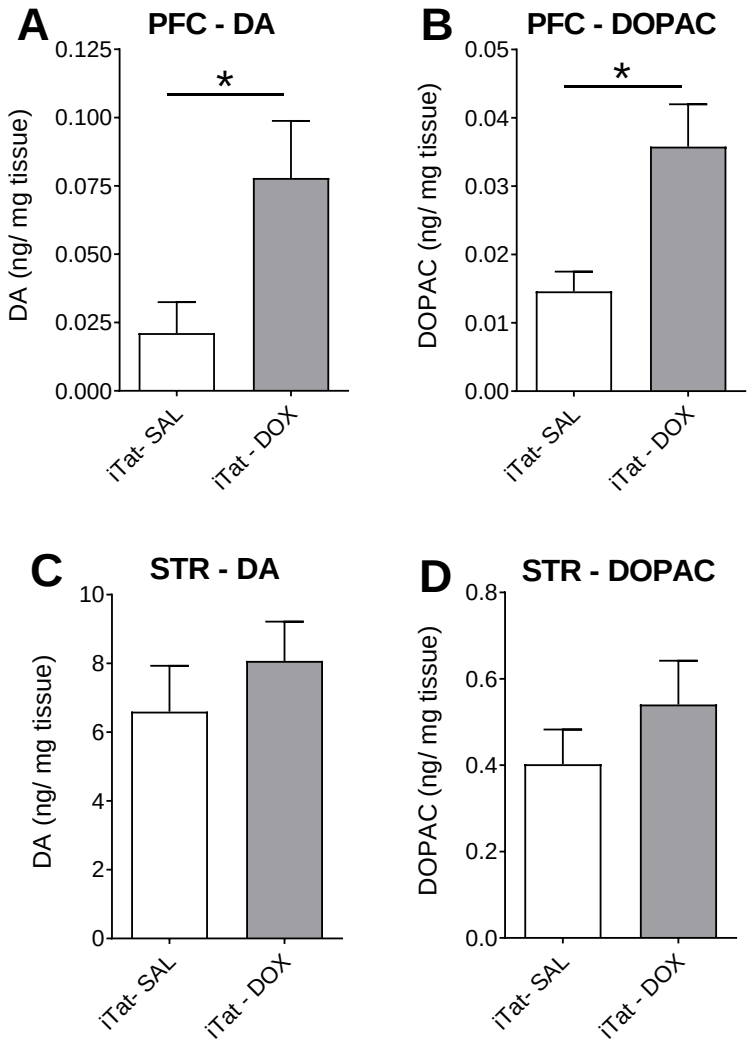

Figure 3.4 DA and dihydroxyphenylacetic acid (DOPAC) tissue content in the PFC and striatum of iTat-tg mice following 7-day administration of saline or Dox. Top panels: DA (A) and DOPAC (B) tissue content in the PFC of iTat-tg (iTat) mice from Dox-treated or saline (SAL) control groups. Bottom panels: DA (C) and DOPAC (D) tissue content in striatum (STR) of iTat-tg mice from Dox-treated or saline control groups. Data are expressed as ng/mg tissue (mean ± S.E.M.) from 5-6 mice per group. * $p < 0.05$, compared to saline control group.

3.3.5 Action potential frequency is decreased in layer V pyramidal neurons of the prelimbic cortex of iTat-tg mice

To determine whether the Tat-induced decrease in DA uptake via DAT/NET in the PFC alters electrical firing signaling of neurons in this region, we performed whole-cell patch clamp electrophysiology on layer V pyramidal neurons in the prelimbic region of PFC from iTat-tg mice following 7-day saline or Dox treatment. As shown in Figure 3.5B, ANOVA analysis revealed a significant main effect of current injection [$F_{(10, 210)} = 82.52$, $p < 0.0001$], and a significant main effect of drug treatment (saline vs dox) [$F_{(1, 21)} = 5.77$, $p = 0.025$], as well as significant current × drug treatment interaction [$F_{(10, 210)} = 2.49$, $p = 0.008$]. Dox-treated iTat-tg mice displayed a reduction of action potential output in this subset of neurons, compared to saline control group (Bonferroni $p < 0.05$). No differences were observed between saline and Dox treated C57BL/6J mice (Figure A.4).

Additionally, to assess the effects of inhibition of DAT or NET in the prelimbic region of PFC by selective inhibitors for the respective transporter on the observed decrease in action potential output, the basal action potentials from pyramidal neurons of iTat-tg mice with Dox or saline treatment were subsequently examined in the presence of DA (10 nM), DA + GBR-12909 (a potent DAT inhibitor; 100 nM), and DA + GBR-12909 + desipramine (DMI; a potent NET inhibitor, 1 µM). A two-way ANOVA with repeated measurement on action potential in iTat-tg mice treated with saline (Figure 3.5C) and Dox (Figure 3.5D) revealed a significant main effect of current injection [saline: $F_{(10, 80)} =$

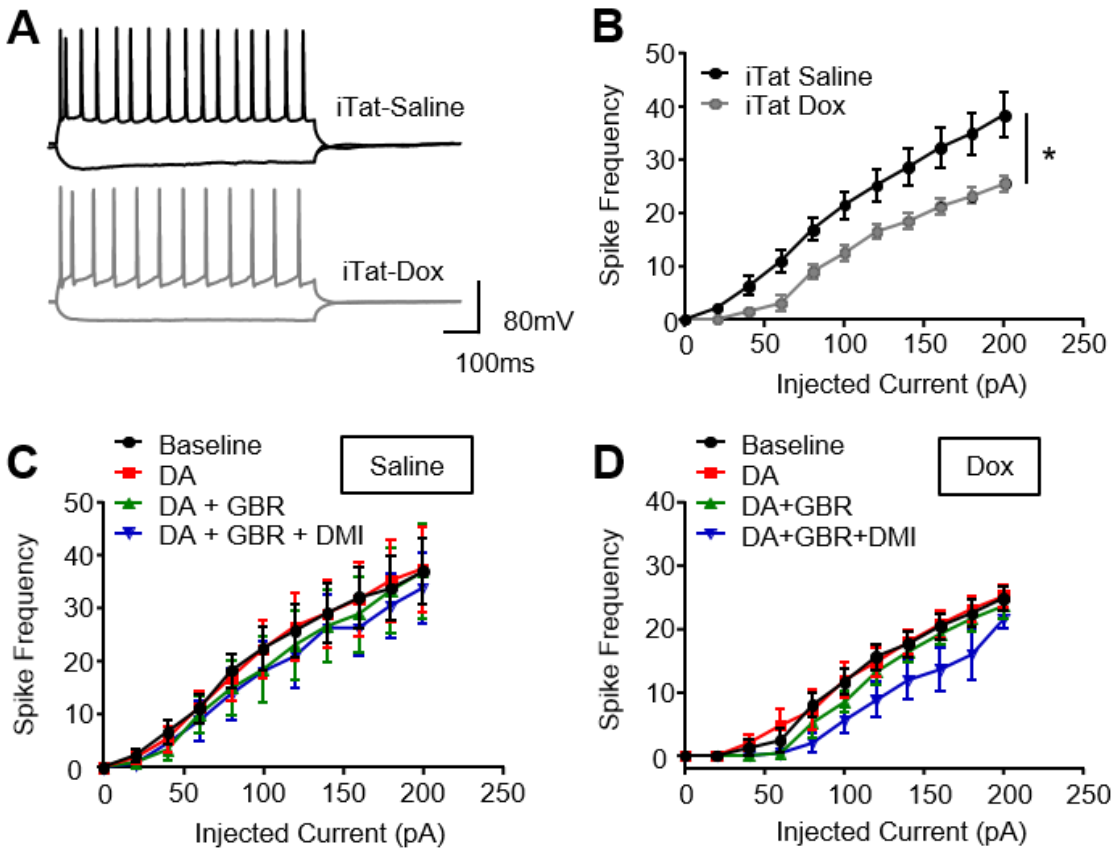

Figure 3.5 Whole-cell patch clamp electrophysiology was performed in layer V pyramidal neurons of the prelimbic region of PFC in iTat-tg mice following 7-day administration of saline or Dox. Coronal slices (300 µm) containing the prelimbic cortex were cut with a Vibratome and incubated in an ice-cold artificial CSF (aCSF) solution at 32–34°C for 45 min and kept at 22–25°C thereafter, until transfer to the recording chamber. (A) Representative traces from iTat-tg mice treated with saline (iTat-Saline) and Dox (iTat-Dox) following hyperpolarizing (-200 pA) and depolarizing (+200 pA) current steps. Summary of basal action potential frequency (B) and action potential frequency in response to acute application of DA (10 nM) or DA + GBR 12909 (100 nM) or DA + GBR 12909 + DMI (1 µM) of neurons from iTat-tg mice treated with saline (C) or Dox (D). * $p < 0.05$, n=15 and n=8 for saline and Dox treated mice, respectively.

21.17, p <0.0001; Dox: $F_{(10, 40)}$ = 145.4, p <0.0001]; however, neither saline- or Dox-treated mice displayed a significant main effect of drug exposure [saline: $F_{(3, 24)}$ = 1.005, p =0.4; Dox: $F_{(3, 12)}$ = 1.945, p = 0.18]. Although the current injection × drug exposure interaction was not significant in saline-treated mice [$F_{(30, 240)}$ = 0.788, p = 0.78], Dox-treated mice displayed a significant interaction between current injection × drug exposure [$F_{(30, 120)}$ = 1.571, p = 0.05].

3.4 DISCUSSION

The current study investigated the mechanism by which inducible Tat expression influences dopaminergic transmission in the PFC of iTat-tg mice. We have demonstrated that *in vitro* HIV-1 recombinant Tat_{1-86} protein reduces [^{3}H]DA uptake though DAT in cells (Midde et al., 2013; Midde et al., 2015; Quizon et al., 2016; Sun et al., 2017) and rat striatal synaptosomes (Zhu et al., 2009b). Our current results show that the V_{max} of [^{3}H]DA uptake through both DAT and NET was decreased in the PFC of iTat-tg mice following 7- or 14-day Dox-induced Tat_{1-86} expression. We also observed corresponding decreases in the B_{max} of [^{3}H]WIN35,428 and [^{3}H]Nisoxitine binding in this region, suggesting that the inhibitory effects of *in vitro* Tat on DAT and NET function can be replicated in the PFC of the iTat-tg mouse model with *in vivo* biological Tat expression. Moreover, we also observed increased DA and DOPAC tissue content in the iTat-tg mice, which was again selective to the PFC, suggesting a neuroadaptive change in the DA system, perhaps in compensation for iTat protein-induced inhibition of DAT and NET function.

The most intriguing observation is that the V_{max} for DA uptake via DAT or NET in the PFC was decreased (~30%) in iTat-tg mice following 7- or 14-day administration of Dox, whereas no differences in V_{max} were observed in the striatum or hippocampus of the iTat-tg mice between saline- and Dox-treated subjects. In addition, no differences in V_{max} were found in these brain regions between saline- and Dox-treated subjects in the control G-tg and C57BL/6J mouse lines. These findings suggest that the Dox-induced Tat reduces DA transport in the PFC by inhibiting both DAT and NET in a region-specific manner. Moreover, following 7-day Dox treatment, the B_{max} value for [^{3}H]WIN 35,428 labeled DAT binding sites in the PFC was decreased by 28% in iTat-tg mice, which is comparable to the magnitude of the decrease in V_{max} for DAT, whereas the B_{max} value for [^{3}H]Nisoxetine labeled NET binding sites in the PFC was decreased by 35%, which was slightly more than the observed decrease in the V_{max} for NET. Interestingly, DA uptake turnover (V_{max}/B_{max}), the efficacy of DA molecules being transported per second per uptake site (Lin et al., 2000), was not altered in the PFC of iTat-tg mice, which is consistent with our previous results showing no change in DA uptake turnover following *in vitro* exposure of rat synaptosomes to Tat (Midde et al., 2012). The efficacy of DA uptake largely depends on DAT expression in the plasma membrane, which is dynamically modulated by a trafficking mechanism (Zhu and Reith, 2008). Results from the surface biotinylation assay did not find any difference in total and plasma membrane expression of DAT or NET in the PFC in iTat-tg mice between Dox- and saline-treated groups, suggesting that the reductions in V_{max} and B_{max} are

not due to Tat-induced transporter protein degradation or surface transporter trafficking. We have demonstrated that DA transport to cytoplasmic pool via DAT is a dynamic conversion of the transporter's conformation between the three states (outward-open, outward-occluded, and inward-open) (Yuan et al., 2016) and that the Tat protein allosterically regulates DAT activity by binding to DAT in the outward-open state (Yuan et al., 2015; Zhu et al., 2018). Considering that DAT and NET share similar binding residues for Tat based on computational and homology modeling (Yuan et al., 2016), the Dox-induced Tat expression could reduce both V_{max} and B_{max} for DAT/NET by interfering with the Tat-DAT/NET binding sites and inducing a conformational change of DAT/NET from the outward-open state to the outward-occluded state.

The equivariant expression of inducible Tat protein across all brain regions in the iTat-tg mice subjected to 7 days of 100 mg/kg/day Dox treatment has been confirmed by detecting Tat mRNA (Kim et al., 2003) and Tat immunoblotting (Carey et al., 2012). A caveat, however, it is unclear what is the actual concentration of Dox-induced Tat expression is at or around the synaptic terminals, and how this effective concentration of Tat might be reflected in the brain of HIV-infected patients remains unclear, as most studies investigating the inhibitory effects of Tat on monoamine transporters are performed *in vitro* using recombinant Tat. For example, exposure to 140 nM recombinant Tat_{1-86} induces about 30% reduction of DA uptake in cells expressing wild-type hDAT (Midde et al., 2013; Midde et al., 2015; Quizon et al., 2016; Sun et al., 2017) and brain synaptosomes (Zhu et al., 2009b). One study reported that a detectable Tat

concentration in frontal cortical brain samples from HIV-1-infected patients is about 140 pmol (Hudson et al., 2000), which is 1000-fold lower than *in vitro* recombinant Tat used in reported studies. The Dox treatment of 100 mg/kg used in this study has been shown to induce ~ 1 ng/mL Tat concentration in the iTat-tg mouse brain (Kim et al., 2003), which is comparable to Tat protein levels detected in sera of HIV+ patients (Westendorp et al., 1995; Xiao et al., 2000). Nevertheless, our studies with *in vitro* and *in vivo* Tat exposure provide molecular insight into the mechanisms underlying Tat-induced dysregulation of dopaminergic transmission via DAT and NET.

Consistent with the decreased V_{max} for DAT and NET in PFC, the current study found an increase in the tissue content of DA and DOPAC in the PFC of iTat-tg mice 24 h after 7-day administration of Dox. Similar studies have demonstrated increased DA content in the caudate putamen of iTat-tg mice 3 days after completing a 7-day Dox regiment (Kesby et al., 2016a), but decreased ratios of DOPAC/DA in the same region 10 days after completing a 7-day Dox regiment without changes in this ratio in PFC (Kesby et al., 2016b). Regarding these results, effects of Tat on DA tissue content in specific brain regions may be influenced by different Dox regiments and the timing of brain collection after Dox treatment. Levels of extracellular DA in the synaptic cleft are controlled by reuptake via plasma membrane transporters and presynaptic vesicle-mediated release. Indeed, we have demonstrated that *in vitro* exposure to Tat inhibits DA uptake via the vesicular monoamine transporter-2 (Midde et al., 2012), which is responsible for monoamine storage and the vesicle-mediated DA release.

Therefore, a very complex influence of Tat protein on the DA system should be taken into consideration when we evaluate the actual DA levels in iTat-tg mice after Dox-induced Tat expression. Given that the DA content reflects the tissue levels of total DA rather than the specific extracellular DA levels, monitoring release and uptake dynamics of endogenous DA levels in iTat-tg mice by an electrochemical technique (e.g. fast scan cyclic voltammetry) is an interesting topic for future investigation.

Another important finding from the current study is that the inhibitory effects of Tat on the kinetic parameters of DA uptake through DAT/NET and the respective substrate binding sites are selective to the PFC. There are several possible explanations for our observations. First, compared to the PFC, the striatum and hippocampus exhibit a higher density of DAT and NET (Horn, 1973b; Raiteri et al., 1977; Borgkvist et al., 2012), which may provide protection from the acute inhibitory effects of HIV-1 Tat on transporter function. Second, HIV-1 Tat may be not expressed throughout different brain regions. Although a previous report showed Tat immunoreactivity was expressed throughout brain of the Tat transgenic mice (Carey et al., 2012), the exact concentration of biological Tat in these brain regions remains unclear. Indeed, our previous study has reported that HIV-1 Tat inhibits DAT function in a concentration-dependent manner (Zhu et al., 2009b). Third, with regards to HIV-1 Tat-induced decrease in DA transport through NET, the NET in the PFC is more concentrated than the DAT and plays a primary role in reuptake of DA (Moll et al., 2000; Moron et al., 2002). For these reasons, it is possible that HIV-1 Tat-induced dysfunction of the

DA system in the PFC could be mediated by inhibition of both DAT and NET. In the early stages of HIV-1 infection, the cognitive impairments associated with the PFC is initially observed (Everall et al., 1991; Melrose et al., 2008), whereas the severe damage such as degradation of the dopaminergic terminals is observed in the striatal area in the late stages of HIV-1 infected patients (Wang et al., 2004; Chang et al., 2008). Moreover, volume loss and thinning of the PFC are found in the patients with AIDS, which is associated with the severity of cognitive impairments (Thompson et al., 2005), suggesting that the PFC is more vulnerable to HIV infection compared to other regions. Thus, the current findings demonstrate that the inhibition of DAT/NET specifically in the PFC may play an important role in mediating Tat-induced neurocognitive impairment observed in HAND".

Whole-cell patch clamp recordings show that the evoked basal action potential firing from layer V pyramidal neurons of the prelimbic cortex is reduced in iTat-tg mice treated with Dox compared to saline controls. This reduced neuronal firing is unlikely to have resulted from the Tat-induced decrease in DA uptake via DAT and NET since DA at the low concentration used in our experiments has no effect on action potentials and previous studies indicate that higher concentrations of DA increase membrane excitability in striatal as well as prefrontocortical projection neurons (Hopf et al., 2003; Ortinski et al., 2015; Buchta et al., 2017; Lahiri and Bevan, 2020). Conversely, reduced neuronal firing is unlikely to have caused a deficit in DAT function via effects on membrane potential, since membrane hypoexcitability has been linked to surface expression

of DAT (Richardson et al., 2016). Finally, DAT-mediated translocation of Na^+ ions across the plasma membrane is not expected to have a pronounced impact on either the membrane potential or spike firing and a trend towards reduced action potential firing with desipramine of AMPA-mediated currents and voltage-gated Ca^{2+} channels (Koncz et al., 2014). Together, these observations suggest that decreased action potential firing of prelimbic cortex pyramidal neurons in iTat-tg mice is not directly related to Tat effects on DA transport. HIV-1 Tat may, however, affect action potential generation through mechanisms independent of DA uptake with a variety of bi-directional effects reported by previous studies (Krogh et al., 2014; Ngwainmbi et al., 2014; Francesconi et al., 2018; Mohseni Ahooyi et al., 2018).

In conclusion, the current findings provide a novel evidence that HIV-1 Tat protein decreases the V_{max} pf [^{3}H]DA uptake and the respective substrate binding sites in the PFC of iTat-tg mice by inhibiting both DAT and NET, which may have important implications for preclinical studies if the role of the prefrontal DAT/NET in neurocognitive impairment observed in HAND. Considering HIV-1 Tat interacting with allosteric modulatory binding sites on these transporters (Zhu et al., 2011; Sun et al., 2017), the current study provides a biological basis for developing allosteric modulators that specifically block Tat binding on these transporters with minimal effect on physiological DA transport, which may have potential for therapeutic application in Tat-induced dysregulation of dopaminergic transmission and its associated cognitive deficits observed in HIV-1 infected patients.

CHAPTER 4

Y88F MUTANT DOPAMINE TRANSPORTER EXPRESSING MICE ATTENUATE HIV-1 TAT-MEDIATED INHIBITION OF DOPAMINE UPTAKE AND LEARNING AND MEMORY DEFICITS IN A TRANSGENIC MOUSE MODEL[3]

[3] Strauss, M., McQuillen, P. Xiao, Z., Farmaki, E., & Zhu, J (2020). Y88F mutant dopamine transporter expressing mice attenuate HIV-1 Tat-mediated inhibition of dopamine uptake and learning and memory deficits in a transgenic mouse model. *In preparation for submission to The Proceeding of the National Academy of Sciences*.

ABSTRACT: Abnormal dopaminergic transmission has been implicated in the neuropathogenesis of HIV-associated neurocognitive disorders. Inducible HIV-1 trans-activator of transcription (Tat) transgenic (iTat-tg) mice display deficits in learning and memory similar to those observed in HAND patients. We previously reported that dopamine (DA) uptake through the DA transporter (DAT) in the prefrontal cortex (PFC) is significantly reduced in these mice. Furthermore, our previous *in vitro* work has demonstrated that HIV-1 Tat inhibits the DAT through a direct allosteric interaction with specific residues on the DAT, and that mutation of these residues can attenuate HIV-1 Tat-mediated inhibition. In order to determine if this phenomenon could be replicated *in vivo*, and to examine the extent to which attenuation of HIV-1 Tat-mediated inhibition of the DAT would prevent the cognitive deficits observed in these mice, we generated a mutant tyrosine88 to phenylalanine (Y88F) DAT expressing mouse model. The Y88F DAT mice do not demonstrate any baseline differences in [^{3}H]DA uptake, [^{3}H]WIN 35,428 binding, total DAT expression, or locomotor activity compared to WT DAT controls, except for a small increase in DA uptake affinity in the striatum. This mouse line was crossed with the iTat-tg mice resulting in a model which is capable of biologically expressing HIV-1 Tat and also possesses the mutant Y88F DAT mutant (iTat-tg/Y88F). In contrast to the iTat-tg/WT mice, the iTat-tg/Y88F mice did not demonstrate any reduction in DA uptake through DAT in the PFC, or deficits in the acquisition of Novel object recognition. Our findings indicate that preventing the HIV-1 Tat/DAT interaction, via a single point mutation

on the DAT, is sufficient to attenuate HIV-1 Tat-mediated inhibition of DAT in the PFC and learning and memory deficits previously observed in this mouse model.

4.1 INTRODUCTION

Despite the widespread use of efficacious combinatorial antiretroviral therapy (cART) to control peripheral HIV infection and improve and extend the lives of Human Immunodeficiency Virus (HIV) patients, HIV-associated neurocognitive disorders (HAND) continue to remain prevalent and pose a significant health problem. HAND constitutes a group of neurological complications including cognitive dysfunction, motor deficits, and dementia (Heaton et la., 2010). These disorders manifest largely because most cART medications do not cross the blood-brain barrier, while infected macrophages carrying the virus can (Buckner et al., 2006), leaving the central nervous system (CNS) as a reservoir for HIV viral replication (Valcour et al., 2012). Considerable evidence has demonstrated that this long-term viral protein exposure can accelerate damage to the mesocorticolimbic dopamine (DA) system (Nath et al., 1987; Berger and Arendt, 2000; Koutsilieri et al., 2002; Wang et al., 2004). Furthermore, converging lines of clinical observations, supported by imaging (Wang et al., 2004; Chang et al., 2008), neuropsychological performance testing (Kumar et al., 2011; Meade et al., 2011), and postmortem examinations (Gelman et al., 2012), have demonstrated that DA dysregulation is correlated with the abnormal neurocognitive function observed in HAND (Berger and Arendt, 2000; Purohit et al., 2011). Among HIV viral proteins, the trans-activator of transcription (Tat) protein has been demonstrated to play a central role in the neurotoxicity

and cognitive impairment evident in HAND (King et al., 2006), and has been detected in DA-rich brain areas (Gray et al., 2014), as well as in the cerebral spinal fluid of patients diagnosed with HAND (Hudson et al., 2000), even those receiving cART (Johnson et al., 2013).

The inducible HIV-1 Tat transgenic (iTat-tg) mouse has been utilized as a clinically relevant model of symptomatic HAND, as it recapitulates many aspects of the neuropathologies and neurocognitive impairments observed in the human population (Kim et al., 2003; Carey et al., 2012). Our recent work (Strauss et al., 2020) has revealed that this mouse model also demonstrates the characteristic dysregulation of the dopaminergic system observed in HAND, specifically through inhibition of the DA transporter (DAT) in the prefrontal cortex (PFC). DAT-mediated DA reuptake is critical for maintaining normal DA homeostasis. Human DAT (hDAT) activity is strikingly reduced in HIV-1-infected patients, particularly those with a history of cocaine abuse, correlating with the severity of HIV-1 associated cognitive deficits (Wang et al., 2004; Chang et al., 2008). Our previous *in vitro* work has shed light on the molecular mechanism of HIV-1 Tat-mediated inhibition of DAT-mediated DA uptake (Midde et al., 2013; Midde et al., 2015; Quizon et al., 2016). Through a computational modeling and experimental validation approach we have shown HIV-1 Tat inhibits DAT activity through a direct allosteric interaction involving several distinct residues on the DAT. One specific residue we have identified is DAT Tyrosine88 (Y88). We demonstrated that mutation of this residue from a tyrosine to a phenylalanine (Y88F) did not alter basal transporter function or expression (Midde et al., 2015) *in vitro*.

Furthermore, this mutation was capable of attenuating the inhibitory effects of recombinant HIV-1 Tat on DAT-mediated DA uptake through the disruption of a hydrogen bond between this residue and HIV-1 Tat lysine19.

These findings raise two critical questions. First, could the ability of the Y88F DAT mutant to attenuate HIV-1 Tat-mediated inhibition of DA uptake be replicated in the iTat-tg mouse model? And second, what effect would this attenuation have on the cognitive deficits observed in these mice? We have generated a mouse model which genetically expresses a mutant Y88F DAT. The Y88F DAT mouse line was then crossed with the iTat-tg mouse line to generate mice which expressed the Y88F DAT mutation, and were also capable of inducible HIV-1 Tat expression (iTat-tg/Y88F). This mouse line was used in the current study to answer these questions.

4.2 MATERIALS AND METHODS

4.2.1.1 Animals

Four distinct mouse lines were used in the current investigation and are abbreviated throughout the manuscript as follows: C57BL/6J mice, obtained from Jackson laboratories, referred to as C57; $Y88F^{+/+}$ homozygous DAT mice which were generated from a C57 background and developed as described below, referred to as Y88F; the inducible HIV-1 Tat transgenic mouse line, originally developed by Dr. Johnny He, referred to as iTat-tg/WT, and the mouse line which was generated by crossing the iTat-tg and Y88F mouse lines and contains the components of both, referred to as iTat-tg/Y88F.

Mice used for all experiments were between the age of 9-14 weeks. Mice were housed (4-5 mice/cage) in a temperature (21 ± 2 °C)- and humidity (50 ± 10%)-controlled vivarium, which were maintained on a 12:12 h light/dark cycle (lights on at 07:00 h) with *ad libitum* access to food and water. Animals were maintained in accordance with the Guide for the Care and Use of Laboratory Animals under the National Institute of Health (NIH) guidelines in the Assessment and Accreditation of Laboratory Animal Care accredited facilities. The experimental protocol was approved by the Institutional Animal Care and Use Committee (IACUC) at the University of South Carolina, Columbia.

4.2.1.2 Y88F DAT mice

Heterozygous Y88F dopamine transporter (DAT) mutant mice were originally generated by Ingenious targeting laboratory (Ronkonkoma, NY) utilizing an embryonic stem cell targeting approach which is detailed in the results section "Generation of a mutant Y88F DAT mice". The heterozygous F1 mice generated by Ingenious were transferred to the animal vivarium at the University of South Carolina, where they were subsequently mated to generate homozygous Y88F mice ($Y88F^{+/+}$). The identification of $Y88F^{+/+}$ mice was determined by PCR which is described below.

4.2.1.3 iTat-tg mice

Male iTat-tg mice breeding stock were provided by Dr. Jay P. McLaughlin at the University of Florida College of Pharmacy (Gainesville, FL). Mice in this colony were established from progenitors originally derived by Dr. Johnny J. He (Kim et al., 2003), currently at the Rosalind Franklin University of Medicine and

Science (Chicago, IL). The iTat-tg mouse line genetically expresses a “tetracycline-on (TETON)” system, which is integrated into the regulator for the astrocyte-specific glial fibrillary acidic protein (GFAP) promoter and coupled to the Tat_{1-86} coding gene, allowing astrocyte (brain)-specific Tat_{1-86} expression induced by doxycycline (Dox) administration (Kim et al., 2003).

4.2.1.4 iTat-tg/Y88F mice

The hybrid iTat-tg/Y88F mice were generated by crossing the two mouse lines described above. A detailed explanation of this process is outlined in the Results section “Generation of mutant Y88F DAT mice” and the detailed PCR protocol is outlined in the “PCR genotyping” section of the Materials and Methods section.

4.2.2 PCR

The PCR protocols for identification of homozygous Y88F (+/+) mice were adapted from the procedures given to us from Ingenious at the time we received the founding six animals. PCR testing for the iTat-tg transgenes was adapted from the original description of this transgenic mouse line (Kim et al., 2003). Each mouse was ear-tagged and tail-clipped between three and four weeks of age. The tail clip was placed into a tube containing 200 µL of tail buffer (10mM Tris HCl, 100mM NaCl, 10mM EDTA, 0.5% SDS) which contained 0.75 mg/mL of proteinase K. The tails in solution were placed in a 56 °C water bath overnight. The following morning the samples were heated to 95 °C on a dry heater for 5 minutes to deactivate the proteinase K. The samples were then spun down to pellet any undissolved tissue, and these samples were subsequently utilized for

PCR analysis. To test the zygosity of the Y88F mutation, 1 µL of sample was placed into 23 µL of PCR solution which contained 10.47 µL of ddH_2O, 6.5 µL Betaine, 0.325 µL DMSO, 2.5 µL 10X PCR buffer, 2 µL $MgCl_2$, 0.5 µL of 200 µM dNTPs, 0.5 µL of 100 µM primer mix (FWD, NDEL1: 5' – ACT CAG GGG TGC AGT GGA GG – 3' and RVS, NDEL2: 5' – AAG CAG CCC CAC TAT CCT ACA GG – 3'), and 0.2 µL of Taq polymerase. This solution was ran using the following PCR parameters: 94 °C for 3 min once, followed by 30 cycles of 94 °C for 30 sec, 60 °C for 30 sec, and 72 °C for 1 min, then held at 4 °C until ready to load into a gel. The resulting PCR samples were loaded into a 2% agarose gel and ran on 80V for 30 min. A band at 420 bp was associated with WT DAT and a band at 522 bp was associated with the Y88F mutation. Therefore, if only one of the bands was present the mouse was determined to be homozygous (-/- if at 420 and +/+ if at 522) for the Y88F mutation or if both bands were present the mouse was determined to be heterozygous for the mutation (see figure 4.1A for example). These mice were additionally tested to verify that a TAC to TTC point mutation was introduced. For this PCR the following conditions were utilized: 1 µL of sample was placed into a PCR tube with 19 µL of PCR solution which contained 11.25 µL of ddH_2O, 4 µL of PCR buffer, 2 µL of MgCl2, 0.5 µL of 200 µM dNTPs, 1 µL of 100 µM primer mix (FWD, SQ1: 5' – GGG ACC AAT GTC TTC TGT GG – 3' and RVS, RNEOGT: 5' – GAA AGT ATA GGA ACT TCG CGA CAC GGA C – 3'), and 0.25 µL of Taq Flex polymerase. This solution was ran using the following PCR parameters: 94 °C for 3 min once, followed by 30 cycles of 94 °C for 30 sec, 55 °C for 30 sec, and 72 °C for 1 min, then held at 4 °C until

ready to load into a gel. The resulting PCR samples were loaded into a 2% agarose gel and ran on 80V for one hour. A band at 771 bp indicated that the point mutation was present (see figure 4.1B for example).

Once homozygous Y88F (+/+) mice were obtained we began to cross this line with the iTat-tg mice as described in the Results section “Generation of mutant Y88F DAT mice”. The efficacy of PCR primers to detect the presence of the Teton-GFAP and TRE-Tat86 transgenes was tested using the following PCR parameters: 1 µL of sample was placed into a PCR tube with 19 µL of PCR solution which contained 11.25 µL of ddH_2O, 4 µL of PCR buffer, 2 µL of MgCl2, 0.5 µL of 200 µM dNTPs, 1 µL of 100 µM primer mix (Teton-GFAP FWD: 5’ – GCT CCA CCC CCT CAG GCT ATT CAA – 3’ and RVS: 5’ – TAA AGG GCA AAA GTG AGT ATG GTG 3’; and TRE-Tat86 FWD: CGG TGG GAG GCC TAT ATA AGC 3’, and RVS: 5’ – AAC TGC AGT TAT TCC TTC GGG CCT GTC GG – 3’), and 0.25 µL of Taq Flex polymerase. This solution was ran using the following PCR parameters: 94 °C for 3 min once, followed by 30 cycles of 94 °C for 30 sec, 55 °C for 30 sec, and 72 °C for 1 min, then held at 4 °C until ready to load into a gel. The resulting PCR samples were loaded into a 2% agarose gel and ran on 80V for one hour. A band at 250 bp indicated the presence of the TRE-Tat86 gene and a band at 420 bp indicated the presence of the Teton-GFAP gene (see figure 4.3A/B for example). Following initial testing the levels of gene expression were determined using qPCR. 0.5 µL of tail sample was placed into a 384 well plate which also contained 4.95 µL of 2XSYBR Green Mix, 0.5 µL of 10 µM Primer mix (as noted above for PCR) and 3.95 µL of ddH_2O. The plate

was then sealed with plastic, spun down, and ran using the following parameters: Initial denaturation at 94 °C for 2 min followed by 40 cycles of 94 °C for 15 sec and 60 °C for 1 min. Results were interpreted using CFX manager software and were compared to iTat-tg mouse transgene expression levels using the ΔΔCq calculation method. Mice which expressed both transgenes at similar levels as the iTat-tg/WT mice were considered to have adequate expression levels of these genes to be used for breeding/experimentation.

4.2.3 Drug administration and Synaptosomal preparation

Male iTat-tg, C57BL/6J, Y88F, and iTat-tg/Y88F mice were administered either Dox (100 mg/kg/day) or saline (10 µl/gram body weight) via intraperitoneal injection for 7 consecutive days. The optimized dose of Dox was chosen because it has been previously proven efficacious for induction of Tat (Zou et al., 2007; Carey et al., 2012; Paris et al., 2014b) and findings showing that iTat so induced is biologically active during the period of behavioral testing (Zou et al., 2007). The 7-day Dox or saline treatment paradigm was chosen for the kinetic analysis of DA uptake and behavioral testing based on the previous physiological and behavioral studies (Strauss et al, 2020; Carey et al., 2012). Selection of animals for saline or Dox treatment was made randomly among littermates.

All mice were rapidly decapitated 24 h after last saline or Dox injection. Brain tissue dissected from prefrontal cortex (PFC, prelimbic and infralimbic cortices combined) and striatum, and was pooled from a group of three mice for [^{3}H]DA uptake and [^{3}H]WIN 35,428 binding (constituting a single sample for each region), which was used as a single replicate (*n*) for conducting independent

experiments. Thus, "*n*" refers the number of independent experiments conducted, rather than the number of mice used. Synaptosomes were prepared using our published method (Strauss et al., 2020). The PFC region was a focus of the current study because it is a critical brain region for higher cognitive function (Miller and Cohen, 2001; Dalley et al., 2004; Ridderinkhof et al., 2004). Given that DA uptake through DAT is not identical throughout various brain regions, the DA uptake through DAT in striatum was examined in addition to the PFC. The striatum was also selected due to its central role in DA neurotransmission. The tissue was homogenized immediately in 20 mL of ice-cold 0.32 M sucrose buffer containing 2.1 mM of NaH_2PO_4 and 7.3 mM of Na_2HPO_4, pH 7.4; with 16 up-and-down strokes using a Teflon pestle homogenizer (clearance approximately 0.003 in.). Homogenates were centrifuged at 1,000g for 10 min at 4°C and the resulting supernatants were then centrifuged at 12,000g for 20 min at 4°C. The resulting pellets were resuspended in the respective buffer for each individual assay as noted below.

4.2.4 Kinetic analysis of synaptosomal [^{3}H]DA uptake assay

To determine the effects of the mutant Y88F DAT on DA uptake compared to WT DAT, and to assess if this mutation would result in attenuation of HIV-1 Tat-mediated inhibition of DA uptake via DAT in the PFC, the maximal velocity (V_{max}) and Michaelis-Menten constant (K_m) of synaptosomal [^{3}H]DA uptake were examined using a previously described method (Strauss et al., 2020). Because DA is transported by DAT, NET, and SERT in the PFC (Moron et al., 2002; Williams and Steketee, 2004), kinetic analysis of [^{3}H]DA uptake via DAT in the

PFC was assessed in the presence of desipramine (1 µM) and fluoxetine (0.1 µM) to prevent DA uptake into norepinephrine- and serotonin-containing nerve terminals, respectively. In brief, the resulting pellets described above were resuspended in Krebs-Ringer-HPES assay buffer (125mM NaCl, 5mM KCl, 1.5mM $MgSO_4$, 1.25mM $CaCl_2$, 1.5mM KH_2PO_4, 10mM glucose, 25mM HEPES, 0.1mM EDTA, 0.1mM pargyline and 0.1mM L-ascorbic acid, saturated with 95% O_2 / 5% CO_2, pH 7.4). Aliquots of synaptosomal tissue (50µg/25 µL) were incubated with one of 6 mixed [^{3}H]DA concentrations containing a range of DA concentrations (1nM - 1µM) and fixed [^{3}H]DA (12nM) for 8 minutes at 37 °C. Incubation was terminated by the addition of 3mL of ice-cold assay buffer, followed by immediate filtration through Whatman GF/B glass fiber filters (presoaked with 1mM pyrocatechol for 2h). Filters were washed three times with 3mL of ice-cold assay buffer using a Brandel cell harvester (Model MP-43RS; Biochemical Research and Development Laboratories Inc., Gaithersburg, MD). Radioactivity was determined by liquid scintillation spectrometry (Model B1600TR, Packard Corporation Inc., Meriden, CT). Bovine serum albumin was used as a standard (Bradford, 1976) to measure protein concentration for all samples. Nonspecific uptake of [^{3}H]DA into DAT was determined in the presence of 10 µM Nomifensine.

4.2.5 [^{3}H]WIN 35,428 binding

[^{3}H]WIN 35,428 represents the substrate binding site on the DAT. To determine the effects of the mutant Y88F DAT on substrate binding sites compared to WT DAT, [^{3}H]WIN 35,428 binding was examined using our

previously described method (Strauss et al., 2020). Saturation binding assays were conducted in duplicate in a final volume of 250 µL for PFC, striatum. 50 µL aliquots (50 µg protein) of synaptosomes were incubated in 0.32M sucrose buffer (pH: 7.4) containing 2.1 mM NaH_2PO_4 and 7.3 mM Na_2HPO_4 with six concentrations of [^{3}H]WIN 35,428 (1, 5, 10, 15, 25, 30 nM) on ice for 2 h. Desipramine (1 µM) was included to inhibit [^{3}H]WIN 35,428 binding to the NET in the PFC. Nonspecific binding was determined in the presence of 10 µM cocaine in the striatum and 10 µM nomifensine in the PFC. The reaction was terminated by rapid filtration onto Whatman GF/B glass filter filters, presoaked for 2 h with assay buffer containing 10% polyethylenimine, through a Brandel cell harvester (Model MP-43RS; Biochemical Research and Development Laboratories Inc., Gaithersburg, MD). Filters were washed three times with 3 mL of ice-cold assay buffer. Radioactivity was determined by liquid scintillation spectrometry (Model B1600TR, Packard Corporation Inc., Meriden, CT), and bovine serum albumin (Sigma-Aldrich; St. Louis, MO) was used as a standard (Bradford, 1976) to measure protein concentration for all samples.

4.2.6 Western blotting

Synaptosomal preparations which were used for DA uptake were stored at -80 with protease inhibitors and subsequently thawed and subjected to gel electrophoresis and western blotting to obtain immunoreactive DAT bands. Samples were separated by 10% SDS-polyacrylamide gel electrophoresis for ~90 min at 125V. Samples were then transferred to Immobilon-P transfer membranes (0.45 µm pore size) in transfer buffer (50 mM Tris, 250 mM glycine,

3.5 mM SDS) using a Mini Trans-Blot Electrophoretic Transfer Cell for 90 min at 75 V. The membranes were then incubated with blocking buffer (5% milk powder in PBS containing 0.5% Tween-20) for 1 h at room temperature, followed by incubation with either goat anti-DAT (Santa Cruz, C-20 polyclonal antibody, diluted 1:500 in blocking buffer) overnight at 4 °C. Transfer membranes were then washed three times with blocking buffer at room temperature followed by incubation with anti-goat-HRP (Jackson Laboratory, catalog number 305-035-045 diluted 1:10,000 in blocking buffer) for 1 h at room temperature. Membranes were then washed an additional three times in PBS containing 0.5% Tween-20 (Sigma-Aldrich; St. Louis, MO). Immunoreactive proteins on the transfer membranes were detected using Amersham ECL prime western blotting detection reagent (GE life sciences; Chicago, IL) and developed on Hyperfilm (GE life sciences; Chicago, IL). After detection and quantification of DAT, each blot was washed and re-probed with rabbit anti-Calnexin (Santa Cruz, Biotechnology, catalog number SC-11397 polyclonal antibody, diluted 1:10,000 in blocking buffer), an endoplasmic reticular protein, to monitor protein loading between all groups. Multiple autoradiographs were obtained using different exposure times, and immunoreactive bands within the linear range of detection were quantified by densitometric scanning using Scion image software. Band density measurements, expressed as relative optical density, were used to determine levels of DAT.

4.2.7 Behavioral Assays

4.2.7.1 Locomotor activity

As locomotor activity in mice is dependent on both motivation and movement capability, which may be impacted by the dopaminergic system, locomotor activity was compared between Y88F and WT (C57BL/6J) mice to determine if the Y88F DAT mutation had any effect on this outcome. The activity monitors were 16” x 16” square plexiglass chambers that detect free movement of animals by infrared photocell interruptions. This equipment uses an infrared photocell grid with 32 emitter/detector airs to measure locomotor activity. All activity monitors are located in an isolated room located within the University of South Carolina vivarium. Mice were habituated to the locomotor activity chambers (San Diego Instruments) for two 60-min sessions once/day prior to testing. Twenty four hours after the second habituation session, all mice were placed into the chamber for a 60 minute session where activity was recorded and is reported as total horizontal activity.

4.2.7.2 Novel Object Recognition

Learning and memory performance was examined using the novel object recognition (NOR) assay adapted from a previous report (Carey et al., 2012). The NOR task for mice is based on their tendency to spontaneously explore their environment; unaffected animals will spend more time exploring a novel object than a familiar one (Frick and Gresack 2003). This task does not require motivation such as food or water deprivation and minimizes external and physical stressors. The NOR task probes both learning and memory function, as the final

output of the assay is affected by both. The paradigm was carried out over three phases as described in Carey et al. 2012. Each phase lasted 10 min with a 10 min inter-trial interval (ITI). During each phase, mice freely explored the environment before being returned to their home cages. During phase 1, objects A and B (e.g., pair of dice) were centered across from each other in a rectangular cage (which was identical to the home cage except that it was placed inside of a brown cardboard box to decrease distraction), 2 cm away from the walls. In phase 2, object B was moved laterally to 1 cm from the edge of the cage whereas object A remained fixed. In phase 3, after completion of the training phases, object B (the die) was replaced with a novel object (a marble). Note that phase 2 served as a control, to demonstrate that subsequent performance in phase 3 was based on novel object recognition, rather than simple changes in object location. In contrast, phase 3 testing assessed both learning and memory, as mice will typically recognize and reject previously encountered objects to spend more time with the novel object Carey et al., 2009. Use of marbles and dice as novel objects was randomized across the study. For each phase, the time mice spent attending to each object was video recorded and analyzed by a blinded team member with a stopwatch. Object attending was defined as the duration of time a mouse spent in physical contact with the object, using any body part other than the tail, or whenever it was within 0.5 cm of the object, facing it, and engaged in active exploration (e.g., sniffing or manipulating). Data are presented as a percent recognition index (RI) for object B: RI = (time attending to object B/time attending to object A+B)*100.

4.2.8 Statistical analysis

Data are expressed as means ± S.E.M., and *n* refers to the number of individual experiments for each group. To analyze the kinetic parameters (V_{max}/K_m and B_{max}/K_d) of [^{3}H]DA uptake or [^{3}H]WIN 35,428, best-fit nonlinear regression analysis using a single-site model was conducted for each individual experiment using GraphPad Prism 8 software. The kinetic parameters were then compared between either the WT (C57) and Y88F DAT expressing mice, the saline- and Dox-treated iTat-tg/Y88F mice, or the iTat-tg/WT mice using unpaired Student's *t* tests, which were conducted using IBM SPSS statistics version 25. Analyses resulting in $P < 0.05$ were considered significant.

4.3 RESULTS

4.3.1 Generation of mutant Y88F DAT mice

Heterozygous Y88F dopamine transporter (DAT) mutant mice were originally generated by Ingenious targeting laboratory (Ronkonkoma, NY) utilizing an embryonic stem cell targeting approach. This technique consisted of six distinct steps in order to generate the mutant mouse model (Figure 4.1A). First, a DNA construct was designed targeting a short homology arm of slc6a3 gene, which was suitable for PCR amplification and placement of the Neo cassette (Figure 4.1B). The construct was designed to create a point mutation of the TAC codon (correlating to tyrosine 88 of DAT) to TTC (Phenylalanine). This construct was generated using homologous recombination, which is ideal for creating single point mutations with a low risk of unwanted mutations. Second, the DNA construct was electroporated into mouse embryonic stem (ES) cells, which were

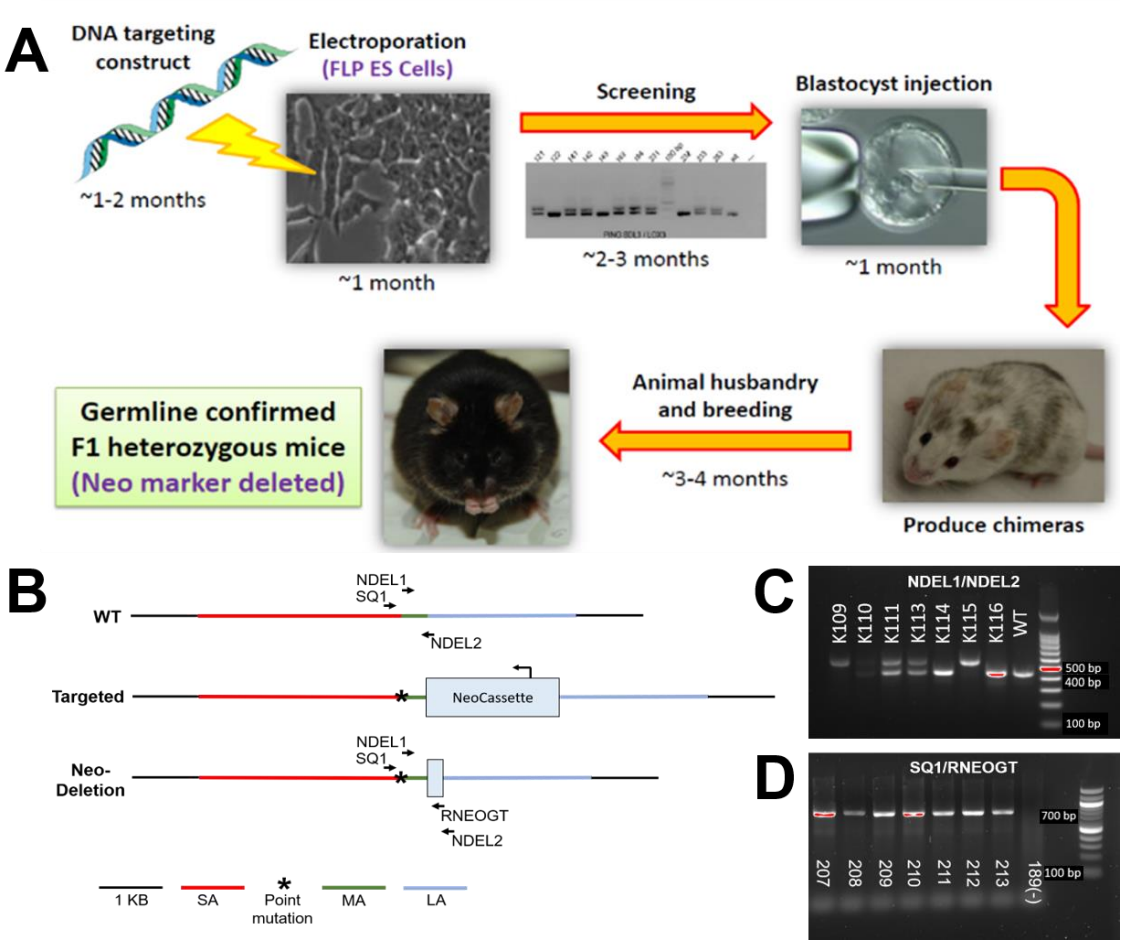

Figure 4.1 Generation of mutant Y88F DAT mouse model and PCR genotyping. (A) Schematic representation of the embryonic stem cell/blastocyst approach used by Ingenious Targeting Laboratory to generate heterozygous Y88F DAT expressing mice. (B) A 7.5 kb genomic region was first sub cloned from a positively identified C57BL/6 BAC clone (RP23-433L1) using a homologous recombination-based technique. The region was designed such that a long homology arm (LA) extends ~4.6 kb 5' to a codon exchange TAC>TTC (Tyrosine to Phenylalanine). A Neo cassette is positioned 471bp (MA; middle arm) downstream of the TTC codon. A short homology arm (SA) extends ~ 2.5 kb downstream of the Neo cassette. NDEL1 and NDEL2 represent the targets of the forward and reverse primers, respectively, which used to screen for deletion of the Neo cassette, and allow for determination of homo/heterozygosity. SQ1 and RNEOGT represent the targets of the forward and reverse primers, respectively, used to verify the presence of the point mutation. (C) Representative result of PCR gel exposure (gel red) using the NDEL1/NDEL2 primer combination. A band at 420 bp only indicates a homozygous WT mouse (example #K116), a band at 522 bp only represents a homozygous Y88F mouse (example #K115), and the presence both bands indicates a heterozygous mouse (example #K111). (D)

Representative result of PCR gel exposure (gel red) using the SQ1/RNEOGT primer combination. A band at 771 kb indicates the presence of the point mutation (#207-213) or the lack thereof (example 189, negative control). Primer sequences are shown in the PCR section of the materials and methods.

then selected based on integration of the Neo cassette into the mouse genome. The DNA from the selected ES cells was extracted and provided to the screening team for vector integration screening. Third, the screening team analyzed DNA samples by optimized PCR to identify potential positive clones and subsequent qPCR was used to assess copy number of the targeted allele. The positive ES cell clones were expanded, and genotyping was reconfirmed. Fourth, the reconfirmed clones were microinjected into mouse host blastocysts (3.5-day old mouse embryos) and the injected blastocysts were subsequently transferred into foster moms (pseudo-pregnant females). Fifth, the chimeric (F0) mice produced from the transferred embryos were assessed by coat color and medium- and high-percentage chimera mice were mated with WT mice to produce the F1 mice. Finally, tail clip DNA from F1 mice were genotyped to determine germline transmission of the target allele (heterozygous). These heterozygous F1 mice were transferred to the animal vivarium at the University of South Carolina. At this time, the heterozygous Y88F mice were mated together and screened for zygosity (Figure 4.1C) and presence of the point mutation was verified (Figure 4.1D). Homozygous mice with confirmed point mutation were mated to create a stable line of homozygous Y88F mice.

4.3.2 Y88F DAT mutant mice do not display baseline differences in dopaminergic function

DAT Tyrosine 88 (Y88) has been suggested to play a role in maintaining a conformational structure of the DAT which is prepared for conformational conversion associated with DA uptake. This role is supported by stabilization of transmembrane helix 1b (TM1b) and transmembrane helix 6a (TM6a) through hydrophobic or electrostatic intramolecular interactions (Midde et al., 2015). Additionally, the aromatic side chain of Y88 is sandwiched between TM1b and extracellular loop 4 (EL4) in a hydrophobic region. These insights indicate that mutation of Y88 to a phenylalanine (Y88F) would not be expected to have a significant effect on the function of the DAT. Our previous report (Midde et al., 2015) examined this mutation in hDAT expressing PC12 cells and found no significant alterations in DA uptake or total/surface expression of DAT. We did report small alterations in the affinity of WIN 35,428 binding, as well as substrate (DA) and inhibitor (cocaine) potencies, which may be due to slight conformational alterations near the primary substrate (S1) binding site. Taken together these results indicate that Y88F mutation to hDAT maintains relatively normal transporter function. In order to verify if similar results could be produced in the Y88F expressing mice, we performed [^{3}H]DA uptake, [^{3}H]WIN 35,428 binding, and examination of total protein expression in the prefrontal cortex (PFC) and striatum of these mice compared to WT DAT controls (C57). As shown in Table 4.1, we did not find any significant differences in the V_{max} or K_m of [^{3}H]DA uptake, the B_{max} or K_d of [^{3}H]WIN 35,428 binding, or total DAT expression in the PFC of

Y88F DAT mice compared to WT controls. In the striatum, we did identify a 32% increase in the Km of [^{3}H]WIN 35,428 binding, indicating an increased affinity at the S1 binding site, although no other significant differences were found. Finally, we assessed locomotor activity in the Y88F DAT mice compared to WT controls (Table 4.1), as locomotor activity is dependent on both motivation and movement capability, which may be impacted by the dopaminergic system, and our results demonstrate that the Y88F mice do not display any significant differences in this behavioral outcome. Taken together our results indicate that the Y88F DAT mice do not display significant alterations in DAT function, or the dopaminergic system compared to WT expressing DAT control mice.

4.3.3 Generation of iTat-tg/Y88F mouse line

Our recent publication demonstrated that following 7-day dox treatment, iTat-tg mice displayed a 27% reduction in the V_{max} of [^{3}H]DA uptake in the PFC compared to saline treated controls (Strauss et al., 2020). Additionally, our previous data has demonstrated that the Y88F DAT mutation is capable of attenuating the inhibitory effects of HIV-1 Tat on DA uptake (Midde et al., 2015) *in vitro*. Thus, the aim of our current work was to determine first, if the attenuation of HIV-1 Tat-mediated inhibition of DAT observed *in vitro* could be replicated in an animal model; second, to determine the extent to which the aforementioned attenuation would prevent cognitive deficits previously reported in this mouse model (Carey et al., 2012). To investigate these possibilities, the Y88F DAT mutant mice were crossed with the iTat-tg mice to generate hybrid iTat-tg/Y88F mice. Importantly, the iTat-tg mice require two distinct transgenes in order to

Table 4.1 Summary of V_{max} and K_m of [^{3}H]DA uptake, B_{max} and K_d of [^{3}H]WIN 35,428 binding, and total dopamine transporter expression in the prefrontal cortex and striatum of C57BL/6J and Y88F mice

	Prefrontal cortex		Striatum	
	V_{max} (pmol/min/mg)	K_m (nM)	V_{max} (pmol/min/mg)	K_m (nM)
C57BL/6J	1.34 ± 0.59	711 ± 307	47.0 ± 10	83 ± 6.1
Y88F	1.57 ± 0.28	794 ± 600	55.8 ± 6.2	110 ± 5.2*
	B_{max} (pmol/mg)	K_d (nM)	B_{max} (pmol/mg)	K_d (nM)
C57BL/6J	0.514 ± 0.036	6.26 ± 0.68	36.2 ± 3.8	37.6 ± 2.6
Y88F	0.622 ± 0.086	9.62 ± 3.6	32.2 ± 2.2	33.1 ± 6.6
	Dopamine transporter/Calnexin Expression (arbitrary units)			
C57BL/6J	1.03 ± 0.13		1.23 ± 0.057	
Y88F	0.729 ± 0.05		1.13 ± 0.076	
	Total horizontal activity (beam breaks)			
C57BL/6J	7142 ± 723			
Y88F	7737 ± 597			

Data are expressed as mean ± S.E.M. values from three to four independent experiments performed in duplicate. * $p < 0.05$, compared to C57BL/6J

produce HIV-1 Tat expression following dox treatment, the Teton-GFAP gene, which encodes the tetracycline-on system and is linked to glial fibrillary acidic protein (GFAP) expression, and the TRE-Tat86 gene, which encodes the Tat_{1-86} protein (Kim et al., 2003). During the crossing of the two mouse lines the zygosity of the Y88F DAT mutant was assessed as described in Figure 4.1, and the presence of the Teton-GFAP and TRE-Tat86 genes was determined by PCR as shown in Figure 4.2 (detailed in the materials and methods PCR section). Importantly, as the number of copies of the Teton-GFAP and TRE-Tat86 genes can vary between mice, qPCR was also used to ensure that the iTat-tg/Y88F mice possessed similar levels of the transgenes as the iTat-tg/WT mice. The crossing of these two mouse lines yielded iTat-tg/Y88F mice, which expressed both the Y88F DAT mutant as well as the two transgenes required for HIV-1 Tat expression.

4.3.4 iTat-tg/Y88F mice demonstrate attenuation of HIV-1 Tat-mediated inhibition of DA uptake

To determine if the Y88F DAT mutation was capable of attenuating our previously reported HIV-1 Tat-mediated inhibition of DA uptake through DAT in the PFC (Strauss et al., 2020) we performed [^{3}H]DA uptake following 7-day administration of saline or dox to both iTat-tg/WT and iTat-tg/Y88F mice. This experimental paradigm allowed us to investigate three key outcomes. First, we determined that our previously reported data could be replicated, as we found a significant reduction of 33% in the V_{max} of [^{3}H]DA uptake (Figure 4.3A) in the dox-treated iTat-tg/WT mice compared to the saline-treated controls [$t_{(8)} = 3.46$, $p <$

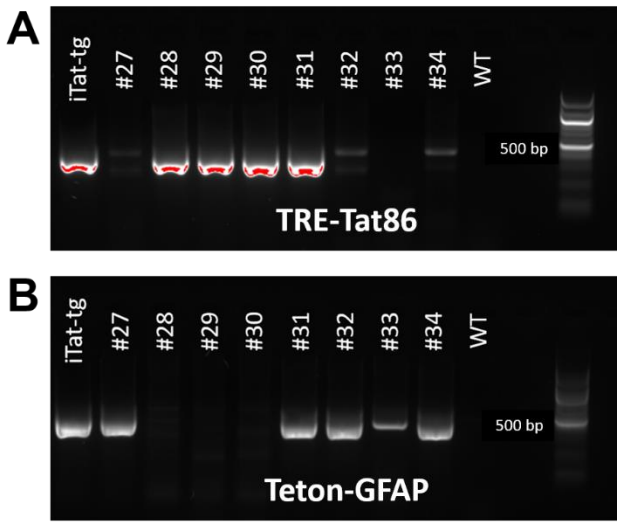

Figure 4.2 Representative PCR results for the TRE-Tat86 and Teton-GFAP genes. (A) Example PCR result for TRE-Tat86 gene expression using the TRE-Tat86 FWD and RVS primers. A band at 250 bp indicates the presence of the gene (example #28) or a lack of a band indicates the gene is not present (example #27). (B) Example PCR result for Teton-GFAP gene expression using the Teton-GFAP FWD and RVS primers. A band at 420 bp indicates the presence of the gene (example #31) or a lack of a band indicates the gene is not present (example #28). The presence of both genes is required for the mice to express the HIV-1 Tat protein following dox administration (example #31). Primer sequences are shown in the PCR section of the materials and methods.

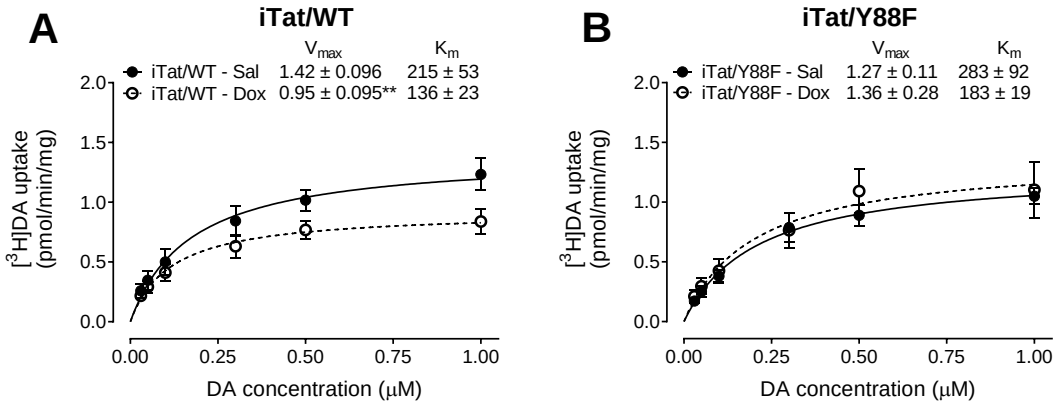

Figure 4.3 Kinetic analysis of synaptosomal [^{3}H]DA uptake in the PFC of iTat-tg/WT and iTat-tg/Y888F mice following 7-administration of saline or Dox. Synaptosomes were incubated with a range of mixed DA concentrations (0.03 – 1 μM, final concentration) containing a fixed concentration (12 nM) of [^{3}H]DA. The V_{max} and K_m values for [^{3}H]DA uptake via DAT in the PFC of iTat-tg/WT (A) and iTat-tg/Y88F (B) mice following 7-day administration of saline (black circles, solid line) or Dox (white circles, dashed line) were calculated using non-linear regression analysis with a one-site binding parameter and represent the means from five independent experiments ± S.E.M. ** $p < 0.01$ compared to saline control group.

0.01], which is similar to our previously reported decrease of 27%, with no significant difference in K_m. Additionally, we did not find any significant differences between the saline- and dox-treated iTat-tg/WT mice in striatal V_{max} (saline: 37.6 ± 3.8; dox: 35.6 ± 1.5 pmol/mg/min) or K_m (saline: 146 ± 7; dox: 145 ± 13 nM), which is consistent with our previous study (Strauss et al., 2020). Second, we did not find any significant differences in V_{max} or K_m between the saline-treated iTat-tg/WT and saline-treated iTat-tg/Y88F in the PFC (Figure 4.3A/B) or striatum (iTat-tg/WT V_{max}: 37.6 ± 3.8, iTat-tg/Y88F V_{max}: 34.0 ± 4.6 pmol/mg/min; iTat-tg/WT K_m: 146 ± 7, iTat-tg/Y88F K_m: 182 ± 18 nM), confirming that this mutation does not alter basal DA uptake capability. Finally, the observed decrease in DA uptake in the iTat-tg/WT mice following dox treatment was not observed in the iTat-tg/Y88F mice (Figure 4.3B). Taken together, this data indicates that preventing the HIV-1 Tat/DAT interaction, via a single point mutation on the DAT which does not alter basal uptake function, is sufficient to prevent the inhibition of DAT function associated with HIV-1 Tat expression in this mouse model.

4.3.5 iTat-tg/Y88F mice do not display learning and memory deficits observed in iTat-tg/WT mice

Learning and memory capabilities were analyzed in the iTat-tg/WT and iTat-tg/Y88F mice using the novel object recognition task (NOR). Both genotypes were assessed following 7-day treatment with saline or dox immediately before being used for [^{3}H]DA uptake assays. Similar to the [3H]DA uptake experimental design, the genotype/treatment groups used for NOR were analyzed for three

key outcomes. First, we were able to replicate previously published data demonstrating that iTat-tg/WT mice treated with dox for 7 days have impaired novel object recognition (Carey et al., 2012), as demonstrated by the significant difference in phase 3 recognition index (RI) compared to the saline-treated controls (iTat-tg/WT-saline-phase 3: 71.5%; iTat-tg/WT-dox-phase 3: 53.9%; [$t_{(22)}$ = 2.086, $p < 0.05$]). Importantly, the dox-treated iTat-tg/WT mice did not show an increase in NOR performance when compared to their phase 1 RI (iTat-tg/WT-dox-phase 1: 49.1%; p = 0.47), whereas their saline-treated counterparts did (iTat-tg/WT-saline-phase 1: 54.3%; [$t_{(26)}$ = 2.427, $p < 0.05$]). Second, we did not find any significant phase 3 RI differences between the saline-treated iTat-tg/WT or iTat-tg/Y88F mice (iTat-tg/Y88F-saline-phase 3: 61.5%; p = 0.18), indicating that the Y88F DAT mutation does not significantly alter NOR response. Finally, the deficit in NOR acquisition identified in the dox-treated iTat-tg/WT mice was not observed in the iTat-tg/Y88F dox-treated mice, as these mice did not show any significant phase 3 RI differences compared to the saline-treated iTat-tg/Y88F controls (iTat-tg/Y88F-dox-phase 3: 62.6%; (p = 0.87), and both the saline- and dox-treated iTat-tg/Y88F mice demonstrated an increase in NOR performance compared to their phase 1 RI values (iTat-tg/Y88F-saline-phase 1: 50.3%; [$t_{(35)}$ = 2.196, $p < 0.05$] compared to phase 3; iTat-tg/Y88F-dox-phase 1: 51.1%; [$t_{(33)}$ = 2.194, $p < 0.05$] compared to phase 3). Taken together, this data indicates that by preventing the HIV-1 Tat-mediated DAT inhibition, via Y88F DAT mutation, is sufficient to prevent deficits in learning and memory associated with the NOR task.

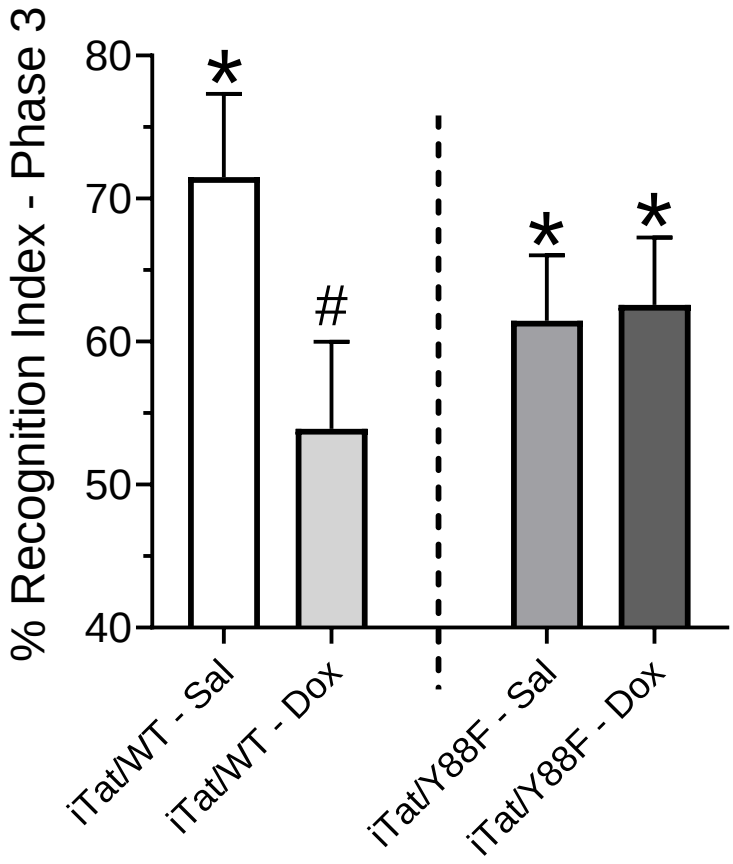

Figure 4.4 iTat-tg/Y88F demonstrate attenuation of phase 3 novel object recognition deficits observed in iTat-tg/WT mice. Following 7-day administration of saline or dox iTat-tg/WT (Sal – white; Dox – light grey) and iTat-tg/Y88F (Sal – medium grey; Dox – dark grey) were subjected to the novel object recognition assay. The phase 3 recognition index was compared to the phase 1 recognition index within each genotype/treatment group, and a $p < 0.05$ was considered significant and is represented by *. Following this analysis, the phase 3 recognition index of the dox-treated iTat-tg/WT and iTat-tg/Y88F was compared to the phase 3 recognition index of their respective controls. A $p < 0.05$ was considered significant and is denoted by #. Data is presented as the mean ± S.E.M. for the phase 3 recognition index calculated as time spent with the novel object/ (time spent with novel object + original object) from n = 16-19 mice/bar).

4.4 DISCUSSION

Through the use of the Y88F DAT mutant and inducible HIV-1 Tat transgenic mouse models, the current study sought to determine the role of HIV-1 Tat-mediated inhibition of DA uptake through DAT on the development of cognitive deficits associated with HAND. This work built upon the findings of several previous studies. First, that biological HIV-1 Tat expression inhibits the DAT in the PFC of iTat-tg mice (Strauss et al., 2020), second, that these mice also demonstrate learning and memory deficits similar to HIV-1 infected patients (Carey et al., 2012), and third, that a tyrosine88 to phenylalanine (Y88F) mutation on the DAT is capable of attenuating the HIV-1 Tat/DAT interaction *in vitro* (Midde et al., 2015). Our results indicate, similar to previous *in vitro* reports (Midde et al., 2015), that an *in vivo* Y88F DAT mutation does not significantly alter DAT function or expression, as evidenced by no changes in [^{3}H]DA uptake, [^{3}H]WIN 35,428 binding, total DAT protein expression, or locomotor activity compared to WT DAT mice. Furthermore, when crossed with the Y88F DAT mice, the iTat-tg mice no longer demonstrated inhibition of DA uptake through DAT in the PFC or deficits in the NOR task, suggesting that HIV-1 Tat-mediated inhibition of DAT may play a critical role in the development of cognitive deficits associated with HAND.

The first aim of our study was to develop a mouse model which expressed a Y88F DAT mutation. This was accomplished with a homologous recombination technique in embryonic stem cells using a replacement type vector with a selectable marker, allowing for the precise and specific mutation of a single

amino acid on a given protein (Rubinstein et al., 1993). Although the recent advent of CRISPR/Cas9 has made gene editing in mammals a much more rapid and inexpensive process, several concerns remain with this technique, primarily off-target effects (Rodríguez-Rodríguez et al., 2019). Because CRISPR/Cas9 is based on complementary target sequences only about 20 nucleotides in length, the system allows for cleavage at genomic locations which are partially complementary, creating the potential for mismatch pairings between the organism's DNA and the guide RNA (gRNA). These off-target cuts remain one of the largest unresolved issues with the CRISPR/Cas9 system, and there is little evidence as what the consequences of these off-target cuts may be (Rodríguez-Rodríguez et al., 2019). In contrast, the technique used in this study to generate the Y88F DAT mutant mice has little evidence of off-target effects (Friedrich and Soriano, 1991), allowing us to examine the specific effects of this mutation on the development of HAND, without concern of unwanted mutations.

The Tyrosine88 residue on the DAT was chosen based on our previous *in vitro* reports (Midde et al., 2015; Sun et al., 2019) demonstrating mutation of this residue to a phenylalanine does not substantially alter transporter function and also attenuates HIV-1 Tat-mediated inhibition of DA uptake. In these *in vitro* studies, the Y88F DAT mutation did not affect the V_{max} or K_m of [^{3}H]DA uptake, but did decrease the B_{max} and increase the K_d of [^{3}H]WIN 35,428 binding without alterations in DAT surface expression, suggesting that this mutation may alter the substrate binding site. This data is consistent with the role of Tyrosine88 in the structure and function of the DAT. Tyrosine88 is located in transmembrane helix

1 (TM1) of the DAT which plays an important role in mediating the structural environment surrounding the DA binding site (Cheng and Bahar, 2019). Specifically, a nearby hydrophobic cluster is essential to the closure of extracellular gates on the DAT, which mediates access to the substrate binding sites (Cheng and Bahar, 2015; Malinauskaite et al., 2014). Therefore, it is possible that mutation of this residue from a polar amino acid (Tyrosine) to a hydrophobic one (Phenylalanine) slightly alters the local molecular environment near the DA binding site, thus altering substrate binding kinetics. Consistent with our *in vitro* reports, we did not demonstrate substantial differences in DAT function or expression between Y88F and WT DAT mice. One exception however is that we did not see the alterations in [^{3}H]WIN 35,428 binding which were observed *in vitro*. Although the human DAT (hDAT) and mouse DAT (mDAT) display a high level of sequence homology (Donovan et al., 1995), since our *in vitro* work utilized the hDAT, this discrepancy may be explained by the small interspecies differences between the human and mouse transporters (Han and Gu, 2006). Ultimately, the Y88F mutant DAT expressing mice demonstrate normal transporter function/expression and locomotor activity, indicating that this is a suitable model to examine the effects of HIV-1 Tat-mediated inhibition of DAT *in vivo*.

Using a computational modeling and molecular dynamics approach, our previous study (Midde et al., 2015) identified residues on the DAT which are likely involved in the HIV-1 Tat/DAT interaction, one of which was Tyrosine88. Specifically, it was predicted that the hydroxyl group on the Tyrosine88 side

chain would form a hydrogen bond with nitrogen on the side chain of the Lysine19 residue of HIV-1 Tat. Therefore, it was anticipated that mutation of the Tyrosine88 residue of the DAT to a Phenylalanine, a structurally similar residue to Tyrosine which lacks the *para* hydroxyl group, would weaken the interaction between the two proteins, thereby preventing the associated inhibitory effects of HIV-1 Tat on the DAT. Experimental validation confirmed this prediction, confirming that Tyrosine88 on the DAT is a critical residue involved in the HIV-1 Tat/DAT interaction. In order to investigate if this interaction involved a similar molecular mechanism *in vivo*, we performed [^{3}H]DA uptake in the PFC and striatum of iTat-tg/WT and iTat-tg/Y88F mice following 7-day treatment of both genotypes with saline or Dox (Figure 4.3). First, we demonstrated that we were able to replicate our previous findings (Strauss et al., 2020) demonstrating that induction of HIV-1 Tat expression decreases the V_{max} of [^{3}H]DA uptake in the PFC by ~30% in iTat-tg/WT mice, with no effect on V_{max} in the striatum. However, when we performed this same experiment in the iTat-tg/Y88F mice we did not identify any alterations in the V_{max} of [^{3}H]DA uptake in the PFC or striatum. These results demonstrate that HIV-1 Tat-mediated inhibition of DA uptake through the DAT involves interactions between specific residues on these two proteins, and furthermore, that a single point mutation on the DAT is capable of attenuating the inhibitory effect by weakening the HIV-1 Tat/DAT molecular interaction.

Normal dopaminergic transmission is critical for maintenance of brain activities involved in attention, learning, memory, and motivation (Nieoullon 2002; Cools, 2006; Tye et al., 2013). Dysregulation of the dopaminergic system has

been suggested to be a mediating factor in the development and progression of HAND (Berger et al., 2000; Purohit et al., 2011; Gaskill et al., 2017), and several studies have demonstrated that, even in the era of cART, HIV-1 infection alters dopamine concentrations and metabolism in the brain (Kumar et al., 2009; Scheller et al., 2010; Horn et al., 2013; Meulendyke et al., 2014). Furthermore, previous studies have found that iTat-tg/WT mice display dopaminergic dysregulation in the PFC (Strauss et al., 2020) and that these mice also exhibit learning and memory deficits, as evidenced by their inability to successfully perform the novel object recognition (NOR) task (Carey et al., 2012). We hypothesized that attenuation of HIV-1 Tat-mediated inhibition of the DAT in iTat-tg mice would prevent the reported deficits in NOR performance. While we were able to replicate these reported deficits in NOR performance in the iTat-tg/WT mice (Carey et al., 2012), strikingly, the iTat-tg/Y88F did not exhibit any decrease in NOR performance following induction of HIV-1 Tat expression. Interestingly, our previous report (Strauss et al., 2020) demonstrated that HIV-1 Tat expression resulted in inhibition of not only DAT, but also the norepinephrine transporter (NET). In the current study, we were able to demonstrate attenuation of HIV-1 Tat-mediated inhibition of DA uptake through the DAT, but we did not alter the HIV-1 Tat/NET interaction. This leads to the question of what the respective impact of DAT versus NET inhibition is in the development of cognitive deficits in HAND. The observed prevention of cognitive deficits associated with the NOR task by only preventing the HIV-1 Tat/DAT interaction is likely due to the respective roles of DAT versus NET in this specific behavioral test.

Decreased DAT function has been linked with deficits in NOR performance (Chang et al., 2018; Chang et al., 2020), whereas inhibition of NET function or changes in PFC norepinephrine levels were not associated with altered NOR performance (Carlini et al., 2012; Ray et al, 2019), but were associated with deficits in the Y-maze. Thus it is possible that the observed prevention of cognitive deficits identified in this study may be specific to the NOR task, and furthermore performance of another behavioral test, such as Y-maze, may not have demonstrated prevention of HIV-1 Tat-mediated cognitive deficits. In this vein, future studies are warranted to determine the specific impact of DAT and NET inhibition in the development of HAND pathology. Ultimately, our data suggests that dopaminergic dysregulation mediated by the HIV-1 Tat/DAT plays a significant role in the development of HAND pathology.

Taken together the current findings demonstrate that attenuation of the HIV-1 Tat/DAT interaction via genetic manipulation of a single residue on the DAT results in prevention of learning and memory deficits associated with HAND. Although useful for research purposes, it is currently very difficult (and likely unethical) to genetically modify human patients. In this vein it is critical to develop novel therapeutic molecules which are capable of attenuating the HIV-1 Tat/DAT interaction, without affecting normal transporter function. A recent report from our laboratory (Sun et al., 2017) demonstrated that *in vitro* application of allosteric modulators (SRI-20041 and SRI-30827) may prevent the inhibitory effects of HIV-1 Tat on DAT function *in vitro*. Future studies investigating the use of these compounds in iTat-tg mice to determine their ability to attenuate HIV-1 Tat-

mediated dopaminergic dysregulation *in vivo* as well as on cognitive deficits observed in this mouse model will be crucial to the progression towards a preventative treatment for HAND.

CHAPTER 5

CONCLUSIONS AND FUTURE DIRECTIONS

5.1 CONCLUSIONS

There are currently over 37 million people living with HIV-1 worldwide, and another nearly 2 million becoming infected every year (HIV.gov). Even with the success of cART, the majority of these patients continue to develop neurocognitive deficits, substantially affecting their quality of life. Due to the continued growth of the HIV-1 infected population, and because there currently are no effective therapies for the treatment of HAND, it is estimated that the number of HIV-1 patients with HAND will increase by 5- to 10-fold by the year 2030 (Cysique et al., 2011). A multitude of studies have suggested the continued presence of the HIV-1 Tat protein in the CNS is a key mediator of the devasting effects of HIV-1 infection (Koutsilieri et al., 2002b; Wang et al., 2004; Scheller et al., 2005), particularly impacting the dopaminergic system (Gaskill et al., 2017; Zhu et al., 2018). Several studies have indicated that the effects of HIV-1 Tat on the dopaminergic system may be due to its interactions with the DAT (Midde et al., 2013; Zhu et al., 2016; Yuan et al., 2016). As the DAT is a key regulator of DA homeostasis in the CNS, HIV-1 Tat-mediated inhibition of transporter function could potentially be linked to the dopaminergic dysregulation observed in HAND patients, leading to neuropsychiatric dysfunction. This dissertation aimed to elucidate the specific mechanisms by which HIV-1 Tat induces dysregulation of

the dopaminergic system, and critically, what the impact of DA dysfunction has on the development of HAND neuropathology and cognitive deficits.

This study demonstrated that biological expression of HIV-1 Tat in a mouse model of HAND was sufficient to dysregulate the dopaminergic system. Furthermore, this study identified, for the first time, that HIV-1 Tat is capable of inhibiting not only the DAT but also the NET, both *in vitro* and in the PFC of HIV-1 Tat expressing mice. These findings not only add to the current evidence that HIV-1 Tat protein is a key mediator of dopaminergic dysregulation in HAND, but additionally identified a novel mechanism underlying the neuropathological abnormalities observed in this disorder.

Through the use of a mouse model which is capable of biological HIV-1 Tat expression and recapitulates the neuropathologies and neurocognitive impairments evident in HAND (Kim et al., 2003; Carey et al., 2012) this study was able to examine the impact of HIV-1 Tat-mediated inhibition of the DAT on the development of HAND related cognitive deficits. It was determined that attenuation of HIV-1 Tat-mediated inhibition of DAT in the PFC of iTat-tg mice via a single point mutation on DAT (Y88F) was sufficient to prevent learning and memory deficits which have previously been reported in this mouse model. This finding identifies the HIV-1 Tat/DAT interaction as a realistic target for the development of novel therapeutics to prevent the development of HAND.

5.2 FUTURE DIRECTIONS

While this dissertation provides key mechanistic insights into the neuropathological developments of HAND, the development of these disorders is

likely multifaceted, and thus future studies are warranted to investigate other potential factors which may be involved. In this vein, a critical problem facing the HIV-1 community is the disproportional amount of drug abuse in this population (Norman et al., 2009). It has been demonstrated that drugs of abuse, particularly cocaine and methamphetamine, can accelerate damage to the mesocorticolimbic DA system in HIV-1 patients (Starace et al., 1998; Langford et al., 2003; Chana et al., 2006; Meyer et al., 2014). Use of drugs of abuse in the HIV-1 population is a double-edged sword, as their use increases the probability of contracting HIV-1, or conversely, contracting HIV-1 increases the likelihood of drug abuse (Soontornniyomkij et al., 2016). Because the DAT is involved in the pharmacologic effects of both cocaine and methamphetamine, the mechanisms underlying the synergistic effects of these drugs of abuse and HIV-1 viral proteins may involve further effects on transporter function than those reported in this dissertation. Thus, future investigation into the underlying mechanisms of these synergistic effects, specifically with the HIV-1 Tat protein, may provide critical information to prevent the devastating effects of these toxins.

This dissertation reported for the first time that the HIV-1 Tat protein is capable of inhibiting DA uptake through the NET. As the HIV-1 Tat protein has been found to interact with a variety of molecular targets within the CNS (King et al., 2006), it is likely that additional pre-synaptic transporters involved in monoaminergic regulation may be affected in HAND. Particularly, the vesicular monoamine transporter (VMAT-2) has been previously found to be inhibited by recombinant HIV-1 Tat protein *in vitro* (Midde et al., 2012). This previous report

raises important questions. Can the inhibitory effects of HIV-1 Tat on VMAT-2 function be replicated in an animal model of HAND, and if so, does this interaction involve a similar allosteric interaction as the identified interactions between HIV-1 Tat and the DA and NE transporters? Furthermore, the VMAT-2 is also a target of drugs of abuse, specifically methamphetamine. Could the synergistic effects of HIV-1 Tat and methamphetamine on the dopaminergic system be mediated by combined effects on VMAT-2 function, expression or localization? Answering these questions may further our mechanistic insight of not only HAND neuropathology, but also mechanisms underlying neurocognitive impairments resulting from methamphetamine abuse.

This dissertation has demonstrated that attenuation of HIV-1 Tat-mediated inhibition of DAT function may be able to prevent some of the neurocognitive impairments evident in HAND. Because there currently is no treatment to prevent the development of HAND, it will be critical to develop novel therapeutic molecules which are capable of attenuating the HIV-1 Tat/DAT interaction, without affecting normal transporter function. Because the HIV-1 virus is capable of penetrating the BBB and damaging the CNS shortly after initial infection, ideally these therapies will be utilized in the early stages of HIV-1 infection. Future studies investigating the use of novel small molecules to attenuate the HIV-1 Tat/DAT and Tat/NET interactions and prevent HIV-1 Tat-mediated dysregulation of the dopaminergic system will be invaluable to the improvement of HIV-1 infected patients' lives.

REFERENCES

A Krogh, Kelly, Matthew V Green, and Stanley A Thayer. "HIV-1 Tat-induced changes in synaptically-driven network activity adapt during prolonged exposure." *Current HIV research* 12.6 (2014): 406-414.

Aksenov, Michael Y., et al. "Oxidative damage induced by the injection of HIV-1 Tat protein in the rat striatum." *Neuroscience letters* 305.1 (2001): 5-8.

Albright, Andrew V., Samantha S. Soldan, and Francisco González-Scarano. "Pathogenesis of human immunodeficiency virus-induced neurological disease." *Journal of neurovirology* 9.2 (2003): 222-227.

Andersen, Jacob, et al. "Binding site residues control inhibitor selectivity in the human norepinephrine transporter but not in the human dopamine transporter." *Scientific reports* 5 (2015): 15650.

Antinori, A1, et al. "Updated research nosology for HIV-associated neurocognitive disorders." *Neurology* 69.18 (2007): 1789-1799.

Bachani, M., et al. "Detection of anti-tat antibodies in CSF of individuals with HIV-associated neurocognitive disorders." *Journal of neurovirology* 19.1 (2013): 82-88.

Barreto, Isabella Cristina Gomes, et al. "Animal models for depression associated with HIV-1 infection." *Journal of Neuroimmune Pharmacology* 9.2 (2014): 195-208.

Beaulieu, Jean-Martin, and Raul R. Gainetdinov. "The physiology, signaling, and pharmacology of dopamine receptors." *Pharmacological reviews* 63.1 (2011): 182-217.

Berger, Joseph R., and Gabriele Arendt. "HIV dementia: the role of the basal ganglia and dopaminergic systems." *Journal of psychopharmacology* 14.3 (2000): 214-221.

Berger, Joseph R., et al. "Cerebrospinal fluid dopamine in HIV-1 infection." *Aids* 8.1 (1994): 67-72.

Bertrand, Sarah J., et al. "HIV-1 Tat protein variants: critical role for the cysteine region in synaptodendritic injury." *Experimental neurology* 248 (2013): 228-235.

Beyrer, Chris, et al. "Epidemiologic links between drug use and HIV epidemics: an international perspective." *JAIDS Journal of Acquired Immune Deficiency Syndromes* 55 (2010): S10-S16.

Bonavia, Rudy, et al. "HIV-1 Tat causes apoptotic death and calcium homeostasis alterations in rat neurons." *Biochemical and biophysical research communications* 288.2 (2001): 301-308.

Bonnet, Fabrice, et al. "Cognitive disorders in HIV-infected patients: are they HIV-related?." *Aids* 27.3 (2013): 391-400.

Borgkvist, Anders, et al. "Dopamine in the hippocampus is cleared by the norepinephrine transporter." *International Journal of Neuropsychopharmacology* 15.4 (2012): 531-540.

Brack-Werner, Ruth. "Astrocytes: HIV cellular reservoirs and important participants in neuropathogenesis." *Aids* 13.1 (1999): 1-22.

Bradford, Marion M. "A rapid and sensitive method for the quantitation of microgram quantities of protein utilizing the principle of protein-dye binding." *Analytical biochemistry* 72.1-2 (1976): 248-254.

Brailoiu, G. Cristina, et al. "HIV Tat excites D1 receptor-like expressing neurons from rat nucleus accumbens." *Drug and alcohol dependence* 178 (2017): 7-14.

Brown, Amanda, et al. "In vitro modeling of the HIV-macrophage reservoir." *Journal of leukocyte biology* 80.5 (2006): 1127-1135.

Bucci, Mirella. "Tat modulates DAT." *Nature chemical biology* 11.4 (2015): 240-240.

Buchta, William C., et al. "Dopamine terminals from the ventral tegmental area gate intrinsic inhibition in the prefrontal cortex." *Physiological reports* 5.6 (2017): e13198.

Buckner, Clarisa M., et al. "Neuroimmunity and the blood–brain barrier: molecular regulation of leukocyte transmigration and viral entry into the nervous system with a focus on neuroAIDS." *Journal of Neuroimmune Pharmacology* 1.2 (2006): 160-181.

Capon, Daniel J., and Rebecca HR Ward. "The CD4-gpl20 interaction and AIDS pathogenesis." *Annual review of immunology* 9.1 (1991): 649-678.

Carey, Amanda N., et al. "Conditional Tat protein expression in the GT-tg bigenic mouse brain induces gray matter density reductions." *Progress in Neuro-Psychopharmacology and Biological Psychiatry* 43 (2013): 49-54.

Carey, Amanda N., et al. "Expression of HIV-Tat protein is associated with learning and memory deficits in the mouse." *Behavioural brain research* 229.1 (2012): 48-56.

Carlini, Valeria Paola, et al. "Differential effects of fluoxetine and venlafaxine on memory recognition: possible mechanisms of action." *Progress in Neuro-Psychopharmacology and Biological Psychiatry* 38.2 (2012): 159-167.

Carpenter, Charles CJ, et al. "Antiretroviral therapy for HIV infection in 1996: recommendations of an international panel." *Jama* 276.2 (1996): 146-154.

Chana, G., et al. "Cognitive deficits and degeneration of interneurons in HIV+ methamphetamine users." *Neurology* 67.8 (2006): 1486-1489.

Chang, Linda, et al. "Decreased brain dopamine transporters are related to cognitive deficits in HIV patients with or without cocaine abuse." *Neuroimage* 42.2 (2008): 869-878.

Cheng, Mary Hongying, and Ivet Bahar. "Molecular mechanism of dopamine transport by human dopamine transporter." *Structure* 23.11 (2015): 2171-2181.

Cheng, Mary Hongying, and Ivet Bahar. "Monoamine transporters: structure, intrinsic dynamics and allosteric regulation." *Nature structural & molecular biology* 26.7 (2019): 545-556.

Choi, Se Joon, et al. "Changes in neuronal dopamine homeostasis following 1-methyl-4-phenylpyridinium (MPP+) exposure." *Journal of Biological Chemistry* 290.11 (2015): 6799-6809.

Cirino, Thomas J., et al. "Region-specific effects of HIV-1 Tat on intrinsic electrophysiological properties of pyramidal neurons in mouse prefrontal cortex and hippocampus." *Journal of Neurophysiology* 123.4 (2020): 1332-1341.

Clements, Janice E., et al. "The central nervous system as a reservoir for simian immunodeficiency virus (SIV): steady-state levels of SIV DNA in brain from acute through asymptomatic infection." *The Journal of infectious diseases* 186.7 (2002): 905-913.

Cools, Roshan. "Dopaminergic modulation of cognitive function-implications for L-DOPA treatment in Parkinson's disease." *Neuroscience & Biobehavioral Reviews* 30.1 (2006): 1-23.

Cysique, Lucette A., et al. "The burden of HIV-associated neurocognitive impairment in Australia and its estimates for the future." *Sexual health* 8.4 (2011): 541-550.

Dalley, Jeffrey W., Rudolf N. Cardinal, and Trevor W. Robbins. "Prefrontal executive and cognitive functions in rodents: neural and neurochemical substrates." *Neuroscience & Biobehavioral Reviews* 28.7 (2004): 771-784.

Deeks, Steven G., Sharon R. Lewin, and Diane V. Havlir. "The end of AIDS: HIV infection as a chronic disease." *The Lancet* 382.9903 (2013): 1525-1533.

Del Valle, Luis, et al. "Detection of HIV-1 Tat and JCV capsid protein, VP1, in AIDS brain with progressive multifocal leukoencephalopathy." *Journal of neurovirology* 6.3 (2000): 221-228.

Desplats, Paula, et al. "Molecular and pathologic insights from latent HIV-1 infection in the human brain." *Neurology* 80.15 (2013): 1415-1423.

Devoto, Paola, and Giovanna Flore. "On the origin of cortical dopamine: is it a co-transmitter in noradrenergic neurons?." *Current neuropharmacology* 4.2 (2006): 115-125.

Donovan, David M., et al. "Human and mouse dopamine transporter genes: conservation of 5′-flanking sequence elements and gene structures." *Molecular brain research* 30.2 (1995): 327-335.

Douglas, Rodney J., and Kevan AC Martin. "Neuronal circuits of the neocortex." *Annu. Rev. Neurosci.* 27 (2004): 419-451.

Eisenhofer, Graeme, Irwin J. Kopin, and David S. Goldstein. "Catecholamine metabolism: a contemporary view with implications for physiology and medicine." *Pharmacological reviews* 56.3 (2004): 331-349.

EngElS, AnnA S., et al. "Co-occurring anxiety influences patterns of brain activity in depression." *Cognitive, Affective, & Behavioral Neuroscience* 10.1 (2010): 141-156.

Everall, I. P., P. J. Luthert, and P. L. Lantos. "Neuronal loss in the frontal cortex in HIV infection." *The Lancet* 337.8750 (1991): 1119-1121.

Feinberg, Mark B., David Baltimore, and Alan D. Frankel. "The role of Tat in the human immunodeficiency virus life cycle indicates a primary effect on transcriptional elongation." *Proceedings of the National Academy of Sciences* 88.9 (1991): 4045-4049.

Ferris, Mark J., et al. "In vivo microdialysis in awake, freely moving rats demonstrates HIV-1 Tat-induced alterations in dopamine transmission." *Synapse* 63.3 (2009): 181-185.

Flatmark, T. "Catecholamine biosynthesis and physiological regulation in neuroendocrine cells." *Acta Physiologica Scandinavica* 168.1 (2000): 1-18.

Fog, Jacob U., et al. "Calmodulin kinase II interacts with the dopamine transporter C terminus to regulate amphetamine-induced reverse transport." *Neuron* 51.4 (2006): 417-429.

Foster, James D., Benchaporn Pananusorn, and Roxanne A. Vaughan. "Dopamine transporters are phosphorylated on N-terminal serines in rat striatum." *Journal of Biological Chemistry* 277.28 (2002): 25178-25186.

Francesconi, Walter, Fulvia Berton, and Maria Cecilia G. Marcondes. "HIV-1 Tat alters neuronal intrinsic excitability." *BMC research notes* 11.1 (2018): 1-7.

Frankel, Alan D., and Carl O. Pabo. "Cellular uptake of the tat protein from human immunodeficiency virus." *Cell* 55.6 (1988): 1189-1193.

Frankel, Alan D., and John AT Young. "HIV-1: fifteen proteins and an RNA." (1998): 1-25.

Friedrich, Glenn, and Philippe Soriano. "Promoter traps in embryonic stem cells: a genetic screen to identify and mutate developmental genes in mice." *Genes & development* 5.9 (1991): 1513-1523.

Gabdoulline, Razif R., and Rebecca C. Wade. "Brownian dynamics simulation of protein–protein diffusional encounter." *Methods* 14.3 (1998): 329-341.

Gallo, Robert, et al. "HIV/HTLV gene nomenclature." *Nature* 333.6173 (1988): 504-504.

Gaskill, Peter J., et al. "HIV, Tat and dopamine transmission." *Neurobiology of disease* 105 (2017): 51-73.

Gaskill, Peter J., et al. "Human immunodeficiency virus (HIV) infection of human macrophages is increased by dopamine: a bridge between HIV-associated neurologic disorders and drug abuse." *The American journal of pathology* 175.3 (2009): 1148-1159.

Gelman, Benjamin B., et al. "Prefrontal dopaminergic and enkephalinergic synaptic accommodation in HIV-associated neurocognitive disorders and encephalitis." *Journal of Neuroimmune Pharmacology* 7.3 (2012): 686-700.

Goodwin, J. Shawn, et al. "Amphetamine and methamphetamine differentially affect dopamine transporters in vitro and in vivo." *Journal of Biological Chemistry* 284.5 (2009): 2978-2989.

Góral, Izabella, Kamil Łątka, and Marek Bajda. "Structure Modeling of the Norepinephrine Transporter." *Biomolecules* 10.1 (2020): 102.

Gorantla, Santhi, Larisa Poluektova, and Howard E. Gendelman. "Rodent models for HIV-associated neurocognitive disorders." *Trends in neurosciences* 35.3 (2012): 197-208.

Göttlinger, Heinrich G., Joseph G. Sodroski, and William A. Haseltine. "Role of capsid precursor processing and myristoylation in morphogenesis and infectivity of human immunodeficiency virus type 1." *Proceedings of the National Academy of Sciences* 86.15 (1989): 5781-5785.

Gray, Lachlan R., et al. "Is the central nervous system a reservoir of HIV-1?." *Current opinion in HIV and AIDS* 9.6 (2014): 552.

Guptaroy, Bipasha, et al. "A juxtamembrane mutation in the N terminus of the dopamine transporter induces preference for an inward-facing conformation." *Molecular pharmacology* 75.3 (2009): 514-524.

Han, Dawn D., and Howard H. Gu. "Comparison of the monoamine transporters from human and mouse in their sensitivities to psychostimulant drugs." *BMC pharmacology* 6.1 (2006): 1-7.

Haughey, Norman J., and Mark P. Mattson. "Calcium dysregulation and neuronal apoptosis by the HIV-1 proteins Tat and gp120." *Journal of acquired immune deficiency syndromes (1999)* 31 (2002): S55-61.

Hayashi, Kentaro, et al. "HIV-TAT protein upregulates expression of multidrug resistance protein 1 in the blood–brain barrier." *Journal of Cerebral Blood Flow & Metabolism* 26.8 (2006): 1052-1065.

Heaton, Robert K., et al. "HIV-associated neurocognitive disorders before and during the era of combination antiretroviral therapy: differences in rates, nature, and predictors." *Journal of neurovirology* 17.1 (2011): 3-16.

Henderson, Lisa J., et al. "Presence of Tat and transactivation response element in spinal fluid despite antiretroviral therapy." *Aids* 33 (2019): S145-S157.

Hevers, W., and H. Lüddens. "Pharmacological heterogeneity of γ-aminobutyric acid receptors during development suggests distinct classes of rat cerebellar granule cells in situ." *Neuropharmacology* 42.1 (2002): 34-47.

Holton, Katherine L., Merewyn K. Loder, and Haley E. Melikian. "Nonclassical, distinct endocytic signals dictate constitutive and PKC-regulated neurotransmitter transporter internalization." *Nature neuroscience* 8.7 (2005): 881-888.

Hong, Weimin C., and Susan G. Amara. "Membrane cholesterol modulates the outward facing conformation of the dopamine transporter and alters cocaine binding." *Journal of Biological Chemistry* 285.42 (2010): 32616-32626.

Hopf, F. Woodward, et al. "Cooperative activation of dopamine D1 and D2 receptors increases spike firing of nucleus accumbens neurons via G-protein βγ subunits." *Journal of Neuroscience* 23.12 (2003): 5079-5087.

Horn, A. S. "Structure activity relations for the inhibition of 5-HT uptake into rat hypothalamic homogenates by serotonin and tryptamine analogues." *Journal of neurochemistry* 21.4 (1973): 883-888.

Horn, A. S. "Structure-activity relations for the inhibition of catecholamine uptake into synaptosomes from noradrenaline and dopaminergic neurons in rat brain homogenates." *British journal of pharmacology* 47.2 (1973): 332.

Hornykiewicz, O. "L-DOPA: from a biologically inactive amino acid to a successful therapeutic agent." *Amino acids* 23.1-3 (2002): 65-70.

Hudson, Lance, et al. "Detection of the human immunodeficiency virus regulatory protein tat in CNS tissues." *Journal of neurovirology* 6.2 (2000): 145-155.

Ikemoto, Satoshi. "Brain reward circuitry beyond the mesolimbic dopamine system: a neurobiological theory." *Neuroscience & biobehavioral reviews* 35.2 (2010): 129-150.

Itoh, Kyoko, Parviz Mehraein, and Serge Weis. "Neuronal damage of the substantia nigra in HIV-1 infected brains." *Acta neuropathologica* 99.4 (2000): 376-384.

J Paris, Jason, Jason Fenwick, and Jay P McLaughlin. "Estrous cycle and HIV-1 Tat protein influence cocaine-conditioned place preference and induced locomotion of female mice." *Current HIV research* 12.6 (2014): 388-396.

Jardetzky, Oleg. "Simple allosteric model for membrane pumps." *Nature* 211.5052 (1966): 969-970.

Jeang, Kuan-Teh, Hua Xiao, and Elizabeth A. Rich. "Multifaceted activities of the HIV-1 transactivator of transcription, Tat." *Journal of Biological Chemistry* 274.41 (1999): 28837-28840.

Johnson, Tory P., et al. "Induction of IL-17 and nonclassical T-cell activation by HIV-Tat protein." *Proceedings of the National Academy of Sciences* 110.33 (2013): 13588-13593.

Johnston, James B., et al. "HIV-1 Tat neurotoxicity is prevented by matrix metalloproteinase inhibitors." *Annals of Neurology: Official Journal of the American Neurological Association and the Child Neurology Society* 49.2 (2001): 230-241.

Jones, Melina, et al. "Intraventricular injection of human immunodeficiency virus type 1 (HIV-1) tat protein causes inflammation, gliosis, apoptosis, and

ventricular enlargement." *Journal of Neuropathology & Experimental Neurology* 57.6 (1998): 563-570.

Joseph, Deepthi, et al. "Structure and gating dynamics of Na+/Cl-coupled neurotransmitter transporters." *Frontiers in molecular biosciences* 6 (2019): 80.

Kesby, James P., Athina Markou, and Svetlana Semenova. "The effects of HIV-1 regulatory TAT protein expression on brain reward function, response to psychostimulants and delay-dependent memory in mice." *Neuropharmacology* 109 (2016): 205-215.

Kesby, James P., et al. "Effects of HIV/TAT protein expression and chronic selegiline treatment on spatial memory, reversal learning and neurotransmitter levels in mice." *Behavioural brain research* 311 (2016): 131-140.

Kesby, James P., et al. "HIV-1 TAT protein enhances sensitization to methamphetamine by affecting dopaminergic function." *Brain, behavior, and immunity* 65 (2017): 210-221.

Kieburtz, Karl D., et al. "Excitotoxicity and dopaminergic dysfunction in the acquired immunodeficiency syndrome dementia complex: therapeutic implications." *Archives of neurology* 48.12 (1991): 1281-1284.

Kim, Byung Oh, et al. "Neuropathologies in transgenic mice expressing human immunodeficiency virus type 1 Tat protein under the regulation of the astrocyte-specific glial fibrillary acidic protein promoter and doxycycline." *The American journal of pathology* 162.5 (2003): 1693-1707.

King, J. E., et al. "HIV tat and neurotoxicity." *Microbes and infection* 8.5 (2006): 1347-1357.

King, Steven R. "HIV: virology and mechanisms of disease." *Annals of emergency medicine* 24.3 (1994): 443-449.

Klanker, Marianne, Matthijs Feenstra, and Damiaan Denys. "Dopaminergic control of cognitive flexibility in humans and animals." *Frontiers in neuroscience* 7 (2013): 201.

Koncz, István, et al. "The tricyclic antidepressant desipramine inhibited the neurotoxic, kainate-induced [Ca2+] i increases in CA1 pyramidal cells in acute hippocampal slices." *Brain research bulletin* 104 (2014): 42-51.

Koutsilieri, E., et al. "Involvement of dopamine in the progression of AIDS Dementia Complex." *Journal of neural transmission* 109.3 (2002): 399-410.

Kristensen, Anders S., et al. "SLC6 neurotransmitter transporters: structure, function, and regulation." *Pharmacological reviews* 63.3 (2011): 585-640.

Kruman, Inna I., Avindra Nath, and Mark P. Mattson. "HIV-1 protein Tat induces apoptosis of hippocampal neurons by a mechanism involving caspase activation, calcium overload, and oxidative stress." *Experimental neurology* 154.2 (1998): 276-288.

Kumar, Adarsh M., et al. "Human immunodeficiency virus infection in the CNS and decreased dopamine availability: relationship with neuropsychological performance." *Journal of neurovirology* 17.1 (2011): 26-40.

Kumar, Adarsh M., et al. "Human immunodeficiency virus type 1 in the central nervous system leads to decreased dopamine in different regions of postmortem human brains." *Journal of neurovirology* 15.3 (2009): 257-274.

Lahiri, Asha K., and Mark D. Bevan. "Dopaminergic Transmission Rapidly and Persistently Enhances Excitability of D1 Receptor-Expressing Striatal Projection Neurons." *Neuron* (2020).

Lamers, Susanna L., et al. "Human immunodeficiency virus-1 evolutionary patterns associated with pathogenic processes in the brain." *Journal of neurovirology* 16.3 (2010): 230-241.

Lammel, Stephan, et al. "Input-specific control of reward and aversion in the ventral tegmental area." *Nature* 491.7423 (2012): 212-217.

Langford, T. D., et al. "Changing patterns in the neuropathogenesis of HIV during the HAART era." *Brain pathology* 13.2 (2003): 195-210.

Lashomb, Abigail L., Michael Vigorito, and Sulie L. Chang. "Further characterization of the spatial learning deficit in the human immunodeficiency virus-1 transgenic rat." *Journal of neurovirology* 15.1 (2009): 14-24.

Lee, Sook-Kyung, Marc Potempa, and Ronald Swanstrom. "The choreography of HIV-1 proteolytic processing and virion assembly." *Journal of Biological Chemistry* 287.49 (2012): 40867-40874.

Li, Chiang J., et al. "Induction of apoptosis in uninfected lymphocytes by HIV-1 Tat protein." *Science* 268.5209 (1995): 429-431.

Lin, Zhicheng, Masanari Itokawa, and George R. Uhl. "Dopamine transporter proline mutations influence dopamine uptake, cocaine analog recognition, and expression." *The FASEB Journal* 14.5 (2000): 715-728.

Lopez, Oscar L., et al. "Dopamine systems in human immunodeficiency virus-associated dementia." *Cognitive and Behavioral Neurology* 12.3 (1999): 184-192.

Ma, Meihui, and Avindra Nath. "Molecular determinants for cellular uptake of Tat protein of human immunodeficiency virus type 1 in brain cells." *Journal of virology* 71.3 (1997): 2495-2499.

Maanen, M., and Richard E. Sutton. "Rodent models for HIV-1 infection and disease." *Current HIV research* 1.1 (2003): 121-130.

Magrane, Michele. "UniProt Knowledgebase: a hub of integrated protein data." *Database* 2011 (2011).

Malinauskaite, Lina, et al. "A mechanism for intracellular release of Na+ by neurotransmitter/sodium symporters." *Nature structural & molecular biology* 21.11 (2014): 1006-1012.

Manepalli, Sankar, et al. "Monoamine transporter structure, function, dynamics, and drug discovery: a computational perspective." *The AAPS journal* 14.4 (2012): 820-831.

Maragos, W. F., et al. "Neuronal injury in hippocampus with human immunodeficiency virus transactivating protein, Tat." *Neuroscience* 117.1 (2003): 43-53.

Marban, Céline, et al. "Targeting the brain reservoirs: toward an HIV cure." *Frontiers in immunology* 7 (2016): 397.

Masana, Mercè, Analía Bortolozzi, and Francesc Artigas. "Selective enhacement of mesocortical dopaminergic transmission by noradrenergic drugs: therapeutic opportunities in schizophrenia." *International Journal of Neuropsychopharmacology* 14.1 (2011): 53-68.

Mathers, Bradley M., et al. "Global epidemiology of injecting drug use and HIV among people who inject drugs: a systematic review." *The Lancet* 372.9651 (2008): 1733-1745.

Mattson, M. P., N. J. Haughey, and A. Nath. "Cell death in HIV dementia." *Cell Death & Differentiation* 12.1 (2005): 893-904.

Meade, Christina S., et al. "fMRI brain activation during a delay discounting task in HIV-positive adults with and without cocaine dependence." *Psychiatry Research: Neuroimaging* 192.3 (2011): 167-175.

Melrose, Rebecca J., et al. "Compromised fronto-striatal functioning in HIV: an fMRI investigation of semantic event sequencing." *Behavioural brain research* 188.2 (2008): 337-347.

Merk, Alan, and Sriram Subramaniam. "HIV-1 envelope glycoprotein structure." *Current opinion in structural biology* 23.2 (2013): 268-276.

Meyer, Vanessa J., et al. "Crack cocaine use impairs anterior cingulate and prefrontal cortex function in women with HIV infection." *Journal of neurovirology* 20.4 (2014): 352-361.

Midde, Narasimha M., Adrian M. Gomez, and Jun Zhu. "HIV-1 Tat protein decreases dopamine transporter cell surface expression and vesicular monoamine transporter-2 function in rat striatal synaptosomes." *Journal of Neuroimmune Pharmacology* 7.3 (2012): 629-639.

Midde, Narasimha M., et al. "Mutation of tyrosine 470 of human dopamine transporter is critical for HIV-1 Tat-induced inhibition of dopamine transport and transporter conformational transitions." *Journal of Neuroimmune Pharmacology* 8.4 (2013): 975-987.

Midde, Narasimha M., et al. "Mutations at tyrosine 88, lysine 92 and tyrosine 470 of human dopamine transporter result in an attenuation of HIV-1 Tat-induced inhibition of dopamine transport." *Journal of Neuroimmune Pharmacology* 10.1 (2015): 122-135.

Miller, Douglas R., et al. "HIV-1 T at regulation of dopamine transmission and microglial reactivity is brain region specific." *Glia* 66.9 (2018): 1915-1928.

Miller, Earl K., and Jonathan D. Cohen. "An integrative theory of prefrontal cortex function." *Annual review of neuroscience* 24.1 (2001): 167-202.

Miller, Michael D., et al. "The human immunodeficiency virus-1 nef gene product: a positive factor for viral infection and replication in primary lymphocytes and macrophages." *The Journal of experimental medicine* 179.1 (1994): 101-113.

Mind Exchange Working Group, et al. "Assessment, diagnosis, and treatment of HIV-associated neurocognitive disorder: a consensus report of the mind exchange program." *Clinical Infectious Diseases* 56.7 (2013): 1004-1017.

Mohseni Ahooyi, Taha, et al. "Network analysis of hippocampal neurons by microelectrode array in the presence of HIV-1 Tat and cocaine." *Journal of cellular physiology* 233.12 (2018): 9299-9311.

Moll, Gunther H., et al. "Age-associated changes in the densities of presynaptic monoamine transporters in different regions of the rat brain from early juvenile life to late adulthood." *Developmental Brain Research* 119.2 (2000): 251-257.

Morón, José A., et al. "Dopamine uptake through the norepinephrine transporter in brain regions with low levels of the dopamine transporter: evidence from knock-out mouse lines." *Journal of Neuroscience* 22.2 (2002): 389-395.

Mortensen, Ole Valente, et al. "Genetic complementation screen identifies a mitogen-activated protein kinase phosphatase, MKP3, as a regulator of dopamine transporter trafficking." *Molecular biology of the cell* 19.7 (2008): 2818-2829.

Nath, Avindra, and Jonathan Geiger. "Neurobiological aspects of human immunodeficiency virus infection: neurotoxic mechanisms." *Progress in neurobiology* 54.1 (1998): 19-33.

Nath, Avindra, Joseph Jankovic, and L. Creed Pettigrew. "Movement disorders and AIDS." *Neurology* 37.1 (1987): 37-37.

Navratna, Vikas, et al. "Thermostabilization and purification of the human dopamine transporter (hDAT) in an inhibitor and allosteric ligand bound conformation." *PLoS One* 13.7 (2018): e0200085.

New, Deborah R., et al. "Human immunodeficiency virus type 1 Tat protein induces death by apoptosis in primary human neuron cultures." *Journal of neurovirology* 3.2 (1997): 168-173.

Ngwainmbi, Joy, et al. "Effects of HIV-1 Tat on enteric neuropathogenesis." *Journal of Neuroscience* 34.43 (2014): 14243-14251.

Nieoullon, André. "Dopamine and the regulation of cognition and attention." *Progress in neurobiology* 67.1 (2002): 53-83.

Norman, Lisa R., et al. "Neuropsychological consequences of HIV and substance abuse: a literature review and implications for treatment and future research." *Current drug abuse reviews* 2.2 (2009): 143-156.

Nutt, David J., et al. "The dopamine theory of addiction: 40 years of highs and lows." *Nature Reviews Neuroscience* 16.5 (2015): 305-312.

Orandle, Marlene S., et al. "Enhanced expression of proinflammatory cytokines in the central nervous system is associated with neuroinvasion by simian immunodeficiency virus and the development of encephalitis." *Journal of virology* 76.11 (2002): 5797-5802.

Ortinski, Pavel I., et al. "Cocaine-seeking is associated with PKC-dependent reduction of excitatory signaling in accumbens shell D2 dopamine receptor-expressing neurons." *Neuropharmacology* 92 (2015): 80-89.

Paris, Jason J., et al. "Anxiety-like behavior of mice produced by conditional central expression of the HIV-1 regulatory protein, Tat." *Psychopharmacology* 231.11 (2014): 2349-2360.

Paris, Jason J., et al. "Effects of conditional central expression of HIV-1 tat protein to potentiate cocaine-mediated psychostimulation and reward among male mice." *Neuropsychopharmacology* 39.2 (2014): 380-388.

Pariser, Joseph J., et al. "Studies of the biogenic amine transporters. 12. Identification of novel partial inhibitors of amphetamine-induced dopamine release." *Journal of Pharmacology and Experimental Therapeutics* 326.1 (2008): 286-295.

Parkin, NEIL T., Mario Chamorro, and HAROLD E. Varmus. "Human immunodeficiency virus type 1 gag-pol frameshifting is dependent on downstream mRNA secondary structure: demonstration by expression in vivo." *Journal of virology* 66.8 (1992): 5147-5151.

Pei, Jimin, Ming Tang, and Nick V. Grishin. "PROMALS3D web server for accurate multiple protein sequence and structure alignments." *Nucleic acids research* 36.suppl_2 (2008): W30-W34.

Persidsky, Yuri, and Howard Fox. "Battle of animal models." *Journal of Neuroimmune Pharmacology* 2.2 (2007): 171-177.

Power, C., et al. "Neuronal death induced by brain-derived human immunodeficiency virus type 1 envelope genes differs between demented and nondemented AIDS patients." *Journal of Virology* 72.11 (1998): 9045-9053.

Pristupa, Zdenek B., et al. "Pharmacological heterogeneity of the cloned and native human dopamine transporter: disassociation of [3H] WIN 35,428 and [3H] GBR 12,935 binding." *Molecular Pharmacology* 45.1 (1994): 125-135.

Purohit, Vishnudutt, Rao Rapaka, and David Shurtleff. "Drugs of abuse, dopamine, and HIV-associated neurocognitive disorders/HIV-associated dementia." *Molecular neurobiology* 44.1 (2011): 102-110.

Quiñones-Mateu, Miguel E., et al. "A dual infection/competition assay shows a correlation between ex vivo human immunodeficiency virus type 1 fitness and disease progression." *Journal of virology* 74.19 (2000): 9222-9233.

Quizon, Pamela M., et al. "Molecular mechanism: the human dopamine transporter histidine 547 regulates basal and HIV-1 Tat protein-inhibited dopamine transport." *Scientific reports* 6 (2016): 39048.

Raiteri, Maurizio, et al. "Effect of sympathomimetic amines on the synaptosomal transport of noradrenaline, dopamine and 5-hydroxytryptamine." *European journal of pharmacology* 41.2 (1977): 133-143.

Rao, Jagadeesh S., et al. "Neuroinflammation and synaptic loss." *Neurochemical research* 37.5 (2012): 903-910.

Rappaport, Jay, et al. "Molecular pathway involved in HIV-1-induced CNS pathology: role of viral regulatory protein, Tat." *Journal of leukocyte biology* 65.4 (1999): 458-465.

Ravna, Aina W., Ingebrigt Sylte, and Svein G. Dahl. "Structure and localisation of drug binding sites on neurotransmitter transporters." *Journal of molecular modeling* 15.10 (2009): 1155-1164.

Ray, Azizi, et al. "Effects of the second-generation" bath salt" cathinone alpha-pyrrolidinopropiophenone (α-PPP) on behavior and monoamine neurochemistry in male mice." *Psychopharmacology* 236.3 (2019): 1107-1117.

Reid, W., et al. "An HIV-1 transgenic rat that develops HIV-related pathology and immunologic dysfunction." *Proceedings of the National Academy of Sciences* 98.16 (2001): 9271-9276.

Reith, Maarten EA, Lijuan C. Wang, and Aloke K. Dutta. "Pharmacological profile of radioligand binding to the norepinephrine transporter: instances of poor indication of functional activity." *Journal of neuroscience methods* 143.1 (2005): 87-94.

Richardson, Ben D., et al. "Membrane potential shapes regulation of dopamine transporter trafficking at the plasma membrane." *Nature communications* 7 (2016): 10423.

Ridderinkhof, K. Richard, et al. "Neurocognitive mechanisms of cognitive control: the role of prefrontal cortex in action selection, response inhibition, performance monitoring, and reward-based learning." *Brain and cognition* 56.2 (2004): 129-140.

Riga, Danai, et al. "Optogenetic dissection of medial prefrontal cortex circuitry." *Frontiers in systems neuroscience* 8 (2014): 230.

Rodríguez-Rodríguez, Diana Raquel, et al. "Genome editing: a perspective on the application of CRISPR/Cas9 to study human diseases." *International Journal of Molecular Medicine* 43.4 (2019): 1559-1574.

Rotello, Vincent M. "The donor atom–π interaction of sulfur with flavin. A density functional investigation." *Heteroatom Chemistry* 9.7 (1998): 605-606.

Rothman, Richard B., et al. "Studies of the biogenic amine transporters. 13. Identification of “agonist” and “antagonist” allosteric modulators of amphetamine-induced dopamine release." *Journal of Pharmacology and Experimental Therapeutics* 329.2 (2009): 718-728.

Ruben, Steven, et al. "Structural and functional characterization of human immunodeficiency virus tat protein." *Journal of virology* 63.1 (1989): 1-8.

Rubinstein, Marcelo, Miguel A. Japón, and Malcolm J. Low. "Introduction of a point mutation into the mouse genome by homologous recombination in embryonic stem cells using a replacement type vector with a selectable marker." *Nucleic acids research* 21.11 (1993): 2613-2617.

Rudnick, Gary. "Mechanisms of biogenic amine neurotransmitter transporters." *Neurotransmitter Transporters*. Humana Press, Totowa, NJ, 2002. 25-52.

Sabatier, J. M., et al. "Evidence for neurotoxic activity of tat from human immunodeficiency virus type 1." *Journal of virology* 65.2 (1991): 961-967.

Sanmarti, Montserrat, et al. "HIV-associated neurocognitive disorders." *Journal of molecular psychiatry* 2.1 (2014): 1-10.

Santana, Noemí, and Francesc Artigas. "Laminar and cellular distribution of monoamine receptors in rat medial prefrontal cortex." *Frontiers in neuroanatomy* 11 (2017): 87.

Sardar, Asif M., Carole Czudek, and Gavin P. Reynolds. "Dopamine deficits in the brain: the neurochemical basis of parkinsonian symptoms in AIDS." *Neuroreport* 7.4 (1996): 910-912.

Scheller, C., et al. "Dopamine activates HIV in chronically infected T lymphoblasts." *Journal of neural transmission* 107.12 (2000): 1483-1489.

Scheller, C., et al. "Increased dopaminergic neurotransmission in therapy-naive asymptomatic HIV patients is not associated with adaptive changes at the dopaminergic synapses." *Journal of neural transmission* 117.6 (2010): 699-705.

Scheller, Carsten, et al. "Early impairment in dopaminergic neurotransmission in brains of SIV-infected rhesus monkeys due to microglia activation." *Journal of neurochemistry* 95.2 (2005): 377-387.

Shan, Jufang, et al. "The substrate-driven transition to an inward-facing conformation in the functional mechanism of the dopamine transporter." *PloS one* 6.1 (2011): e16350.

Shi, Lei, et al. "The mechanism of a neurotransmitter: sodium symporter—inward release of Na+ and substrate is triggered by substrate in a second binding site." *Molecular cell* 30.6 (2008): 667-677.

Silvers, Janelle M., et al. "Dopaminergic marker proteins in the substantia nigra of human immunodeficiency virus type 1-infected brains." *Journal of neurovirology* 12.2 (2006): 140-145.

Silvers, Janelle M., et al. "Neurotoxicity of HIV-1 Tat protein: involvement of D1 dopamine receptor." *Neurotoxicology* 28.6 (2007): 1184-1190.

Simioni, Samanta, et al. "Cognitive dysfunction in HIV patients despite long-standing suppression of viremia." *Aids* 24.9 (2010): 1243-1250.

Soontornniyomkij, Virawudh, et al. "Effects of HIV and methamphetamine on brain and behavior: evidence from human studies and animal models." *Journal of Neuroimmune Pharmacology* 11.3 (2016): 495-510.

Starace, F., et al. "Early neuropsychological impairment in HIV-seropositive intravenous drug users: evidence from the Italian Multicentre Neuropsychological HIV Study." *Acta Psychiatrica Scandinavica* 97.2 (1998): 132-138.

Strauss, Matthew, et al. "[3H] Dopamine Uptake through the Dopamine and Norepinephrine Transporters is Decreased in the Prefrontal Cortex of Transgenic Mice Expressing HIV-1 Transactivator of Transcription Protein." *Journal of Pharmacology and Experimental Therapeutics* 374.2 (2020): 241-251.

Sun, Wei-Lun, et al. "Allosteric modulatory effects of SRI-20041 and SRI-30827 on cocaine and HIV-1 Tat protein binding to human dopamine transporter." *Scientific reports* 7.1 (2017): 1-12.

Sun, Wei-Lun, et al. "Mutational effects of human dopamine transporter at tyrosine88, lysine92, and histidine547 on basal and HIV-1 Tat-inhibited dopamine transport." *Scientific reports* 9.1 (2019): 1-13.

Tatko, Chad D., and Marcey L. Waters. "Investigation of the nature of the methionine–π interaction in β-hairpin peptide model systems." *Protein science* 13.9 (2004): 2515-2522.

Tejani-Butt, S. M. "[3H] nisoxetine: a radioligand for quantitation of norepinephrine uptake sites by autoradiography or by homogenate binding." *Journal of Pharmacology and Experimental Therapeutics* 260.1 (1992): 427-436.

Teo, Min-Yau, et al. "Differential effects of nicotine on the activity of substantia nigra and ventral tegmental area dopaminergic neurons in vitro." *Acta neurobiologiae experimentalis* 64.2 (2004): 119-130.

Thompson, Katherine A., et al. "Brain cell reservoirs of latent virus in presymptomatic HIV-infected individuals." *The American journal of pathology* 179.4 (2011): 1623-1629.

Thompson, Paul M., et al. "Thinning of the cerebral cortex visualized in HIV/AIDS reflects CD4+ T lymphocyte decline." *Proceedings of the National Academy of Sciences* 102.43 (2005): 15647-15652.

Toborek, Michal, et al. "Mechanisms of the blood–brain barrier disruption in HIV-1 infection." *Cellular and molecular neurobiology* 25.1 (2005): 181-199.

Tye, Kay M., et al. "Dopamine neurons modulate neural encoding and expression of depression-related behaviour." *Nature* 493.7433 (2013): 537-541.

Vahlne, Anders. "A historical reflection on the discovery of human retroviruses." *Retrovirology* 6.1 (2009): 1-9.

Valcour, Victor, et al. "Central nervous system viral invasion and inflammation during acute HIV infection." *The Journal of infectious diseases* 206.2 (2012): 275-282.

Van Duyne, Rachel, et al. "The utilization of humanized mouse models for the study of human retroviral infections." *Retrovirology* 6.1 (2009): 76.

Vercruysse, Thomas, and Dirk Daelemans. "HIV-1 Rev multimerization: mechanism and insights." *Current HIV research* 11.8 (2013): 623-634.

Vigorito, Michael, Abigail L. LaShomb, and Sulie L. Chang. "Spatial learning and memory in HIV-1 transgenic rats." *Journal of Neuroimmune Pharmacology* 2.4 (2007): 319-328.

Vives, Eric, Priscille Brodin, and Bernard Lebleu. "A truncated HIV-1 Tat protein basic domain rapidly translocates through the plasma membrane and accumulates in the cell nucleus." *Journal of Biological Chemistry* 272.25 (1997): 16010-16017.

Wall, Stephen C., Howard Gu, and Gary Rudnick. "Biogenic amine flux mediated by cloned transporters stably expressed in cultured cell lines: amphetamine specificity for inhibition and efflux." *Molecular pharmacology* 47.3 (1995): 544-550.

Wang, Ching-I. A., et al. "A second extracellular site is required for norepinephrine transport by the human norepinephrine transporter." *Molecular pharmacology* 82.5 (2012): 898-909.

Wang, Gene-Jack, et al. "Decreased brain dopaminergic transporters in HIV-associated dementia patients." *Brain* 127.11 (2004): 2452-2458.

Wang, Kevin H., Aravind Penmatsa, and Eric Gouaux. "Neurotransmitter and psychostimulant recognition by the dopamine transporter." *Nature* 521.7552 (2015): 322-327.

Webb, Katy M., et al. "Evidence for developmental dopaminergic alterations in the human immunodeficiency virus-1 transgenic rat." *Journal of neurovirology* 16.2 (2010): 168-173.

Westendorp, Michael O., et al. "Sensitization of T cells to CD95-mediated apoptosis by HIV-1 Tat and gp120." *Nature* 375.6531 (1995): 497-500.

Williams, Jason M., and Jeffery D. Steketee. "Characterization of dopamine transport in crude synaptosomes prepared from rat medial prefrontal cortex." *Journal of neuroscience methods* 137.2 (2004): 161-165.

Wu, Sijia, et al. "Ack1 is a dopamine transporter endocytic brake that rescues a trafficking-dysregulated ADHD coding variant." *Proceedings of the National Academy of Sciences* 112.50 (2015): 15480-15485.

Xiao, Hua, et al. "Selective CXCR4 antagonism by Tat: implications for in vivo expansion of coreceptor use by HIV-1." *Proceedings of the National Academy of Sciences* 97.21 (2000): 11466-11471.

Yamashita, Atsuko, et al. "Crystal structure of a bacterial homologue of Na+/Cl--dependent neurotransmitter transporters." *Nature* 437.7056 (2005): 215-223.

Yuan, Yaxia, et al. "Computational modeling of human dopamine transporter structures, mechanism and its interaction with HIV-1 transactivator of transcription." *Future medicinal chemistry* 8.17 (2016): 2077-2089.

Yuan, Yaxia, et al. "Molecular mechanism of HIV-1 Tat interacting with human dopamine transporter." *ACS chemical neuroscience* 6.4 (2015): 658-665.

Zapp, Maria L., and Michael R. Green. "Sequence-specific RNA binding by the HIV-1 Rev protein." *Nature* 342.6250 (1989): 714-716.

Zauli, Giorgio, et al. "HIV-1 Tat-mediated inhibition of the tyrosine hydroxylase gene expression in dopaminergic neuronal cells." *Journal of Biological Chemistry* 275.6 (2000): 4159-4165.

Zhen, Juan, et al. "Characterization of [3H] CFT binding to the norepinephrine transporter suggests that binding of CFT and nisoxetine is not mutually exclusive." *Journal of neuroscience methods* 203.1 (2012): 19-27.

Zhou, Zheng, et al. "Antidepressant specificity of serotonin transporter suggested by three LeuT–SSRI structures." *Nature structural & molecular biology* 16.6 (2009): 652.

Zhou, Zheng, et al. "LeuT-desipramine structure reveals how antidepressants block neurotransmitter reuptake." *Science* 317.5843 (2007): 1390-1393.

Zhu, J., and M. E. A. Reith. "Role of the dopamine transporter in the action of psychostimulants, nicotine, and other drugs of abuse." *CNS & Neurological Disorders-Drug Targets (Formerly Current Drug Targets-CNS & Neurological Disorders)* 7.5 (2008): 393-409.

Zhu, Jun, et al. "Environmental enrichment enhances sensitization to GBR 12935-induced activity and decreases dopamine transporter function in the medial prefrontal cortex." *Behavioural brain research* 148.1-2 (2004): 107-117.

Zhu, Jun, et al. "HIV-1 Tat protein-induced rapid and reversible decrease in [3H] dopamine uptake: dissociation of [3H] dopamine uptake and [3H] 2β-carbomethoxy-3-β-(4-fluorophenyl) tropane (WIN 35,428) binding in rat striatal synaptosomes." *Journal of Pharmacology and Experimental Therapeutics* 329.3 (2009): 1071-1083.

Zhu, Jun, et al. "HIV-1 transgenic rats display an increase in [3 H] dopamine uptake in the prefrontal cortex and striatum." *Journal of neurovirology* 22.3 (2016): 282-292.

Zhu, Jun, et al. "Recombinant human immunodeficiency virus-1 transactivator of transcription1-86 allosterically modulates dopamine transporter activity." *Synapse (New York, NY)* 65.11 (2011): 1251-1254.

Zhu, Jun, Subramaniam Ananthan, and Chang-Guo Zhan. "The role of human dopamine transporter in NeuroAIDS." *Pharmacology & therapeutics* 183 (2018): 78-89.

Zou, Wei, et al. "Protection against human immunodeficiency virus type 1 Tat neurotoxicity by Ginkgo biloba extract EGb 761 involving glial fibrillary acidic protein." *The American journal of pathology* 171.6 (2007): 1923-1935.

APPENDIX A

CHAPTER 3 SUPPLEMENTARY INFORMATION

Table A.1 Kinetic properties of [^{3}H]DA uptake and [^{3}H]WIN 35,428 binding for DAT in C57BL/6J mice

			Prefrontal cortex		Striatum	
			V_{max} (pmol/min/mg)	K_m (nM)	V_{max} (pmol/min/mg)	K_m (nM)
Treatment duration	7-days	C57 - Saline	0.590 ± 0.080	90.8 ± 16	15.1 ± 1.1	100 ± 12
		C57 - Dox	0.647 ± 0.044	77.6 ± 26	14.7 ± 1.2	103 ± 5.7
	14-days	C57 - Saline	0.685 ± 0.048	109 ± 10	51.9 ± 4.0	149 ± 7.5
		C57 - Dox	0.708 ± 0.11	84.3 ± 8.3	54.7 ± 5.5	154 ± 8.2
			B_{max} pmol/mg	K_d (nM)	B_{max} pmol/mg	K_d (nM)
	7-days	C57 - Saline	0.423 ± 0.19	9.02 ± 1.3	26.9 ± 3.5	14.6 ± 0.89
		C57 - Dox	0.395 ± 0.065	7.84 ± 1.5	29.9 ± 4.9	16.9 ± 2.1

Data are expressed as mean ± S.E.M. values from five to seven independent experiments performed in duplicate

Table A.2 Kinetic properties of [^{3}H]DA uptake and [^{3}H]Nisoxetine binding for NET in C57BL/6J mice

			Prefrontal cortex		Hippocampus	
			V_{max} (pmol/min/mg)	K_m (nM)	V_{max} (pmol/min/mg)	K_m (nM)
Treatment duration	7-days	C57 - Saline	1.15 ± 0.063	158 ± 42	0.972 ± 0.047	86.0 ± 16
		C57 - Dox	1.14 ± 0.064	156 ± 35	0.962 ± 0.12	93.3 ± 18
	14-days	C57 - Saline	2.02 ± 0.25	92.2 ± 15	2.30 ± 0.29	86.5 ± 38
		C57 - Dox	1.98 ± 0.24	83.9 ± 17	2.26 ± 0.22	88.9 ± 28
			B_{max} pmol/mg	K_d (nM)	B_{max} pmol/mg	K_d (nM)
	7-days	C57 - Saline	0.553 ± 0.051	12.9 ± 3.2	0.636 ± 0.11	7.39 ± 0.72
		C57 - Dox	0.591 ± 0.12	11.0 ± 3.0	0.645 ± 0.13	8.59 ± 1.1

Data are expressed as mean ± S.E.M. values from five to seven independent experiments performed in duplicate.

Table A.3 Kinetic properties of [^{3}H]DA uptake via DAT in PFC and striatum or NET in PFC and hippocampus in G-tg mice following 7-day administration of saline or Dox

		Prefrontal cortex		Striatum	
		V_{max} (pmol/min/mg)	K_m (nM)	V_{max} (pmol/min/mg)	K_m (nM)
DAT	G-tg - Saline	0.343 ± 0.037	61.0 ± 18	33.3 ± 4.7	78.1 ± 5.3
	G-tg - Dox	0.317 ± 0.065	55.5 ± 17	32.3 ± 2.7	73.1 ± 1.4
		Prefrontal cortex		Hippocampus	
		V_{max} (pmol/min/mg)	K_m (nM)	V_{max} (pmol/min/mg)	K_m (nM)
NET	G-tg - Saline	0.945 ± 0.058	89.3 ± 23	1.39 ± 0.13	110 ± 10
	G-tg - Dox	1.09 ± 0.20	75.7 ± 2.5	1.41 ± 0.10	113 ± 23

Data are expressed as mean ± S.E.M. values from three independent experiments performed in duplicate.

Table A.4 Average age and total number of mice used for each experiment type by genotype and treatment.

	iTat-tg Saline	iTat-tg Dox	C57 Saline	C57 Dox	Total mice used
7-day [^{3}H]DA uptake	11.3 ± 0.41	10.8 ± 0.30	11.8 ± 0.11	12.0 ± 0.09	168
14-day [^{3}H]DA uptake	11.8 ± 0.34	11.2 ± 0.26	11.4 ± 0.24	11.4 ± 0.24	144
Surface Biotinylation	11.1 ± 0.14	11.1 ± 0.14	10.9 ± 0.15	10.9 ± 0.15	36
[^{3}H]WIN and [^{3}H]NXT binding	10.6 ± 0.28	10.3 ± 0.19	12.0 ± 0.27	12.0 ± 0.27	120
DA and DOPAC tissue content	11.9 ± 0.17	11.9 ± 0.17	12.6 ± 0.21	12.6 ± 0.21	24
Patch Clamp Ephys.	10.3 ± 0.44	10.4 ± 0.23	10.6 ± 0.30	11.0 ± 0.25	12

Age of mice is shown in weeks ± S.E.M.. Note that for several experiments the saline and dox groups are exactly the same age; this is because they were tested simultaneously, and treatment was able to be distributed amongst littermates in these experiments.

Table A.5 Pearson's correlation coefficient of age versus experimental output

		PFC – DAT	STR – DAT	PFC – NET	HIP – NET
7-day [^{3}H]DA uptake (V_{max})		0.018	0.031	0.273	0.018
14-day [^{3}H]DA uptake (V_{max})		0.024	0.216	0.345	0.260
Biotinylation	Total	-0.433	-0.101	-0.048	-0.516
	Surface	-0.258	-0.040	-0.200	0.193
[^{3}H]WIN and [^{3}H]NXT binding (B_{max})		-0.166	0.445	-0.020	0.423
		PFC – DA	PFC – DOPAC	STR – DA	STR – DOPAC
DA and DOPAC tissue content		-0.275	0.192	-0.365	-0.166

Pearson's correlation coefficient was determined using Graphpad Prism 8 software. Age was used as the x-axis and experimental output was used for the y-axis. No significant correlations were found between age and any experimental output.

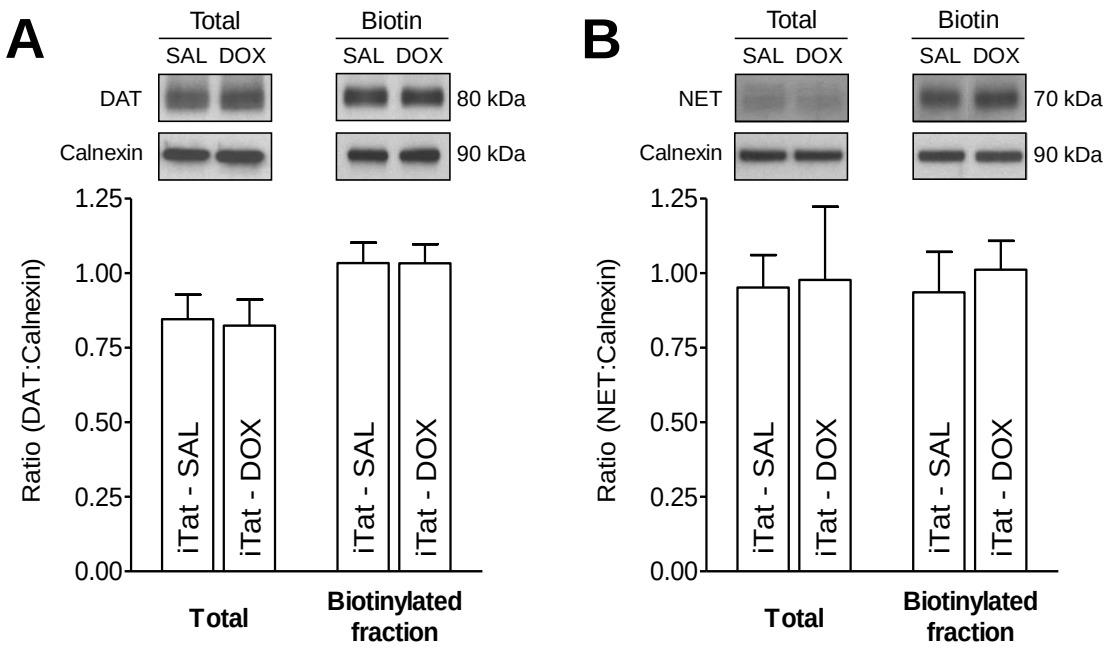

Figure A.1 Analysis of plasmalemmal surface expression of DAT and NET was determined in the striatum and hippocampus of iTat-tg mice following 7-day administration of saline or Dox. Synaptosomes were incubated with sulfo-NHS-biotin and Pierce monomeric avidin beads and washed multiple times to isolate the DAT or NET which was present on the plasmalemmal membrane. Top panels: representative immunoblots of the total and biotinylated (Biotin) fraction of DAT in the striatum (A) or NET in hippocampus (B) from iTat-tg mice from Dox-treated and saline (SAL) control groups. Calnexin was used as control protein. Bottom panels: the ratio of total or biotinylated DAT (A) and NET (B) immunoreactivity to calnexin immunoreactivity expressed as mean ± S.E.M. from five independent experiments.

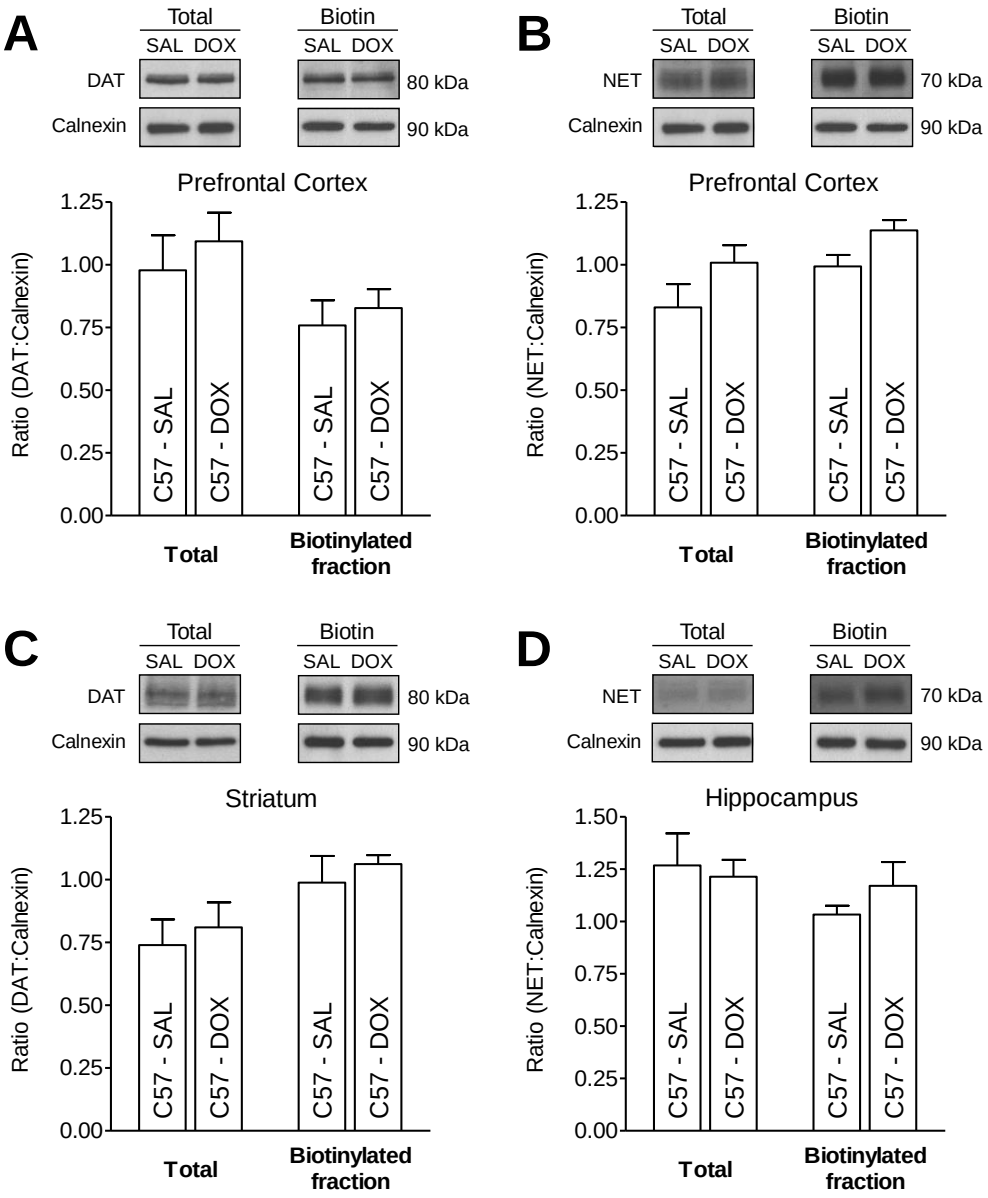

Figure A.2 Analysis of plasmalemmal surface expression of DAT (in PFC and striatum) and NET (in PFC and hippocampus) was determined in C57BL/6J mice following 7-day administration of saline or Dox. Synaptosomes were incubated with sulfo-NHS-biotin and Pierce monomeric avidin beads and washed multiple times to isolate the DAT or NET which was present on the plasmalemmal membrane. Top panels: representative immunoblots for the total and biotinylated (Biotin) fraction of DAT in the PFC (A) and striatum (C) or NET in the PFC (B) and hippocampus (D) from C57BL/6J (C57) from Dox-treated and saline (SAL) control groups. Calnexin was used as control protein. Bottom panels: the ratio of total or biotinylated DAT or NET immunoreactivity to calnexin immunoreactivity (A-D) expressed as mean ± S.E.M. from 3-5 independent experiments.

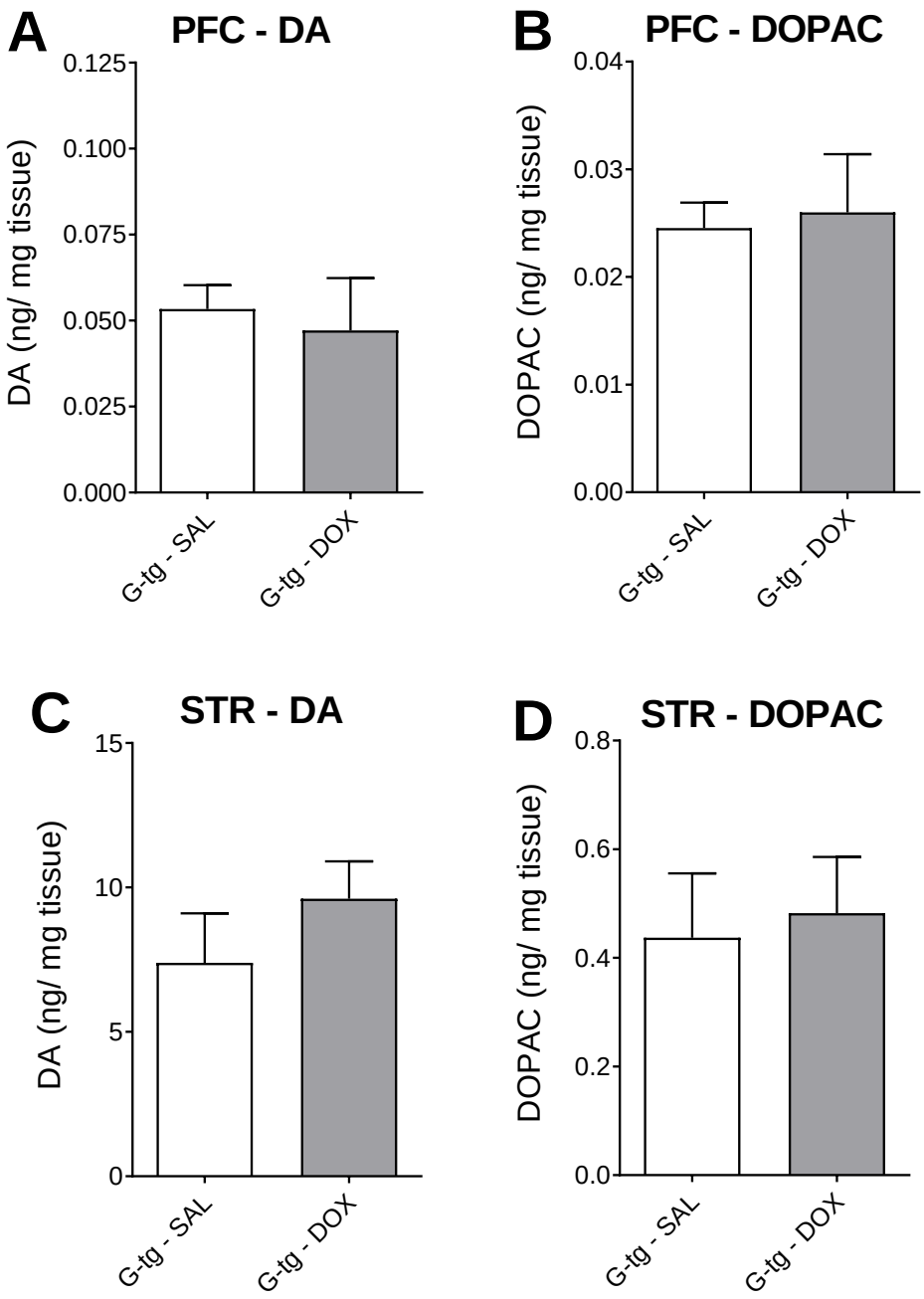

Figure A.3 DA and dihydroxyphenylacetic acid (DOPAC) tissue content in the PFC and striatum of G-tg mice following 7-day administration of saline or Dox. Top panels: DA (A) and DOPAC (B) tissue content in the PFC of G-tg mice from Dox-treated or saline (SAL) control groups. Bottom panels: DA (C) and DOPAC (D) tissue content in striatum (STR) of G-tg mice from Dox-treated or saline (SAL) control groups. Data are expressed as ng/mg tissue (mean ± S.E.M.) from 5-6 independent experiments.

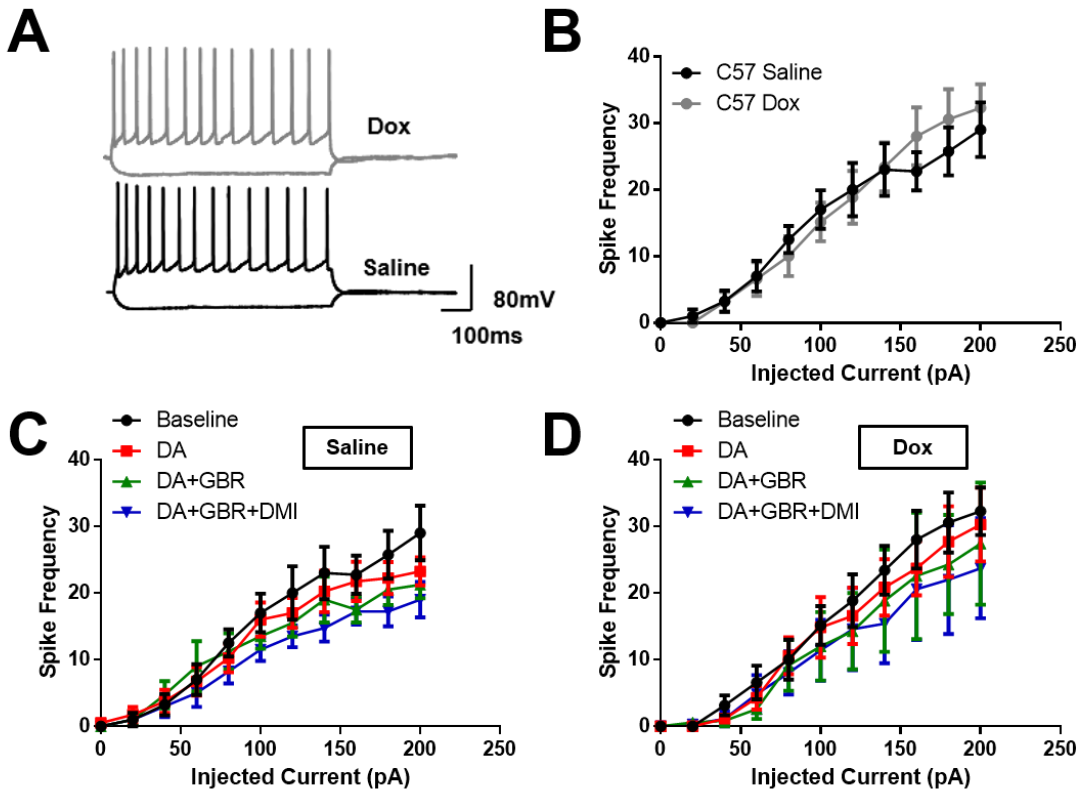

Figure A.4 Whole-cell patch clamp electrophysiology was performed in layer V pyramidal neurons of the prelimbic region of PFC in C57BL/6J mice following 7-day administration of saline or Dox. Coronal slices (300 µm) containing the prelimbic cortex were cut with a Vibratome and incubated in an ice-cold artificial CSF (aCSF) solution at 32–34°C for 45 min and kept at 22–25°C thereafter, until transfer to the recording chamber. (A) Representative traces from C57BL/6J (C57) mice treated with saline (C57-Saline) and Dox (C57-Dox) following hyperpolarizing (-200 pA) and depolarizing (+200 pA) current steps. Summary of basal action potential frequency (B) and action potential frequency in response to acute application of DA (10 nM) or DA + GBR 12909 (100 nM) or DA + GBR 12909 + DMI (1 µM) of neurons from C57BL/6J mice treated with saline (C) or Dox (D).

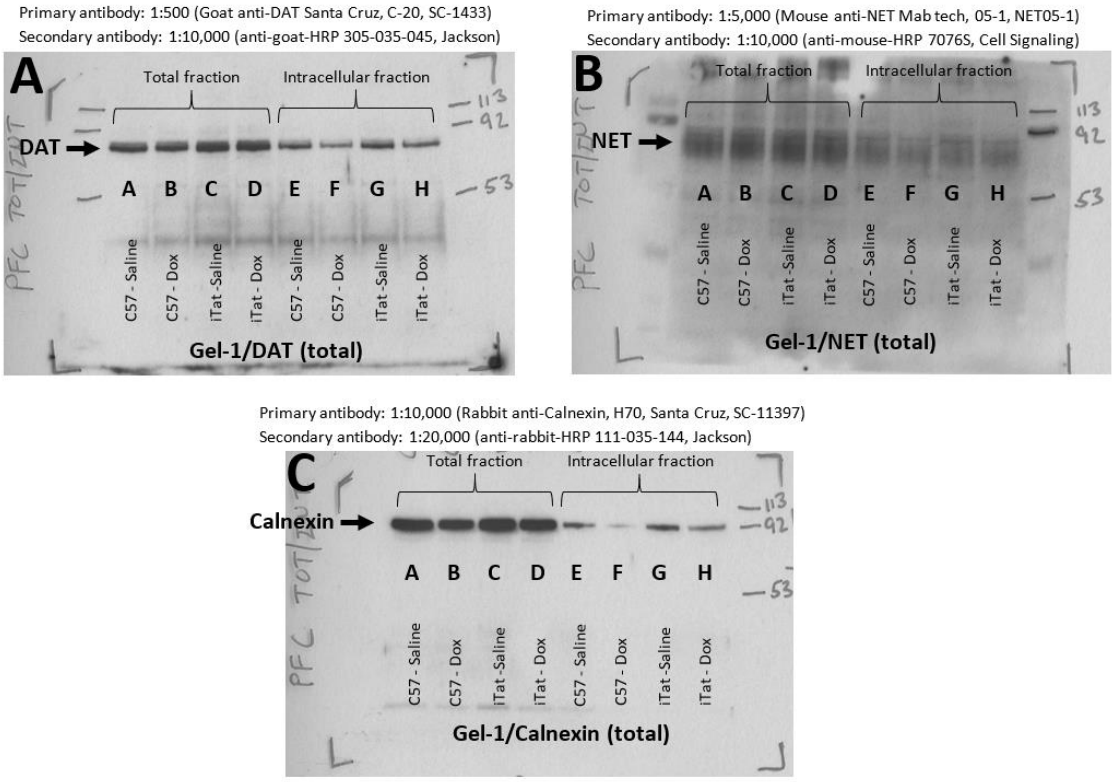

Figure A.5 Representative immunoblots for total DAT (A), NET (B), and Calnexin (C) in C57 or iTat mice treated with saline or dox. Total and intracellular DAT (A), NET (B), and Calnexin (C) expression in C57 and iTat mice following 7-days of saline or dox treatment. The total and intracellular fractions were prepared and loaded as described in the methods section under the biotinylation and western blot heading. The membrane was first probed using the C-20 anti-DAT antibody (A), then stripped using Restore^{TM} Western Blot Stripping Buffer (ThermoFisher, cat# 21059), and re-probed with NET05-1 anti-NET antibody (B). The same membrane was then stripped again and re-probed with H70 anti-calnexin antibody (C) to monitor protein loading between all lanes. Lanes C and D from panel A are shown in Figure 3.2A as total DAT fraction, and lanes C and D from panel B are shown in Figure 3.2B as total NET fraction. Lanes C and D from panel C are shown as the loading control for both total DAT (Figure 3.2A) and NET (Figure 3.2B) as the same sample was used to determine the expression of both proteins. Lanes A and B from all panels were used in Figure A.2A and A.2B in an identical manner.

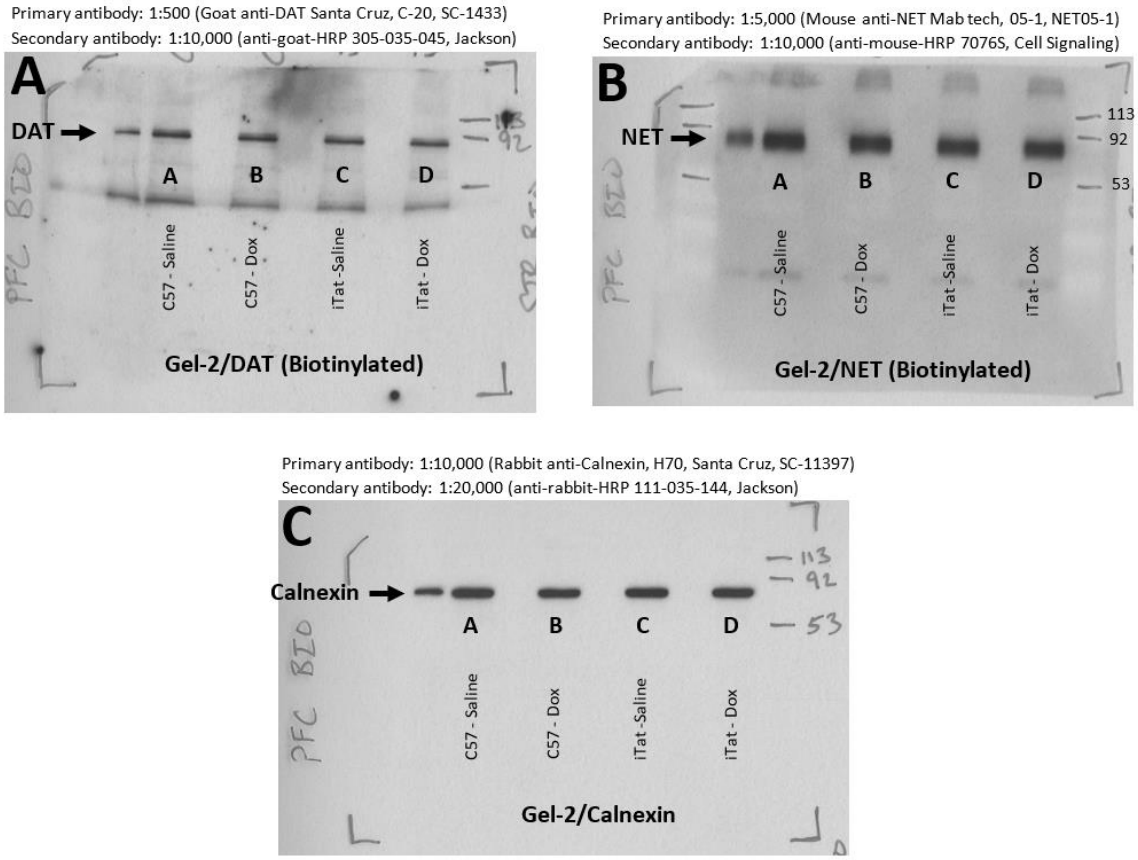

Figure A.6 Representative immunoblots for biotinylated DAT (A), NET (B), and Calnexin (C) in C57 or iTat mice treated with saline or dox. Biotinylated DAT (A), NET (B), and Calnexin (C) expression in C57 and iTat mice following 7-days of saline or dox treatment. The biotinylated fraction was prepared and loaded as described in the methods section under the biotinylation and western blot heading. The membrane was first probed using the C-20 anti-DAT antibody (A), then stripped using Restore^{TM} Western Blot Stripping Buffer (ThermoFisher, cat# 21059), and re-probed with NET05-1 anti-NET antibody (B). The same membrane was then stripped again and re-probed with H70 anti-calnexin antibody (C) to monitor protein loading between all lanes. Lanes C and D from panel A are shown in Figure 3.2A as biotinylated DAT fraction, and lanes C and D from panel B are shown in Figure 3.2B as biotinylated NET fraction. Lanes C and D from panel C are shown as the loading control for both biotinylated DAT (Figure 3.2A) and NET (Figure 3.2B) as the same sample was used to determine the expression of both proteins. Lanes A and B from all panels were used in Figure A.2A and A.2B in an identical manner.

APPENDIX B

CHAPTER 3 COPYRIGHT PERMISSION

August 18, 2020

Matthew Strauss
College of Pharmacy
University of South Carolina
700 Sumter St.
Columbia, SC 29201

Email: strausmj@email.sc.edu

Dear Matthew Strauss:

This is to grant you permission to include the following article in your dissertation entitled "The Role of HIV-1 Tat-mediated inhibition of the Dopamine and Norepinephrine Transporters in the Neuropathology of HIV-1 Associated Neurocognitive Disorders" for the University of South Carolina:

> M Strauss, B O'Donovan, Y Ma, Z Xiao, S Lin, MT Bardo, PI Ortinski, JP McLaughlin, and J Zhu (2020) [^{3}H]Dopamine Uptake through the Dopamine and Norepinephrine Transporters is Decreased in the Prefrontal Cortex of Transgenic Mice Expressing HIV-1 Transactivator of Transcription Protein, *J Pharmacol Exp Ther*, 374(2): 241-251; DOI: https://doi.org/10.1124/jpet.120.266023

The following must be included with your citation to the article:

> Reprinted with permission of the American Society for Pharmacology and Experimental Therapeutics. All rights reserved.

If you present the article as it was published in the journal, the original copyright line published with the paper must be shown on the copies included with your dissertation.

Sincerely yours,

Richard Dodenhoff
Journals Director